ALMA MATER STUDIORUM - UNIVERSITÁ DI BOLOGNA

SCUOLA DI SCIENZE

Corso di Laurea Magistrale in Fisica

FORECASTS ON THE DARK ENERGY ANISOTROPIC STRESS FOR THE ESA *EUCLID* SURVEY

Relatore:

Prof. LAURO MOSCARDINI

Presentata da:

SIMONE FOGLI

Correlatore:

Prof. LUCA AMENDOLA

Sessione I

Anno Accademico 2012/2013

Die Liebe steht dem Tod entgegen, nur sie, nicht die Vernunft, ist stärker als er.

Thomas Mann, “Der Zauberberg”

È l’amore, non la ragione, che è più forte della morte.

Thomas Mann, “La montagna incantata”

It is love, not reason, that is stronger than death.

Thomas Mann, “The Magic Mountain”

Riassunto La costante cosmologica Λ sembra non essere una spiegazione soddisfacente dell'espansione accelerata dell'universo della quale si hanno ormai chiare evidenze sperimentali; si è reso pertanto necessario negli ultimi anni considerare modelli alternativi di *energia oscura*, intesa come causa dell'espansione accelerata. Nello studio dei modelli di energia oscura è importante capire quali quantità possono essere determinate a partire dalle osservazioni sperimentali senza assumere ipotesi di fondo sul modello cosmologico; tali quantità sono determinate in Amendola, Kunz *et al.*, 2012. Nello stesso articolo si è inoltre dimostrato che è possibile stabilire una relazione tra i parametri indipendenti dal modello cosmologico e lo stress anisotropico η, il quale può inoltre essere espresso come combinazione delle funzioni che appaiono nella lagrangiana più generale per le teorie scalare-tensore nell'ambito dei modelli di energia oscura, la lagrangiana di Horndeski. Nel presente elaborato si utilizza il formalismo della matrice di Fisher per formulare una previsione sui vincoli che sarà possibile porre relativamente allo stress anisotropico η nel futuro, a partire dagli errori stimati per le misurazioni in ambito di clustering galattico e lensing gravitazionale debole che verranno effettuate dalla missione *Euclid* dell'Agenzia Spaziale Europea, che verrà lanciata nel 2020. Vengono inoltre considerati i vincoli provenienti da osservazioni di supernovae-Ia. Tale previsione viene effettuata in due casi in cui (a) η viene considerato dipendente unicamente dal redshift e (b) η è costante e uguale a 1, come per esempio nel modello ΛCDM.

Abstract The cosmological constant Λ seems to be a not satisfactory explanation of the late-time accelerated expansion of the Universe, for which a number of experimental evidences exist; therefore, it has become necessary in the last years to consider alternative models of *dark energy*, meant as cause of the accelerated expansion. In the study of dark energy models, it is important to understand which quantities can be determined starting from observational data, without assuming any hypothesis on the cosmological model; such quantities have been determined in Amendola, Kunz *et al.*, 2012. In the same paper it has been further shown that it is possible to estabilish a relation between the model-independent parameters and the anisotropic stress η, which can be also expressed as a combination of the functions appearing in the most general Lagrangian for the scalar-tensor theories, the Horndeski Lagrangian. In the present thesis, the Fisher matrix formalism is used to perform a forecast on the constraints that will be possible to make on the anisotropic stress η in the future, starting from the estimated uncertainties for the galaxy clustering and weak lensing measurements which will be performed by the European Space Agency *Euclid* mission, to be launched in 2020. Further, constraints coming from supernovae-Ia observations are considered. The forecast is performed for two cases in which (a) η is considered as depending from redshift only and (b) η is constant and equal to one, as in the ΛCDM model.

Contents

Introduction

The late-time accelerated expansion of the Universe has been proved with several independent tests (e.g. [1, 2]), and nowadays it is considered as a fact that our Universe is expanding with increasing velocity. But from Friedmann equations (that is, from standard General Relativity with the assumptions that (1) the Universe is homogeneous and isotropic and (2) the Universe content behaves as a perfect fluid), we have that such a result is not understandable, if we deal with ordinary matter with positive pressure. The first attempt to explain this observational evidence was to introduce a cosmological constant Λ in the Einstein equations, which can be interpreted as the vacuum energy density; however, some problems still remain (the so-called coincidence and fine-tuning problems), and the cosmological constant cannot be held as the definitive explanation of late-time cosmic acceleration.

A number of alternative models have been proposed and investigated in the last years as an alternative to cosmological constant, modifying Einstein equations by introducing a new form of matter (*modified matter models*) or modifying Einstein's gravity (*modified gravity models*); all of them are referred to as *dark energy models*, and we simply indicate as *dark energy* the source of the late-time accelerated expansion. The class of the models called scalar-tensor theories, which includes a large part of all the dark energy models, has been shown to be described by a general Lagrangian depending on some functions, namely the Horndeski Lagrangian (HL) [3].

Since many dark energy models have been proposed, it is very important to constrain them by means of observations. To this purpose, the European Space Agency (recenlty joined by the NASA) has therefore planned a mission, called *Euclid*, in order to produce data which will be used to constrain cosmological parameters and maybe cross out some of the models.

Another interesting question to answer is, whether there are some quantities which can be determined from observations without making assumptions on the cosmology, that is, if some model-independent parameters exist. This question has been faced in [4]. In this paper, such parameters have been found, and a relation has been found to hold between the model-independent parameters and the anisotropic stress $\eta = -\Psi/\Phi$. On the other hand, the anisotropic stress can be written as a combination of the functions appearing in the Horndeski Lagrangian, in the so-called quasi-static limit. That is, a relation between the model-independent

parameters and the Horndeski Lagrangian functions (via η) is found to hold. This relation can be used to constrain the HL functions, therefore constraining the dark energy models, starting from observations, from which we can determine the model-independent parameters.

In this Thesis, we deal with the first step of this chain, namely the determination of the constraints on the anisotropic stress η. We use *Euclid* specifications to forecast the uncertainties that this survey will give on the model-independent parameters, starting from uncertainties on rough data, and then project them onto the anisotropic stress η. A supernovae-Ia survey will also be considered in order to put stronger constraints on the dimensionless Hubble parameter $E(z) = H(z)/H_0$. The forecast will be performed in two cases, assuming (a) that η depends on redshift only, and (b) that η is constant and equal to one, respectively.

The determination of the errors on the model-independent parameters and the projection on η are performed by means of a powerful tool: the Fisher matrix formalism, based on Bayesian statistics.

The Thesis is structured as follows.

In Chapter 1, we derive briefly the Friedmann equations from standard General Relativity and introduce the cosmological constant Λ as a possible explanation for the late-time cosmic acceleration; evidences for dark energy from supernovae-Ia are also exposed. In Chapter 2, basics of cosmological perturbation theory are discussed; in particular, the perturbed Friedmann-Lemaître-Robertson-Walker is introduced. The key concept of power spectrum is presented in Chapter 3.

In Chapter 4 we discuss the problems related to the cosmological constant and the reasons why it cannot be considered as a completely satisfactory explanation for cosmic acceleration. We further give an overview on the classes of dark energy models that have been proposed and introduce the Horndeski Lagrangian as the most general Lagrangian for scalar-tensor theories with second-order equations of motion.

In Chapter 5 the two main probes of *Euclid*, galaxy clustering and weak gravitational lensing are presented; the Fisher matrix formalism is also introduced here, describing also how it can be applied to supernovae, galaxy clustering and weak lensing surveys.

Finally, in Chapter 6, the model-independent parameters from [4] and the relation between them, the anisotropic stress η and the HL functions in the quasi-static limit are introduced. The calculations of the Fisher matrices in order to estimate the errors on η are performed, and the results are shown.

Chapter 1

The Concept of Dark Energy in Modern Cosmology

1.1 Friedmann equations

The concept of dark energy has become of great importance in modern Cosmology, after astronomical observations have found the expansion of the Universe to be accelerated. To explain this accelerated expansion, we have to take into account a new form of energy in the Universe, which cannot be matter nor radiation. Let us see briefly how this concept arises.

According to General Relativity, the equations of motion in the Universe can be obtained from the *Einstein field equations* [5]:

$$G_\mu^\nu = 8\pi G T_\mu^\nu, \tag{1.1}$$

where we have set the constant c equal to unity (natural units) and the tensor $G_{\mu\nu}$ is expressed in terms of the Ricci scalar and tensor by:

$$G_{\mu\nu} \equiv R_{\mu\nu} - \frac{1}{2} R g_{\mu\nu}. \tag{1.2}$$

To obtain the form of the Einstein tensor $G_{\mu\nu}$ for a homogeneous and isotropic Universe, we have to extract the form of the Ricci terms from the *Friedmann-Lamaître-Robertson-Walker (FLRW) metric*, which is the line element obtained by applying the cosmological principle hypotheses (homogeneity and isotropy) to the generic Einstein line element:

$$ds^2 = -dt^2 + a^2(t) d\sigma^2, \tag{1.3}$$

where

$$d\sigma^2 = \frac{dr^2}{1-Kr^2} + r^2(d\theta^2 + \sin^2\theta d\phi^2), \tag{1.4}$$

$a(t)$ is the scale factor at time t and K is the curvature parameter, which can be equal to -1, 0 or 1 depending on the geometry of the Universe (open, flat or closed respectively).

The equation (1.3) corresponds to a metric tensor:

$$g_{\mu\nu} = \begin{pmatrix} -1 & 0 & 0 & 0 \\ 0 & \frac{a^2(t)}{1-Kr^2} & 0 & 0 \\ 0 & 0 & a^2(t)r^2 & 0 \\ 0 & 0 & 0 & a^2(t)r^2\sin^2\theta \end{pmatrix}. \tag{1.5}$$

From the metric tensor, we can evaluate the Christoffel symbol

$$\Gamma^{\mu}_{\nu\lambda} = \frac{1}{2}g^{\mu\alpha}(g_{\alpha\nu,\lambda} + g_{\alpha\lambda,\nu} - g_{\nu\lambda,\alpha}) \tag{1.6}$$

and then the Ricci tensor and the Ricci scalar

$$R_{\mu\nu} = \Gamma^{\alpha}_{\mu\nu,\alpha} - \Gamma^{\alpha}_{\mu\alpha,\nu} + \Gamma^{\alpha}_{\mu\nu}\Gamma^{\beta}_{\alpha\beta} - \Gamma^{\alpha}_{\mu\beta}\Gamma^{\beta}_{\alpha\nu}; \tag{1.7}$$

$$R = g^{\mu\nu}R_{\mu\nu}. \tag{1.8}$$

The expression of the Einstein tensor is then obtained; for the FLRW metric, it is given by:

$$G^0_0 = -3(H^2 + K/a^2); \tag{1.9}$$

$$G^i_0 = G^0_i = 0; \tag{1.10}$$

$$G^i_j = -(3H^2 + 2\dot{H} + K/a^2)\delta^i_j, \tag{1.11}$$

where we have defined the Hubble parameter H

$$H \equiv \dot{a}/a \tag{1.12}$$

and the dot indicates the derivative with respect to t.

We now make the assumption of perfect fluid form for the energy-momentum tensor; this means that we are considering the content of the Universe to be a perfect fluid:

$$T^{\mu}_{\nu} = (\rho + P)u^{\mu}u_{\nu} + P\delta^{\mu}_{\nu}, \tag{1.13}$$

where ρ, P are the density and the pressure of the fluid, respectively, and $u^{\mu} = (-1,0,0,0)$ is the four-velocity of the fluid in comoving coordinates.

At this point, we are able to write the explicit form of the Einstein equations; the only non trivial equations are the (00) and the (*ii*) components:

$$H^2 = \frac{8\pi G}{3}\rho - \frac{K}{a^2}, \tag{1.14}$$

$$3H^2 + 2\dot{H} = -8\pi G P - \frac{K}{a^2}. \tag{1.15}$$

Eliminating the K/a^2 term, we can easily get:

$$\frac{\ddot{a}}{a} = -\frac{4\pi G}{3}(\rho + 3P). \tag{1.16}$$

Equations (1.16) and (1.14) are usually referred to as *Friedmann equations*; they describe the dynamics of a homogeneous and isotropic Universe, assuming a perfect fluid form for the energy-momentum tensor (representing a single fluid component). The Friedmann equations are linked to each other by the adiabaticity condition $dU = -PdV$, that is in our case:

$$d(\rho a^3) = -P da^3. \tag{1.17}$$

Multiplying equation (1.14) by a^2, differentiating and using (1.16), we can also write the continuity equation

$$\dot{\rho} + 3H(\rho + P) = 0. \tag{1.18}$$

Equation (1.14) can also be written in the form

$$\Omega + \Omega_K = 1 \tag{1.19}$$

defining the density parameters

$$\Omega \equiv \frac{8\pi G\rho}{3H^2} \tag{1.20}$$

$$\Omega_K \equiv -\frac{K}{(aH)^2}. \tag{1.21}$$

If we deal with more than one fluid component with density parameters Ω_i, we can write

$$\sum_i \Omega_i + \Omega_K = 1. \tag{1.22}$$

For example, in an Universe containing radiation, matter and dark energy with curvature K we have, at the present time (apex (0)):

$$\Omega_r^{(0)} = \frac{8\pi G\rho_r^{(0)}}{3H_0^2} \tag{1.23}$$

$$\Omega_m^{(0)} = \frac{8\pi G\rho_m^{(0)}}{3H_0^2} \tag{1.24}$$

$$\Omega_{DE}^{(0)} = \frac{8\pi G\rho_{DE}^{(0)}}{3H_0^2} \tag{1.25}$$

$$\Omega_K^{(0)} = -\frac{K}{(a_0H_0)^2} \tag{1.26}$$

and the combination

$$\rho_{cr}(t) = \frac{3H^2(t)}{8\pi G} \tag{1.27}$$

is called the *critical density* at time t. The adjective "critical" is due to the fact that, from equation (1.14), one has:

$$\frac{K}{a^2H^2} = \frac{8\pi G\rho}{3H^2} - 1 = \frac{\rho}{\rho_{cr}} - 1, \tag{1.28}$$

and for $\rho > \rho_{cr}$ one has $K > 0$, that is, a *closed* Universe, while for $\rho < \rho_{cr}$ one has $K < 0$ (*open* Universe). If $\rho = \rho_{cr}$, we have a *flat* Universe ($K = 0$).

One can describe the whole thing in terms of the density parameter $\Omega = \rho/\rho_{cr}$: when $\Omega > 1$, we have $K > 0$, etc.

1.2 Cosmic acceleration and cosmological constant

We assume ρ and P to be related by an equation of state of the form

$$P = w\rho \tag{1.29}$$

for example, we have $w \simeq 0$ for non-relativistic matter and $w \simeq 1/3$ for radiation.

Let us now take into account equation (1.16). We can immediately notice that, to have a cosmic acceleration $\ddot{a} > 0$, we need to have $P + \rho/3 < 0$, that means

$$w < -1/3. \tag{1.30}$$

This value of w, representing a fluid with negative pressure, cannot be reached by ordinary matter or radiation. Therefore, we call a form of energy satisfying this property *"dark energy"*.

As already said, in the last decades evidence has arised that our Universe is in accelerated expansion [1, 2]. This means that the Einstein field equations (1.1), taken as they are, are not suitable to explain the observations, and need therefore to be modified. The simplest way to modify them is by adding a constant term, obtaining:

$$R_{\mu\nu} - \frac{1}{2}Rg_{\mu\nu} + \Lambda g_{\mu\nu} = 8\pi G T_{\mu\nu} \tag{1.31}$$

For historical reasons, Λ is called *cosmological constant*, and was first introduced by Einstein himself to allow static solutions $\dot{a} = \ddot{a} = 0$ ([7]).

To deal with equations (1.31), it is useful to bring the Λ term on the right hand side and to define the modified energy-momentum tensor

$$\tilde{T}_{\mu\nu} = T_{\mu\nu} + \frac{\Lambda}{8\pi G}g_{\mu\nu}. \tag{1.32}$$

Now, repeating the steps of the previous section, we can obtain the modified Friedmann equations:

$$\frac{\ddot{a}}{a} = -\frac{4\pi G}{3}(\tilde{\rho} + 3\tilde{P}), \tag{1.33}$$

$$H^2 = \frac{8\pi G}{3}\tilde{\rho} - \frac{K}{a^2}, \tag{1.34}$$

which are formally identical to equations (1.16), (1.14), but where ρ and P are replaced by the effective density and pressure

$$\tilde{P} = P + P_\Lambda = P - \frac{\Lambda}{8\pi G}, \tag{1.35}$$

$$\tilde{\rho} = \rho + \rho_\Lambda = \rho + \frac{\Lambda}{8\pi G}. \tag{1.36}$$

It is easy to see from equation (1.35) that Λ gives a negative contribution to the effective pressure, now therefore allowing solutions with $\ddot{a} > 0$.

In particular, we can see that the Λ contributions to pressure and density satisfy the equation of state

$$P_\Lambda = -\rho_\Lambda \tag{1.37}$$

which is equation (1.29) with $w = -1$.

The quantity Λ can thus explain the cosmic acceleration that comes out from the observations; however, there are some crucial problems, which do not allow us to take Λ as the definitive explanation. This problems will be discussed in Section 4.1.

1.3 The Friedmann models

Here we shall mention some useful relations valid in the context of Friedmann models.

From the adiabaticity relation (1.17) and the equation of state (1.29), we can obtain the relation between the density and the scale factor:

$$\rho \propto a^{-3(1+w)} = \rho_0 (\frac{a}{a_0})^{-3(1+w)}. \tag{1.38}$$

For example, we have $\rho_r \propto a^{-4}$ for radiation, $\rho_m \propto a^{-3}$ for pressureless matter, $\rho_\Lambda = const$ for the cosmological constant.

In observations, the *redshift* z of an electromagnetic source is defined by

$$z \equiv \frac{\lambda_o - \lambda_e}{\lambda_e}, \tag{1.39}$$

where λ_e is the wavelength of the emitted wave and λ_o is the observed wavelength. It turns out that the following relation exists between the redshift and the scale factor:

$$1 + z = \frac{a_0}{a}, \tag{1.40}$$

where a is the scale factor at the epoch of emission and a_0 is the one at present epoch. We can then write equation (1.38) in the form:

$$\rho(z) = \rho_0 (1+z)^{3(1+w)}. \tag{1.41}$$

Let us now take into account a Friedmann Universe filled with radiation, pressureless matter and dark energy with an equation of state w_{DE}, assumed here for simplicity not to depend on z.

From the Friedmann equation (1.14) we have:

$$H^2 = \frac{8\pi G}{3}(\rho_r + \rho_m + \rho_{DE}) - \frac{K}{a^2}. \tag{1.42}$$

Substituting equation (1.41) with different values of w for the components, we can get the expression for the Hubble parameter as a function of the redshift:

$$H^2(z) = H_0^2 \left[\Omega_r^{(0)}(1+z)^4 + \Omega_m^{(0)}(1+z)^3 + \Omega_{DE}^{(0)}(1+z)^{3(1+w_{DE})} + \Omega_K^{(0)}(1+z)^2\right]. \tag{1.43}$$

In the case of the cosmological constant ($w_{DE} = -1$) we have

$$H^2(z) = H_0^2 \left[\Omega_r^{(0)} (1+z)^4 + \Omega_m^{(0)} (1+z)^3 + \Omega_\Lambda^{(0)} + \Omega_K^{(0)} (1+z)^2 \right]. \tag{1.44}$$

1.3.1 Cosmic distances

In Cosmology, it is not possible to define the distance of an object in an unique way. The method we use to estimate distances is different, depending on the quantities we can measure about that object. We define the distances in order to reproduce known relations of the ordinary Physics.

Let us first write the spatial element of the FLRW metric in the form

$$d\sigma^2 = d\chi^2 + (f_K(\chi))^2 (d\theta^2 + \sin^2\theta d\phi^2) \tag{1.45}$$

where we have set

$$r = f_K(\chi) = \begin{cases} \sin\chi & (K=+1) \\ \chi & (K=0) \\ \sinh\chi & (K=-1) \end{cases} . \tag{1.46}$$

The function $f_K(\chi)$ can also be written in a unified form

$$f_K(\chi) = \frac{1}{\sqrt{-K}} \sinh(\sqrt{-K}\chi). \tag{1.47}$$

The *comoving distance* d_c is defined, in physical units, as

$$d_c(z) = \chi = \frac{c}{a_0 H_0} \int_0^z \frac{d\tilde{z}}{E(\tilde{z})} \tag{1.48}$$

where

$$E(z) \equiv H(z)/H_0. \tag{1.49}$$

Suppose now we have an object of which we can determine the absolute luminosity L (such objects in Cosmology are named as *standard candles*). We know that in ordinary Physics the luminosity flux is given by $\mathscr{F} = L/(4\pi d^2)$, where d is the distance of the object. Then, to estimate the distance of such an object we can define the *luminosity distance* d_L as follows:

$$d_L^2 \equiv \frac{L_s}{4\pi\mathscr{F}}, \tag{1.50}$$

where L_s is the absolute luminosity of the source, $\mathscr{F}$ is the observed flux, defined by $\mathscr{F} = \frac{L_0}{4\pi(a_0 f_K(\chi))^2}$, and L_0 is the observed luminosity.

It can be shown that the ratio L_s/L_0 is given by

$$\frac{L_s}{L_0} = (1+z)^2. \tag{1.51}$$

We then have an expression for the luminosity distance:

$$d_L(z) = a_0 f_K(\chi)(1+z), \tag{1.52}$$

or, more explicitly,

$$d_L(z) = \frac{c(1+z)}{H_0\sqrt{\Omega_K^{(0)}}} \sinh\left(\sqrt{\Omega_K^{(0)}}\int_0^z \frac{d\tilde{z}}{E(\tilde{z})}\right), \tag{1.53}$$

where, this time, the parameter $\Omega_K^{(0)}$ is given in physical units as

$$\Omega_K^{(0)} = -\frac{Kc^2}{(a_0H_0)^2}, \tag{1.54}$$

which is equation (1.26) multiplied by a factor c^2.

For a flat universe ($K = 0$) we have the simple relation:

$$d_L(z) = a_0 d_c(z)(1+z) = \frac{c(1+z)}{H_0}\int_0^z \frac{d\tilde{z}}{E(\tilde{z})}. \tag{1.55}$$

In order to estimate the distance of not point-like sources, such as galaxy clusters, we can define the *angular diameter distance* d_A as:

$$d_A \equiv \frac{\Delta x}{\Delta\theta}, \tag{1.56}$$

where Δx is the linear dimension of the object orthogonal to the line of sight and $\Delta\theta$ is the angle subtended by the object as seen by the observer. This definition reproduces the well-known relation $x = d\sin\theta \sim \theta d$ for small θ.

The source lies on the surface of a sphere of radius χ with the observer at the center; the size Δx at the time t_1 corresponding to the object's redshift z is then given by

$$\Delta x = a(t_1) f_K(\chi)\Delta\theta = \frac{a_0}{1+z} f_K(\chi)\Delta\theta. \tag{1.57}$$

The angular diameter distance is then given by:

$$d_A(z) = \frac{a_0}{1+z} f_K(\chi) = \frac{c}{(1+z)H_0\sqrt{\Omega_K^{(0)}}} \sinh\left(\sqrt{\Omega_K^{(0)}}\int_0^z \frac{d\tilde{z}}{E(\tilde{z})}\right), \tag{1.58}$$

that is

$$d_A(z) = \frac{d_L(z)}{(1+z)^2}. \tag{1.59}$$

In the case of a flat Universe ($K = 0$) we have

$$d_A(z) = \frac{c}{H_0(1+z)} \int_0^z \frac{d\tilde{z}}{E(\tilde{z})}. \tag{1.60}$$

1.4 Observational evidences of dark energy

As stated before, there are several observational evidences for late-time cosmic acceleration and thus for the existence of dark energy. The most important ones come from:

1. the comparison of the age of the Universe with oldest stars;
2. supernovae observations;
3. Cosmic Microwave Background (CMB);
4. baryon acoustic oscillations (BAO);
5. large-scale-structure (LSS).

Below we shall talk briefly about the supernovae observations, as they are of interest for the purposes of this thesis and for historical reasons, being the first observational evidence of late-time cosmic acceleration.

1.4.1 Supernovae Ia observations

The first evidence of late-time cosmic acceleration came in 1998 with two independent works by Riess *et al.* [1] and Perlmutter *et al.* [2] based on observation of supernovae of type Ia.

As a matter of fact, supernovae can be classified according to the absorption lines of chemical elements appearing in their spectra. Supernovae whose spectrum contains a spectral line of hydrogen are called Type II; otherwise Type I. Type I supernovae are further subdivided in three different categories: Type Ia contains an absorption line of ionised silicon, Type Ib contains a line of helium, Type Ic neither of these elements.

The crucial property of the Type Ia supernovae (SN Ia) is that their absolute luminosity is almost constant at the peak of brightness: this means that they can be used as *standard candles* to calculate their luminosity distance by measuring their apparent luminosity (in fact, it would be more correct to talk of *standardizable candles,* since the magnitude has to be corrected with the light curve width).

A common way to measure the brightness of a star observed on Earth is by measuring its *apparent magnitude m*.

Given two stars whose apparent fluxes are $\mathscr{F}_1$ and $\mathscr{F}_2$, we define the difference between their apparent magnitudes as

$$m_1 - m_2 = -\frac{5}{2}\log_{10}\left(\frac{\mathscr{F}_1}{\mathscr{F}_2}\right). \tag{1.61}$$

Of course, the apparent magnitude depends on the (luminosity) distance of the object. To compare the absolute brightness of two objects at a different distance, it is then useful to define the *absolute magnitude* M. An object with apparent magnitude m and luminosity distance d_L has an absolute magnitude defined by the following relation:

$$m - M = 5\log_{10}\left(\frac{d_L}{10pc}\right). \tag{1.62}$$

That is, the absolute magnitude is the apparent magnitude that the object would have if it were at a luminosity distance of 10 parsec from the observer. If the distance is expressed in Megaparsec, the *distance modulus* $m-M$ can be written as

$$m - M = 5\log_{10} d_L + 25. \tag{1.63}$$

Let us consider a Universe dominated by dark energy and a non-relativistic matter fluid. We can obtain a formula for the luminosity distance at low redshift by expanding equation (1.53) around $z = 0$, setting $\Omega_r^{(0)} \simeq 0$. We have:

$$d_L(z) = \frac{c}{H_0}\left[z + \frac{1}{4}(1 - 3w_{DE}\Omega_{DE}^{(0)} + \Omega_K^{(0)})z^2 + \mathscr{O}(z^3)\right]. \tag{1.64}$$

If we observe some SN Ia at very low redshift (say $z \lesssim 0.1$), where the distance d_L is well approximated by $d_L \simeq \frac{cz}{H_0}$, then independent from the cosmological model, we can use the data to calculate the absolute magnitude M from equation (1.63). By doing this, it has been found that the absolute magnitude is nearly constant for SN Ia and equal to $M \simeq -19$ at the peak of brightness [6]. We can then use high-redshift supernovae ($z \sim 1$) to evaluate the luminosity distance from equation (1.63) (we now know that the value of M is fixed). Assuming a flat Universe where dark energy is identified with the cosmological constant ($w_{DE} = -1$), we can use equation (1.55) to estimate the parameter $\Omega_{DE}^{(0)}$, and this can be done for each supernova. Perlmutter *et al.* found that dark energy is present ($\Omega_{DE}^{(0)} > 0$) at 99% of confidence level.

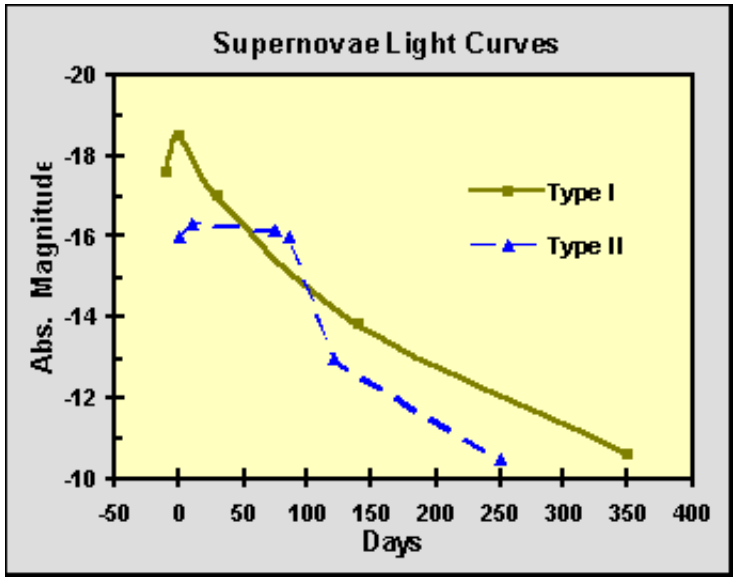

Figure 1.1: Typical light curves for supernovae of Type I and II [8].

Chapter 2

Cosmological Perturbation Theory

In the first chapter we have presented the Friedmann models, based on the FLRW homogeneous and isotropic metric. However, a description like this one can often be not enough satisfying, because the real Universe is more complicated and isotropy and homogeneity hold (in certain limits) only on large scales. The simplest way to describe a Universe that deviates from the FLRW spacetime is to write a metric as a sum of an unperturbed (or background) FLRW term and a "perturbed" deviation term, assumed to be small with respect to the unperturbed one.

We then assume that the metric tensor $g_{\mu\nu}$ is given by

$$g_{\mu\nu} = g^{(0)}_{\mu\nu} + \delta g_{\mu\nu}, \tag{2.1}$$

where $|\delta g_{\mu\nu}| \ll |g^{(0)}_{\mu\nu}|$ for every couple of indexes $\{\mu,\nu\}$.

It is convenient to use the conformal time

$$\eta = \int a^{-1} dt \tag{2.2}$$

and the conformal Hubble quantity

$$\mathscr{H} = \frac{1}{a}\frac{da}{d\eta} = Ha. \tag{2.3}$$

The FLRW metric can be written, as a function of η, as

$$ds^2 = g^{(0)}_{\mu\nu} dx^\mu dx^\nu = a^2(-d\eta^2 + \delta_{ij} dx^i dx^j). \tag{2.4}$$

In General Relativity, the field equations are invariant under a general coordinate change. This means that the unperturbed tensor $g^{(0)}_{\mu\nu}$ and the perturbed one $\delta g_{\mu\nu}$ in equation (2.1) are not unique. However, in order to avoid confusion, we would like to keep the background FLRW metric fixed, and let only the perturbation

term vary. Therefore, we select a class of infinitesimal transformations that leaves $g^{(0)}_{\mu\nu}$ as it is, and makes only $\delta g_{\mu\nu}$ change. These coordinate changes are called *gauge transformations*.

In the unperturbed Universe, we have defined comoving coordinates in a way that the matter particles expanding with the Universe remain at fixed comoving coordinates. If perturbations are added, we have three possibilites: either to use the same coordinates, or to introduce a new system of coordinates that free-fall with the particles in the perturbed gravitational field, or to use a completely different frame not related to the matter particles. Let us focus on the first two cases.

In the first case, we actually choose to attach the observers to the points in the unperturbed frame; this choice is called *Newtonian* or *longitudinal gauge*. The observers will then detect a velocity field of particles falling into the clumps of matter and will measure a gravitational potential. In the second case, instead, the observers are attached to the free-falling particles and therefore they do not see any velocity field nor measure a gravitational potential. This choice is called *comoving proper-time gauge*. In the following we will discuss some concepts of cosmological perturbation theory in the Newtonian gauge.

2.1 Newtonian gauge

The most general perturbed metric can be written as equation. The perturbed term $\delta g_{\mu\nu}$ can be decomposed in the following way, which holds for every rank-two tensor:

$$\delta g_{\mu\nu} = a^2 \begin{pmatrix} -2\Psi & w_i \\ w_i & 2\Phi\delta_{ij} + h_{ij} \end{pmatrix}, \tag{2.5}$$

where Ψ and Φ are spatial scalars, called the *gravitational potentials*, w_i is a 3-vector and h_{ij} is a traceless 3-tensor; all of these quantities depend on space and time.

The vector w_i can be itself decomposed into a longitudinal and a transverse component

$$w_i = w_i^{||} + w_i^{\perp}, \tag{2.6}$$

which by construction satisfy

$$\nabla \cdot w_i^{\perp} = \nabla \times w_i^{||} = 0. \tag{2.7}$$

The transverse component is curl-free and is therefore the gradient of a scalar. When we derive the Einstein equations for the (0i) components, we will have longitudinal and transverse terms. Taking the curl of the equations, we are left with the transverse equations only, whereas taking the divergence, we are left with the longitudinal ones. This means that the two components completely decouple from each other and evolve independently, and can be treated separately. The density perturbation δ is a scalar quantity: this means that only the longitudinal terms couple to the density perturbations.

A similar argument holds for the 3-tensor h_{ij}. We can write it as a sum of three traceless terms:

$$h_{ij} = h_{ij}^{||} + h_{ij}^{\perp} + h_{ij}^{T} \tag{2.8}$$

where the divergences $\partial^i h_{ij}^{||}$ is longitudinal (or curl-free), the divergence $\partial^i h_{ij}^{\perp}$ is transverse (which means it has null divergence) and h_{ij}^{T} is also transverse:

$$\varepsilon_{ijk}\partial_i\partial_k h_{ij}^{||} = \partial_i\partial_j h_{ij}^{\perp} = \partial_i h_{ij}^{T} = 0. \tag{2.9}$$

Since $\partial_i h_{ij}^{||}$ is curl-free, it can be written in terms of a scalar function B; it can be easily checked that $\varepsilon_{ijk}\partial_i\partial_k h_{ij}^{||} = 0$ is verified if

$$h_{ij}^{||} = \left(\partial_i\partial_j - \frac{1}{3}\delta_{ij}\nabla^2\right)B \equiv D_{ij}B. \tag{2.10}$$

The other two terms $\left(h_{ij}^{\perp}, h_{ij}^{T}\right)$, which cannot be derived from a scalar function, give rise to rotational velocity perturbations and to gravitational waves, respectively. Anyway, they decouple completely from the scalar term, and it can be shown that, if they are present, they decrease as a^{-1}. For the reasons previously exposed, we can then consider only the longitudinal term.

That is, to study the field equations in perturbation theory we need to take into account only the part of w_i and h_{ij} derived from scalars. If we introduce two new scalar functions E, B (in analogy to the electromagnetic formalism), we can write the perturbed term (2.5) as

$$\delta g_{\mu\nu} = a^2 \begin{pmatrix} -2\Psi & E_{,i} \\ E_{,i} & 2\Phi\delta_{ij} + D_{ij}B \end{pmatrix}, \tag{2.11}$$

where $E_{,i} = \nabla E$ and $D_{ij}B$ is given by equation (2.10).

The situation can be simplified if we work in a specific gauge; this can be done if we impose up to four conditions on the metric. We choose them to be $w_i = 0$ (from which $E = 0$) and $B = 0$. We then obtain the perturbed metric in the Newtonian or longitudinal gauge:

$$ds^2 = a^2(\eta)\left[-(1+2\Psi)d\eta^2 + (1+2\Phi)\delta_{ij}dx^i dx^j\right]. \tag{2.12}$$

Our next step is then to derive the first-order Einstein equations. To achieve this, we decompose the Einstein and the energy-momentum tensor in a background and a perturbed part

$$G_\nu^\mu = G_\nu^{\mu(0)} + \delta G_\nu^\mu, \tag{2.13}$$

$$T_\nu^\mu = T_\nu^{\mu(0)} + \delta T_\nu^\mu. \tag{2.14}$$

The background cosmological evolution is obtained by solving the zero-th order Einstein equations $G_\nu^{\mu(0)} = 8\pi G T_\nu^{\mu(0)}$; the first-order Einstein equations are instead given by

$$\delta G_\nu^\mu = 8\pi G \delta T_\nu^\mu. \tag{2.15}$$

In order to compute the l.h.s. of equation (2.15), we have to calculate the perturbed Christoffel symbols $\delta\Gamma^\mu_{\nu\lambda}$ by using the formula

$$\delta\Gamma^\mu_{\nu\lambda} = \frac{1}{2}\delta g^{\mu\alpha}\left(g_{\alpha\nu,\lambda} + g_{\alpha\lambda,\nu} - g_{\nu\lambda,\alpha}\right) + \frac{1}{2}g^{\mu\alpha}\left(\delta g_{\alpha\nu,\lambda} + \delta g_{\alpha\lambda,\nu} - \delta g_{\nu\lambda,\alpha}\right) \tag{2.16}$$

and then the perturbation in the Ricci tensor and scalar

$$\delta R_{\mu\nu} = \delta\Gamma^\alpha_{\mu\nu,\alpha} - \delta\Gamma^\alpha_{\mu\alpha,\nu} + \delta\Gamma^\alpha_{\mu\nu}\Gamma^\beta_{\alpha\beta} + \Gamma^\alpha_{\mu\nu}\delta\Gamma^\beta_{\alpha\beta} - \delta\Gamma^\alpha_{\mu\beta}\Gamma^\beta_{\alpha\nu} - \Gamma^\alpha_{\mu\beta}\delta\Gamma^\beta_{\alpha\nu} \tag{2.17}$$

$$\delta R = \delta g^{\mu\alpha} R_{\alpha\mu} + g^{\mu\alpha}\delta R_{\alpha\mu}. \tag{2.18}$$

The perturbations δG_ν^μ for the Einstein are then given by

$$\delta G_{\mu\nu} = \delta R_{\mu\nu} - \frac{1}{2}\delta g_{\mu\nu} R - \frac{1}{2} g_{\mu\nu}\delta R \tag{2.19}$$

$$\delta G_\nu^\mu = \delta g^{\mu\alpha} G_{\alpha\nu} + g^{\mu\alpha}\delta G_{\alpha\nu}. \tag{2.20}$$

In particular, for the FLRW metric (2.12), we get:

$$\delta G_0^0 = 2a^{-2}\left[3\mathscr{H}\left(\mathscr{H}\Psi - \Phi'\right) + \nabla^2\Phi\right], \tag{2.21}$$

$$\delta G_i^0 = 2a^{-2}\left(\Phi' - \mathscr{H}\Psi\right)_{|i}, \tag{2.22}$$

$$\delta G_j^i = 2a^{-2}\left[\left(\mathscr{H}^2 + 2\mathscr{H}'\right)\Psi + \mathscr{H}\Psi' - \Phi'' - 2\mathscr{H}\Phi'\right]\delta_j^i + a^{-2}\left[\nabla^2\left(\Psi+\Phi\right)\delta_j^i - \left(\Psi+\Phi\right)^{|i}_{|j}\right], \tag{2.23}$$

where the prime represents the derivative with respect to the conformal time η, the subscript $_|$ represents a covariant derivative with the spatial 3-metric, δ_j^i is the Kronecker delta and $\nabla^2 f = f^{;\mu}_{;\mu}$.

The calculation of the r.h.s. of equation (2.15) requires the assumption of a form for the energy-momentum tensor $T_{\mu\nu}$; given the form, the perturbation $\delta T_{\mu\nu}$ can be derived. From it we could also get the first-order part of the continuity equation

$$\delta T^\mu_{\nu;\mu} = 0. \tag{2.24}$$

In the following paragraph we will perform the calculation for the case of a single perfect fluid.

2.2 Single-fluid model

For a general fluid the energy-momentum tensor is given by

$$T_{\mu\nu} = (\rho + P)\, u_\mu u_\nu + P g_{\mu\nu} + \left[q_\mu u_\nu + q_\nu u_\mu + \pi_{\mu\nu}\right], \tag{2.25}$$

where u_μ is the four-velocity vector of the fluid, q_μ is the heat flux vector and $\pi_{\mu\nu}$ is the viscous shear tensor.

We will make the following assumptions for the fluid:

1. the fluid is a perfect fluid: that is, $q_\mu = 0$ and $\pi_{\mu\nu} = 0$;
2. the perturbed fluid remains a perfect fluid: $\delta T^i_j = 0$ $(i \neq j)$.

It is useful to define two perturbed quantities: the density contrast δ and the velocity divergence θ:

$$\delta \equiv \frac{\rho(x) - \bar{\rho}}{\bar{\rho}} = \frac{\delta\rho}{\rho}, \tag{2.26}$$

$$\theta \equiv \nabla_i v^i. \tag{2.27}$$

In models with more than one fluid, there are several pairs δ_i, θ_i, one for each fluid.

The perturbed energy-momentum tensor for a perfect fluid can be written as

$$\delta T_{\mu\nu} = \rho\left[\delta\left(1 + c_s^2\right) u_\nu u^\mu + (1+w)\left(\delta u_\nu u^\mu + u_\nu \delta u^\mu\right) + c_s^2 \delta \delta^\mu_\nu\right], \tag{2.28}$$

where the sound speed

$$c_s^2 \equiv \frac{\delta P}{\delta \rho} \tag{2.29}$$

has been introduced. Pay attention to the difference between δ and δ^μ_ν.

If P depends on ρ alone, and we are in the FLRW metric, then we can write

$$c_s^2 = \frac{dP}{d\rho} = \frac{\dot{P}}{\dot{\rho}}. \tag{2.30}$$

The perturbations of the four velocity $u^\mu = \frac{dx^\mu}{ds}$ can be calculated from the first-order expressions

$$u^\mu = \left[\frac{1}{a}(1 - \Psi), \frac{v^i}{a}\right], \tag{2.31}$$

$$u_\mu = \left[-a(1+\Psi), a v^i\right], \tag{2.32}$$

where $v^i = \frac{dx^i}{d\eta} = a\frac{dx^i}{dt}$ is the matter peculiar velocity with respect to the general expansion.

The components of the perturbed energy-momentum tensor are

$$\delta T_0^0 = -\delta\rho, \tag{2.33}$$

$$\delta T_i^0 = -\delta T_0^i = (1+w)\rho v_i, \tag{2.34}$$

$$\delta T_i^i = c_s^2\delta\rho. \tag{2.35}$$

We finally obtain for the perturbed Einstein equations (2.15):

$$3\mathscr{H}\left(\mathscr{H}\Psi - \Phi'\right) + \nabla^2\Phi = -4\pi G a^2\rho\delta \tag{2.36}$$

$$\nabla^2\left(\Phi' - \mathscr{H}\Psi\right) = 4\pi G a^2(1+w)\rho\theta \tag{2.37}$$

$$\Psi = -\Phi \tag{2.38}$$

$$\Phi'' + 2\mathscr{H}\Phi' - \left(\mathscr{H}^2 + 2\mathscr{H}'\right)\Psi - \mathscr{H}\Psi' = -4\pi G a^2 c_s^2\rho\delta \tag{2.39}$$

for the (00), (0i), (ij) and (ii) components respectively, where the assumption $\delta T_j^i = 0$ has been used.

From the continuity equation (2.24), we can obtain the so-called perturbation equations: the perturbed continuity equation (0-component)

$$\delta' + 3\mathscr{H}\left(c_s^2 - w\right)\delta = -(1+w)\left(\theta + 3\Phi'\right) \tag{2.40}$$

and the Euler equation (divergence of the i-component)

$$\theta' + \left[\mathscr{H}(1-3w) + \frac{w'}{1+w}\right]\theta = -\nabla^2\left(\frac{c_s^2}{1+w}\delta + \Psi\right). \tag{2.41}$$

In the case of non-relativistic matter ($w = 0$, $c_s = 0$) we get:

$$\delta' = -\theta - 3\Phi' \tag{2.42}$$

$$\theta' + \mathscr{H}\theta = -\nabla^2\Psi - \nabla^2(c_s^2\delta). \tag{2.43}$$

We can also write the Einstein and the perturbation equations in the Fourier space.

Every perturbation quantity ϕ can be expanded as:

$$\phi = \int e^{ik\cdot r}\phi_k d^3k \tag{2.44}$$

where ϕ_k are the Fourier modes of ϕ. In practice, this means we can transform the quantities from the real to the Fourier space by performing the following replacements:

$$\phi(x,\eta) \to \phi_k(\eta)$$
$$\nabla\phi(x,\eta) \to ik\phi_k(\eta)$$
$$\nabla^2\phi(x,\eta) \to -k^2\phi_k(\eta)$$

We apply this expansion to the quantities $\Phi, \Psi, \delta, \theta$ and obtain, for the equations (2.36)-(2.41):

$$k^2\Phi + 3\mathscr{H}\left(\Phi' - \mathscr{H}\Psi\right) = 4\pi G a^2 \rho\delta \tag{2.45}$$
$$k^2\left(\Phi' - \mathscr{H}\Psi\right) = -4\pi G a^2(1+w)\rho\theta \tag{2.46}$$
$$\Psi = -\Phi \tag{2.47}$$
$$\Phi'' + 2\mathscr{H}\Phi' - \left(\mathscr{H}^2 + 2\mathscr{H}'\right)\Psi - \mathscr{H}\Psi' = -4\pi G a^2 c_s^2 \rho\delta \tag{2.48}$$
$$\delta' + 3\mathscr{H}\left(c_s^2 - w\right)\delta = -(1+w)\left(\theta + 3\Phi'\right) \tag{2.49}$$
$$\theta' + \left[\mathscr{H}(1-3w) + \frac{w'}{1+w}\right]\theta = k^2\left(\frac{c_s^2}{1+w}\delta + \Psi\right) \tag{2.50}$$

where we dropped the k subscripts and now $\theta = ik\cdot v$.

From equations (2.45), (2.46) we can obtain the relativistic Poisson equation:

$$k^2\Phi = 4\pi G a^2\rho\left[\delta + 3\mathscr{H}(w+1)\theta/k^2\right] = 4\pi G a^2\rho\delta* \tag{2.51}$$

where $\delta* \equiv \delta + 3\mathscr{H}(w+1)\theta/k^2$ is the total matter variable.

By combining equations (2.45), (2.47), (2.48), we can also obtain a useful relation for Φ alone:

$$\Phi'' + 3\mathscr{H}(1+c_s^2)\Phi' + (c_s^2k^2 + 3\mathscr{H}^2c_s^2 + 2\mathscr{H}' + \mathscr{H}^2)\Phi = 0. \tag{2.52}$$

In order to solve the perturbed equations, we will consider two different regimes: the large-scale limit $k \ll \mathscr{H} = aH$ and the small-scale limit $k \gg \mathscr{H} = aH$.

2.2.1 Scales larger than the Hubble radius

Let us begin with the large-scale limit $k \ll \mathscr{H} = aH$. In this regime the scale on which the physical wavelength $\lambda_p = \frac{2\pi}{k}a$ is larger than the Hubble radius H^{-1}.

If the pressure P depends only on ρ and the equation of state of the fluid w is a constant (i.e. matter, radiation), we have $c_s^2 = w$ and equation (2.52) takes the form

$$\Phi'' + 3\mathscr{H}(1+c_s^2)\Phi' = 0. \tag{2.53}$$

It is clear that $\Phi' = 0$ ($\Phi = constant$) is a solution, and it is the dominating one (growing mode) at least for $c_s^2 > -1$. Then we can say that the gravitational potential is constant for scales outside the Hubble radius in the hypotheses specified above. Let us now see what happens to the density contrast δ.

Equation (2.45) becomes

$$3\mathscr{H}^2\Phi = 4\pi G a^2 \rho \delta \tag{2.54}$$

and using the Friedmann equation $3\mathscr{H}^2 = 8\pi G a^2 \rho$, we get

$$\delta = 2\Phi. \tag{2.55}$$

So we have that, at large scales, Φ constant implies δ constant.

It is important to remark that the condition $c_s^2 = w$, which we assumed before, is violated during the transition from radiation to matter era, and therefore the gravitational potential changes.

2.2.2 Scales smaller than the Hubble radius

Now we will discuss the small-scale limit, $k \gg \mathscr{H} = aH$, deriving the equations for a pressureless fluid ($w = 0$) in the absence of perturbations, with a small sound speed $c_s^2 \ll 1$. Equation (2.45) becomes then

$$k^2\Phi = 4\pi G a^2 \rho \delta = \frac{3}{2}\mathscr{H}^2\delta. \tag{2.56}$$

Deriving and substituting into equation (2.49) yields:

$$\delta' = -\theta - \frac{9}{2}\frac{\mathscr{H}^2}{k^2}\delta\left(2\frac{\mathscr{H}'}{\mathscr{H}} + \frac{\delta'}{\delta}\right) \simeq -\theta \tag{2.57}$$

and the perturbation equations in this limit are

$$\delta' = -\theta \tag{2.58}$$

$$\theta' = -\mathscr{H}\theta + c_s^2 k^2 \delta - k^2\Phi \tag{2.59}$$

plus equation (2.56).

From the two previous equation we get, after differentiating the first one with respect to η,

$$\delta'' + \mathscr{H}\delta' + \left(c_s^2 k^2 - \frac{3}{2}\mathscr{H}^2\right)\delta = 0. \tag{2.60}$$

This shows that the perturbation does not grow if $c_s^2 k^2 - \frac{3}{2}\mathscr{H} > 0$, that is, if the physical wavelength of the perturbation $\lambda_p = \frac{2\pi}{k}a$ is smaller than the *Jeans length*

$$\lambda_J = c_s \sqrt{\frac{\pi}{G\rho}}. \tag{2.61}$$

For scales smaller than λ_J the perturbations vanish through damping oscillations. In the cases of CDM and radiation, however, the scale λ_J is not larger than the Hubble radius ($c_S \simeq 0$ for CDM, $c_s = \frac{c}{\sqrt{3}}$ for photons), so that perturbations never grow under the Hubble radius.

For baryons, the sound speed is comparable to the photons' one before the decoupling epoch, so that baryon perturbation are damped out and the baryons are free to fall into the dark matter potential wells (*baryonic catch-up*).

On the other hand, when $c_s k \ll \mathscr{H}$, the perturbations grow because gravity is stronger than pressure (*gravitational instability*).

We have:

$$\delta'' + \mathscr{H}\delta' - \frac{3}{2}\mathscr{H}^2\delta = 0 \tag{2.62}$$

and the growing and decaying modes during the matter era evolve as

$$\delta_+ \propto a, \tag{2.63}$$

$$\delta_- \propto a^{-3/2}. \tag{2.64}$$

Chapter 3

Statistical Properties of the Universe

3.1 Correlation function

We want to describe a random distribution of points (i.e. astrophysical sources) in a compact way, using statistical quantities. Given N points in a volume V , the first quantity of statistical interest is the average density $\rho_0 = N/V$; however, the average density does not tell us how the points are distributed in the volume V: they could be homogeneously distributed or concentrated in some regions. We need then more useful descriptors, which carry more information.

Let us consider an infinitesimal volume dV chosen randomly inside the volume V. The average number of points inside the volume dV is $\rho_0 dV$. If we take into account two volumes dV_a and dV_b separated by a distance r_{ab}, the average number of pairs with the first element in the volume dV_a and the second in the volume dV_b is $dN_{ab} = \langle n_a n_b \rangle$. We can define the next important descriptor, the *2-point correlation function* $\xi(r_{ab})$ as:

$$dN_{ab} = \langle n_a n_b \rangle = \rho_0^2 dV_a dV_b \left[1 + \xi(r_{ab})\right]. \tag{3.1}$$

Before getting inside the physical meaning of the 2-point correlation function, it is worth to spend some words on the concept of "average". The word "average" can be used in two possible meanings. The first meaning is the so-called *ensemble average*: one can take many realizations of the distribution, all produced in the same way, and then take the volumes dV_a and dV_b at the same locations and then averaging the pair number $n_a n_b$.

The second is the *sample average*: one can take the pairs at different spots, always separated by the same distance r_{ab}, within the same realization. To make the two definitions coincide, the spots must be sufficiently distant to each other, so that they are uncorrelated and can be considered to be coming from different realizations. The problem is, however, that we do not know *a priori* what this "sufficiently distant" means, we

need to compare the spots with an ensemble of realizations to know if they are effectively uncorrelated, and this cannot be done in astrophysics since we only have a single Universe to deal with. In the following, we will always assume the sample average to be a good approximation of the ensemble one: this assumption is called *ergodic hypothesis*.

Now, let us explain the physical meaning of $\xi(r_{ab})$: if the distribution has been obtained by throwing the N particles at random, the average number of pairs dN_{ab} will not depend on the location, and it will be equal to the product of the average number of particles in the two volumes: $dN_{ab} = \langle n_a n_b \rangle = \langle n_a \rangle \langle n_b \rangle = \rho_0^2 dV_a dV_b$. That is, $\xi(r_{ab}) = 0$, and the particles are uncorrelated. Instead, if $\xi(r_{ab}) \neq 0$, we say that the particles are correlated. This means, the correlation function gives a measure of the difference between the given distribution of particles and a random distribution.

The correlation function can be written as a function of the density contrast $\delta(r_a) = \frac{n_a}{\rho_0 dV_a} - 1$ at two different points:

$$\xi(r_{ab}) = \frac{dN_{ab}}{\rho_0^2 dV_a dV_b} - 1 = \langle \delta(r_a)\delta(r_b) \rangle . \tag{3.2}$$

Of course, $\langle \delta(r_a) \rangle = \langle \delta(r_b) \rangle = 0$. If the average is the sample average, we have to average over all possible positions. We will consider a *statistically homogeneous* system, this means a system for which the correlation function depends only on the separation $\mathbf{r}$ between the infinitesimal volumes and not on $\mathbf{r_a}$ and $\mathbf{r_b}$. If $\mathbf{y}$ is the position of the first infinitesimal volume, and $\mathbf{r}$ is the separation between the two volumes, then we can write

$$\xi(\mathbf{r}) = \frac{1}{V} \int \delta(\mathbf{y})\delta(\mathbf{y}+\mathbf{r}) dV_y. \tag{3.3}$$

The correlation function can be derived in practice as the average density of particles at a given distance r from another particle, that is, dV_a is chosen to be such that $\rho_0 dV_a = 1$. The number of pairs is then given by the number of particles in dV_b:

$$dN_b = \rho_0 dV_b \left[1 + \xi(r_b)\right] \tag{3.4}$$

and the correlation function can be evaluated as

$$\xi(r) = \frac{dN(r)}{\rho_0 dV} - 1, \tag{3.5}$$

where $dN(r)/dV$ is the average density of particles at distance r from any given particle (i.e., we choose a particle and count the number of particles in the volume dV at a distance r, then we do the same for each of the particles, and finally we take the average of the counts), and ρ_0 is the average density, which represents the expected number of particles at the same distance in a uniform distribution. Since we are interested only in the dependence on the modulus r, the volume at distance r is chosen to be a shell of thickness dr. But

since is difficult to estimate the density $dN(r)/dV$ in every shell for each of the particles, the estimation of the correlation function via equation (3.5) is rather difficult. There is an easier way to achieve this: ξ can be estimated by comparing the real number of galaxies at distance r from the observer (i.e. our galaxy) with the number of galaxies at the same distance in a random catalog with exactly the same boundaries and selection function:

$$\xi(r) = \frac{N_{data}(r)}{N_{random}(r)} - 1. \tag{3.6}$$

The idea of the 2-point correlation function can be generalized to higher order functions; for example we can define the *3-point correlation function* as

$$\zeta_{abc}(r_a, r_b, r_c) = \langle \delta(r_a)\delta(r_b)\delta(r_c) \rangle . \tag{3.7}$$

A random field (as $\delta(r)$ can be assumed to be) is said to be *Gaussian* when ζ_{abc} and all odd higher-order correlation functions are equal to zero, and therefore the 2-point correlation function describes completely the statistical properties of the field.

3.2 Power spectrum

An alternative way to describe a density field is by using its *power spectrum.* The power spectrum of the density contrast is of great importance in the study of dark energy and cosmolog in general.

Given a function in real space $f(\mathbf{x})$, we can define its *3-dimensional Fourier decomposition* as

$$f(\mathbf{x}) = \frac{V}{(2\pi)^3} \int f_{\mathbf{k}} e^{i\mathbf{k}\cdot\mathbf{x}} d^3k \tag{3.8}$$

and

$$f_{\mathbf{k}} = \frac{1}{V} \int f(\mathbf{x}) e^{-i\mathbf{k}\cdot\mathbf{x}} d^3x \tag{3.9}$$

is called the *Fourier transform* of the field $f(\mathbf{x})$. The values of $f_{\mathbf{k}}$ for different values of $\mathbf{k}$ can be also called *Fourier coefficients* to underline the decomposition aspect of the transformation.

The power spectrum of $f(\mathbf{x})$ is then defined as

$$P_f(\mathbf{k}) = A|f_{\mathbf{k}}|^2 \tag{3.10}$$

where A is some normalization constant.

We can see the Fourier transform as a decomposition of the field $f(\mathbf{x})$ into orthonormal modes $\mathbf{k}$. The power spectrum quantifies then how "strong" is the contribution of the Fourier mode $\mathbf{k}$ to the construction of the field.

In our case, we will be particularly interested in the power spectrum for the density contrast field $\delta(\mathbf{x})$. The Fourier transform is

$$\delta_{\mathbf{k}} = \frac{1}{V}\int \delta(\mathbf{x}) e^{-i\mathbf{k}\cdot\mathbf{x}} dV \tag{3.11}$$

and the power spectrum is defined as

$$P(\mathbf{k}) = V|\delta_{\mathbf{k}}|^2 = V\delta_{\mathbf{k}}\delta^*_{\mathbf{k}}. \tag{3.12}$$

We have straightforward

$$P(\mathbf{k}) = \frac{1}{V}\int \delta(\mathbf{x})\delta(\mathbf{y}) e^{-i\mathbf{k}\cdot(\mathbf{x}-\mathbf{y})} dV_x dV_y \tag{3.13}$$

and, setting $\mathbf{r} = \mathbf{x} - \mathbf{y}$, we get

$$P(\mathbf{k}) = \int \xi(\mathbf{r}) e^{-i\mathbf{k}\cdot\mathbf{r}} dV \tag{3.14}$$

that is, the power spectrum is the Fourier transform of the correlation function. This result is known as *Wiener-Khinchin theorem*. Of course, also the converse property holds:

$$\xi(\mathbf{r}) = \frac{1}{(2\pi)^3}\int P(\mathbf{k}) e^{i\mathbf{k}\cdot\mathbf{r}} d^3k. \tag{3.15}$$

This means that the statistical descriptions of a random field through the correlation function and through the power spectrum are essentially equivalent.

The power spectrum of the density contrast is a fundamental quantity in Cosmology. The matter density contrast field is assumed to be traced by the galaxies, which therefore form a discrete sampling of the field. However, the only way to get information about the field is to study this discrete sample; furthermore, the observations can be made only in a limited volume.

We then have to select the sampling galaxies in some way, and this can be made by means of a *window function* $W(\mathbf{x})$.

Given a collection of N dimensionless particles of unitary masses at positions $\mathbf{x}_i$, the simplest way to select a sample for the underlying field is to take all particles inside a given region of volume V, and no particles outside that region. This selection can be made through a so-called *top-hat window function*, which is a constant inside the survey volume, and zero outside. If we choose the normalization to be

$$\int W(\mathbf{x}) dV = 1 \tag{3.16}$$

then we have that the top-hat window function in real space is given by $W(\mathbf{x}) = 1/V$ inside the survey volume and zero elsewhere.

The density contrast field for a specific sample is then given by

$$\delta_{sample}(\mathbf{x}) = \delta(\mathbf{x})VW(\mathbf{x}). \tag{3.17}$$

Now, if we want to calculate the power spectrum for the sample density contrast field, we have to take into account its Fourier transform. It is useful to write the density $\rho(\mathbf{x})$ as a sum of Dirac deltas $\rho(\mathbf{x}) = \sum_i \delta_D(\mathbf{x}-\mathbf{x}_i)$, so that we can write:

$$\delta_{sample}(\mathbf{x}) = \left(\frac{\rho(\mathbf{x})}{\rho_0} - 1\right) VW(\mathbf{x}) = \frac{V}{N}\sum_i w_i \delta_D(\mathbf{x}-\mathbf{x}_i) - VW(\mathbf{x}) \tag{3.18}$$

where $w_i = VW(\mathbf{x}_i)$ and $\rho_0 = N/V$. The Fourier transform is

$$\delta_{\mathbf{k}} = \frac{1}{V}\int \left(\frac{V}{N}\sum_i w_i \delta_D(\mathbf{x}-\mathbf{x}_i) - VW(\mathbf{x})\right) e^{-i\mathbf{k}\cdot\mathbf{x}} dV = \frac{1}{N}\sum_i w_i e^{-i\mathbf{k}\cdot\mathbf{x}_i} - W_k \tag{3.19}$$

where we have introduced the Fourier space window function

$$W_k = \int W(\mathbf{x}) e^{-i\mathbf{k}\cdot\mathbf{x}} dV \tag{3.20}$$

with the normalization condition $W_0 = 1$.

It is very common to choose a spherical volume for the survey. The *spherical top-hat function* for a volume V of radius R is

$$\begin{cases} W(x) = 1/V, & x \in V \\ W(x) = 0, & x \notin V \end{cases} \tag{3.21}$$

The corresponding spherical top-hat function in the momentum space is then

$$W_k = \frac{3}{R^3}\int_0^R \frac{r\sin(kr)}{k} dr = \frac{3(\sin(kR) - kR\cos(kR))}{(kR)^3} \tag{3.22}$$

Now, averaging and squaring $\delta_{\mathbf{k}}$ given by equation (3.19), we should get the power spectrum for the density contrast field $\delta_{sample}(\mathbf{x})$ in the particular chosen sample. However, this can be split in two components: the "true" power spectrum $P(\mathbf{k})$ and the noise contribution P_n, given by the $i = j$ terms in equation (3.19), which corresponds to the power spectrum for a distribution with no intrinsic correlation, that is, for a Poissonian distribution. As a matter of fact, we have:

$$V\langle \delta_{\mathbf{k}} \delta_{\mathbf{k}}^* \rangle \equiv \left\langle \Delta^2(\mathbf{k}) \right\rangle = P(\mathbf{k}) + P_n \tag{3.23}$$

with

$$P(\mathbf{k}) = \frac{V}{N^2}\sum_{i\neq j}\left\langle w_i w_j\right\rangle e^{-i\mathbf{k}\cdot(\mathbf{x_i}-\mathbf{x_j})} - VW_k^2 \tag{3.24}$$

$$P_n = \frac{V}{N^2}\sum_i w_i^2 = \frac{V}{N}. \tag{3.25}$$

The noise becomes negligible for large densities; however, this is not always true, and it may be necessary to subtract the noise from $\left\langle \Delta^2(\mathbf{k})\right\rangle$ to obtain the "true" power spectrum.

The power spectrum is usually normalized by quoting the quantity σ_8, defined as

$$\sigma_8^2 = \frac{1}{2\pi}\int P(k)W_8^2(k)k^2dk \tag{3.26}$$

where $W_8(k)$ is the spherical window function (3.22) for a radius of 8 h^{-1}Mpc.

3.3 Velocity field

The mass power spectrum can be studied by analyzing the peculiar motion of the galaxies. In fact, a more clustered distribution of matter will induce stronger peculiar velocities. The velocity field will depend on the total mass distribution, therefore also from the invisible massive components.

Taking the Fourier transform of the perturbed continuity equation for non-relativistic matter (2.58), considering that $\theta = \nabla_i v^i$, we obtain

$$\delta_k' = -ik_i v^i. \tag{3.27}$$

We assume that the velocity field v can be represented by the galaxy velocity field v_g, thus there is no bias. This statement is based on the fact that the gravitational field under which matter moves is the same for galaxies and for dark matter, on the universality of gravitational interaction and on the assumption of similar initial conditions and same equation of state and sound speed for all matter components.

From equation (2.50) with $w = c_s = 0$ we have

$$(v^i)' = -\mathscr{H}v^i + ik^i\Phi_k. \tag{3.28}$$

Since we are dealing with scalar perturbations, we can write the velocity as the gradient of a velocity potential v, that is, in Fourier space, $v^i = ik^i v$. Therefore, v^i is parallel to k^i and we can look for solutions of equation (3.27) in the form $v^i = F(k,a)k^i$. By solving (3.27), we obtain the relation between the peculiar velocity field and the density fluctuation in linear perturbation regime:

$$v^i = i\mathscr{H}f\delta_k\frac{k^i}{k^2} \tag{3.29}$$

where $f = f(a)$ is the *growth rate* of matter perturbations:

$$f = \frac{d\ln\delta_m}{d\ln a} \simeq \Omega_m(a)^\gamma \tag{3.30}$$

with $\gamma = 0.545$ for the ΛCDM model.

At present epoch, equation (3.29) yields:

$$v = iH_0 f \delta_k \frac{k}{k^2} \tag{3.31}$$

and the peculiar velocity $v(r)$ at position r can be obtained via Fourier antitransformation:

$$v(x) = iH_0 f \frac{V}{(2\pi)^3} \int \delta_k \frac{k}{k^2} e^{i\mathbf{k}\cdot\mathbf{r}} d^3k \tag{3.32}$$

3.4 Redshift distortions

The distances of the observed galaxies are usually measured through their redshift; but the measured redshift contains a contribution due to the peculiar velocity of the galaxies, so that the distances of the galaxies are affected by an error. On small scales (i.e. in the cluster cores), the peculiar velocity of a galaxy has a random orientation and the error in the distance is statistical: we have the so-called fingers-of-god effect, that is, galaxies in a cluster get an additional random velocity that distorts the cluster distribution in the redshift map, so that it appears elongated along the line of sight. Instead, on large scales the galaxies tend to fall towards more dense regions because of gravitational attraction, and the velocity field is then coupled to the density field. We can account for this effect and correct it. Let us see in particular what are the consequences of this correction on the density contrast and on the power spectrum.

Given a peculiar velocity $\mathbf{v}$ of a source at a position $\mathbf{r}$, the line-of-sight component of the velocity can be defined as:

$$u(r) = \mathbf{v} \cdot \frac{\mathbf{r}}{r} \tag{3.33}$$

with $r = |\mathbf{r}|$. The coordinate transformation that connects the real space (r) with the redshift space (s) is given by

$$\mathbf{s} = \mathbf{r}\left[1 + \frac{u(r) - u(0)}{r}\right]. \tag{3.34}$$

The following relation holds between the volume elements and the number densities in the two spaces:

$$n(r)dV_r = n(s)dV_s \tag{3.35}$$

and we can express the volume element dV_s in terms of the r coordinates:

$$dV_s = \left(1+\frac{\Delta u(r)}{r}\right)^2 |J|(r^2\sin\theta)drd\theta d\phi = \left(1+\frac{\Delta u(r)}{r}\right)^2 |J|dV_r \tag{3.36}$$

where $\Delta u(r) = u(r) - u(0)$ and $|J|$ is the Jacobian of the transformation:

$$|J| = \left|\frac{\partial s}{\partial r}\right| = 1+\frac{du}{dr}. \tag{3.37}$$

We can then get an expression for the density contrast in the redshift space as a function of the quantities in real space

$$\delta_s = \frac{n(s)dV_s}{n_0 dV_s} - 1 = \frac{n(r)dV_r}{n_0 dV_s} - 1 = \frac{n(r)}{n_0(1+\Delta u(r)/r)^2|J|} - 1 \tag{3.38}$$

which, to the first order, yields:

$$\delta_s \simeq \delta_r - 2\frac{\Delta u(r)}{r} - \frac{du}{dr}. \tag{3.39}$$

From the last expression, we see clearly that the density contrast is different in the two spaces; that is, also the correlation function and the power spectrum, measured in the redshift space, need to be corrected in order to be expressed in real space.

First of all, we have to take into account the fact that what we observe is the galaxy density contrast δ_g, which is not the total matter density contrast δ_m. We can assume them to be related by a linear bias factor b:

$$b = \frac{\delta_g}{\delta_m} \tag{3.40}$$

and we can replace $\delta_k f$ with $\delta_{(g)k} f/b = \delta_{(g)k}\beta$ in equation (3.31). Equation (3.32) becomes then:

$$v = iH_0\beta \int \delta_{(g)k} e^{ik\cdot r}\frac{k}{k^2}d^3k^* \tag{3.41}$$

with $d^3k^* = \frac{V}{(2\pi)^3}d^3k$.

For instance, the matter and galaxy power spectra are related by the bias factor in the following way:

$$P_g(k) = b^2 P_m(k). \tag{3.42}$$

Now we want to obtain a relation between the power spectrum in redshift space and the one in the real space, that is, we want to quantify the redshift distortion effect.

Using equation (3.41), we can get an expression for the line-of-sight component $u(r)$ that appears in equation (3.39):

$$u(r) = i\beta \int \delta_{rk} e^{ik\cdot r}\frac{k\cdot r}{k^2 r}d^3k^* \tag{3.43}$$

and for its derivative:

$$\frac{du}{dr} = -\beta \int \delta_{rk} e^{ik\cdot r} \left(\frac{k\cdot r}{kr}\right)^2 d^3k^* \tag{3.44}$$

Equation (3.39) becomes then:

$$\delta_s = \delta_r - \frac{du}{dr} = \delta_r + \beta \int \delta_{rk} e^{ik\cdot r} \left(\frac{k\cdot r}{kr}\right)^2 d^3k^* \tag{3.45}$$

Multiplying by $V^{-1}e^{-ik'\cdot r}d^3r$ and integrating, we obtain the Fourier transform

$$\delta_{sk} = \delta_{rk} + \beta \int \delta_{rk'} I(k,k') d^3k', \tag{3.46}$$

where

$$I(k,k') = (2\pi)^{-3} \int e^{i(k'-k)\cdot r} \left(\frac{k'\cdot r}{k'r}\right)^2 d^3r. \tag{3.47}$$

The formula (3.46) simplifies in the limit of surveys with very small angular scales, that is, when the cosine

$$\mu = \frac{k\cdot r}{kr} \tag{3.48}$$

is almost constant. In this case, $I(k,k') = \mu^2 \delta_D(k'-k)$ and

$$\delta_{sk} = \delta_{rk}(1+\beta\mu^2). \tag{3.49}$$

We then obtain the relation between the power spectra in redshift and real space:

$$P_s(k) = V\delta_{rk}^2 \left(1+\beta\mu^2\right)^2 = P_r(k)(1+\beta\mu^2)^2. \tag{3.50}$$

Chapter 4

Dark Energy Models and the Horndeski Lagrangian

4.1 Problems of the cosmological constant

In Section 1.2 we talked about the fact that the cosmological constant does not explain the cosmic acceleration in a completely satisfactory way. Now we will describe briefly what are the issues with this approach.

4.1.1 Fine tuning problem

We can explicit the Λ term in Friedmann equations with cosmological constant (1.33), (1.34)

$$H^2 = \frac{8\pi G}{3}\rho - \frac{K}{a^2} + \frac{\Lambda}{3} \tag{4.1}$$

$$\frac{\ddot{a}}{a} = -\frac{4\pi G}{3}(\rho + 3P) + \frac{\Lambda}{3} \tag{4.2}$$

and see that, in order to have a cosmic acceleration at present time, the cosmological constant has to be of the order of the square of the present Hubble parameter H_0:

$$\Lambda \approx H_0^2 = (2.1332h \times 10^{-42} GeV)^2. \tag{4.3}$$

We can interpret Λ as an energy density. This energy density is equivalent to:

$$\rho_\Lambda \approx \frac{\Lambda m_{pl}^2}{8\pi} \approx 10^{-47} GeV^4 \approx 10^{-123} m_{pl}^4, \tag{4.4}$$

where $h \approx 0.7$ and $m_{pl} \approx 10^{19} GeV$.

The most reasonable thing to do would be to associate Λ to the energy density of the vacuum. From Field Theory, the zero-point energy of a field of mass m, momentum k and frequency ω, in the units $\hbar = c = 1$ is $E = \omega/2 = \sqrt{k^2+m^2}/2$. The vacuum energy density can be obtained by summing over the zero-point energies up to a cut-off scale k_{max}:

$$\rho_{vac} = \int_0^{k_{max}} \frac{d^3k}{(2\pi)^3} \frac{1}{2} \sqrt{k^2+m^2}, \tag{4.5}$$

whose dominating contribution is given by the large k modes; that is,

$$\rho_{vac} \approx \frac{k_{max}^4}{16\pi^2}. \tag{4.6}$$

We can set $k_{max} \approx m_{pl}$, since General Relativity is believed to be valid up to the Planck scale. We then have

$$\rho_{vac} \approx 10^{74} GeV^4. \tag{4.7}$$

Comparing the results (4.4) and (4.7), we can see that they differ by a factor of 10^{121}, which is enormously large: the Λ value must be incredibly smaller than the value predicted from the theory. On the other hand, it cannot be exactly zero, because in this case we would not have the cosmic acceleration. This is the so-called fine tuning problem.

In principle, there are two possible ways to solve this problem. The first one is to find a way to get a very tiny value of Λ: in this case the explanation of dark energy as cosmological constant would be still valid. The other way would be to find a mechanism that makes Λ completely vanish: in this case, the fine tuning problem is solved, but an alternative explanation for dark energy must be provided.

4.1.2 Coincidence problem

The second problem concerning the cosmological constant is the fact that Λ starts to have an effect on the expansion of the Universe at a time which is very close to the present (i.e. the cosmic acceleration starts very late), and the value of the density parameter $\Omega_\Lambda^{(0)}$ is of the same order of magnitude as the matter density parameter $\Omega_m^{(0)}$.

The matter density $\rho_m = \rho_m^{(0)}(1+z)^3$ coincides with the cosmological density $\rho_\Lambda^{(0)}$ at

$$z_{coinc} = \left(\frac{\Omega_\Lambda^{(0)}}{1-\Omega_\Lambda^{(0)}} \right)^{1/3} - 1, \tag{4.8}$$

that is, $z_{coinc} \approx 0.3$ for $\Omega_\Lambda^{(0)} \approx 0.7$. In fact, the question arises, why Λ becomes important right now, when we can see its effects. This is the so called coincidence problem.

However, this problem is not specific to the cosmological constant: almost all dark energy models have a z_{coinc} very close to zero. Many explanations have been proposed, but it is still far from solved.

4.2 Overview on alternative dark energy models

We can imagine to find a way to make Λ completely vanish, but then we have to find an alternative model to explain the cosmic acceleration. All alternative dark energy models that have been proposed are in this framework.

There are essentially two approaches to construct a dark energy model. The first approach is to modify the right-hand side of the Einstein equations (1.1), so that the energy-momentum tensor $T_{\mu\nu}$ contains an exotic term with negative pressure. Models based on this approach are called *modified matter models*.

The second approach is the one of the *modified gravity models*, in which the Einstein tensor $G_{\mu\nu}$ on the left-hand side is modified.

This is, however, only a practical division to classify models; there is no real fundamental difference between the two categories of models, since every modified matter model can be transformed in an equivalent modified gravity model and viceversa (i.e. the modifications in $T_{\mu\nu}$can be absorbed in $G_{\mu\nu}$ or the other way round).

In this section we will give a general overview of the most popular dark energy models, without entering the details.

4.2.1 Modified matter models

We know from General Relativity that the Einstein field equations (1.1) can be obtained by applying the principle of least action to the following Einstein-Hilbert action:

$$S = \int d^4x\sqrt{-g}\frac{1}{2\kappa^2}R + S_m, \tag{4.9}$$

where $\kappa^2 = 8\pi G$, g is the determinant of the metric tensor and R is the Ricci scalar. A certain matter action $S_m = \int d^4x\mathscr{L}_m$ has been included.

We can then obtain a modified model by modifying the Einstein-Hilbert action. For example, the cosmological constant can be obtained from the modified action

$$S = \int d^4x\sqrt{-g}\frac{1}{2\kappa^2}(R - 2\Lambda) + S_m. \tag{4.10}$$

Depending on how we modify the action (4.9), we can have a different dark energy model.

Quintessence We introduce a scalar field ϕ which interacts with all other components only through standard gravity. This model is described by the action

$$S = \int d^4x\sqrt{-g}\left[\frac{1}{2\kappa^2}R + \mathscr{L}_\phi\right] + S_m, \tag{4.11}$$

where $\mathscr{L}_\phi = -\frac{1}{2}g^{\mu\nu}\partial_\mu\phi\partial_\nu\phi - V(\phi)$ is the Lagrangian density of the scalar field ϕ.

k-essence In this class of models a scalar field ϕ with non-canonical kinetic terms is introduced; the general form of the action is then

$$S = \int d^4x\sqrt{-g}\left[\frac{1}{2\kappa^2}R + P(\phi,X)\right] + S_m, \tag{4.12}$$

where $P(\phi,X)$ is a function of the scalar field and its kinetic energy $X = -(1/2)\partial_\mu\phi\partial_\nu\phi$. The cosmic acceleration can be realized by the kinetic energy of the field.

If $P(\phi,X) = -X - V(\phi)$, the field having a negative kinetic energy, then it can be shown that this gives rise to a value $w < -1$ for the equation of state. In this case we talk about *phantom* models.

Quintessence and k-essence models can have *scaling solutions* when the ratio of the field density ρ_ϕ to the matter density ρ_m and the field equation of state w_ϕ are non-zero constants: $\rho_\phi/\rho_m = constant$ and $w_\phi = constant$.

Coupled dark energy These models suppose that a coupling exists between non-relativistic matter and dark energy; this is based on the fact that the energy density for dark energy today is the same order of magnitude as that of dark matter.

For example, one could consider a quintessence field ϕ coupled to dark matter. An interaction term $\mathscr{L}_{int}$ must then be added to the Lagrangian density of the field ϕ appearing in the action (4.11).

$$\mathscr{L}_\phi = -\frac{1}{2}g^{\mu\nu}\partial_\mu\phi\partial_\nu\phi - V(\phi) - \mathscr{L}_{int}. \tag{4.13}$$

Chamaeleon scalar fields This model is based on a coupled quintessence field whose effective mass depends on the environment it is in. The action is similar to (4.11):

$$S = \int d^4x\sqrt{-g}\left[\frac{1}{2\kappa^2}R + -\frac{1}{2}g^{\mu\nu}\partial_\mu\phi\partial_\nu\phi - V(\phi)\right] - \int d^4x\mathscr{L}_m(g^{(i)}_{\mu\nu},\Psi^{(i)}_m), \tag{4.14}$$

where $\mathscr{L}_m$ is the matter Lagrangian and the $\Psi^{(i)}_m$ are the matter fields coupled to a metric $g^{(i)}_{\mu\nu} = e^{2Q_i\phi}g_{\mu\nu}$, Q_i being the strengths of the couplings for each matter component with the field ϕ.

Unified models of dark energy and dark matter These models use a single fluid or a single scalar field in order to unify dark matter and dark energy in a single entity. For example, the Chaplygin gas is a unified fluid model, while unified models using a single scalar field can be build from k-essence.

4.2.2 Modified gravity models

Here we propose a quick overview on modified gravity models. Scalar-tensor theories will play a role in the continuation.

$f(R)$ gravity One of the simplest modified gravity models is the so-called $f(R)$ gravity, in which some general function $f(R)$ of the Ricci scalar appears in the 4-dimensional action:

$$S = \int d^4x\sqrt{-g}\frac{1}{2\kappa^2}f(R) + S_m(g_{\mu\nu,}\Psi_m). \tag{4.15}$$

Notice that the constant G which appears in κ is a bare gravitational constant; the observed value will be different in general.

Scalar-tensor theories This general category of models is one of the most studied alternatives to General Relativity, and has been investigated a lot in order to generalize the cosmological constant and to explain the fine-tuning and coincidence problems. They link the gravitational constant to a cosmic field φ, that is, they add a degree of freedom to the gravitational tensor field.

The action for scalar-tensor theories is given by

$$S = \int d^4x\sqrt{-g}\left[\frac{1}{2}f(\varphi,R) - \frac{1}{2}\zeta(\varphi)(\nabla\varphi)^2\right] + S_m(g_{\mu\nu},\Psi_m), \tag{4.16}$$

where f is a general function of the scalar field φ and the Ricci scalar R, and ζ is a function of φ. We have set $\kappa^2 = 1$ for simplicity.

Scalar-tensor theories include $f(R)$ gravity as a particular case, and also Brans-Dicke theory and dilaton gravity.

Gauss-Bonnet theories In this models, gravity is modified with a combination of Ricci and Riemann tensors that keeps the equations at second order in the metric, avoiding instabilities. The action is given by (with $\kappa^2 = 1$)

$$S = \int d^4x\sqrt{-g}\left[\frac{1}{2}R - \frac{1}{2}(\nabla\phi)^2 - V(\phi) - f(\phi)R^2_{GB}\right] + S_m(g_{\mu\nu},\Psi_m), \tag{4.17}$$

where R_{GB} is the Gauss-Bonnet term

$$R^2_{GB} \equiv R^2 - 4R_{\mu\nu}R^{\mu\nu} + R_{\mu\nu\alpha\beta}R^{\mu\nu\alpha\beta}. \tag{4.18}$$

Braneworld models of dark energy These models are based on superstring and M-theory; extra dimensions are compactified on some manifolds in order to obtain 4-dimensional effective gravity theories. Examples are Kaluza-Klein theories, Ramdall-Sundrum model and Dvali-Gabadadze-Porrati (DGP) model.

4.3 Horndeski Lagrangian and observational constraints

The most general scalar-tensor theories keeping the field equations of motion at second order, and therefore avoiding instabilities, are described by the Horndeski Lagrangian [3].

It has been shown to be equivalent to the following one [9]:

$$\mathscr{L} = \sum_{i=2}^{5} \mathscr{L}_i, \tag{4.19}$$

where

$$\mathscr{L}_2 = K(\phi, X), \tag{4.20}$$

$$\mathscr{L}_3 = -G_3(\phi, X)\Box\phi, \tag{4.21}$$

$$\mathscr{L}_4 = G_4(\phi, X)R + G_{4,X}\left[(\Box\phi)^2 - (\nabla_\mu\nabla_\nu\phi)(\nabla^\mu\nabla^\nu\phi)\right] \tag{4.22}$$

$$\mathscr{L}_5 = G_5(\phi, X)G_{\mu\nu}(\nabla^\mu\nabla^\nu\phi) - \frac{1}{6}G_{5,X}\left[(\Box\phi)^3 - 3(\Box\phi)(\nabla_\mu\nabla_\nu\phi)(\nabla^\mu\nabla^\nu\phi) + 2(\nabla^\mu\nabla_\alpha\phi)(\nabla^\alpha\nabla_\beta\phi)(\nabla^\beta\nabla_\mu\phi)\right]. \tag{4.23}$$

K and G_i $(i = 3,4,5)$ are functions of the scalar field ϕ and its kinetic energy $X = -\partial^\mu\phi\partial_\mu\phi/2$, with the partial derivatives $G_{i,X} \equiv \partial G_i/\partial X$.

Up to now, we have described the different theoretical dark energy models that have been proposed. In dark energy research it is very important to collect data from observations, in order to constrain the models and rule out those which do not match with the observations. In the next chapters we will talk about the statistic methods (Fisher matrix formalism) that allow us to turn the errors on observed quantities in errors and constraints on theoretical parameters, i.e. the Horndeski Lagrangian functions or combinations of them. This methods will be applied in the case of the ESA *Euclid* survey, and we will perform a forecast for a specific parameter.

Chapter 5

ESA *Euclid* Mission and Fisher Matrix Formalism

5.1 ESA *Euclid* mission: a dark energy survey

As we stated at the end of the last chapter, it is important to obtain more and more precise data from observations in order to put stronger constraints on cosmological models. To this purpose, the European Space Agency (ESA) has planned a mission with the goal to investigate the nature of the dark Universe (which includes dark matter and dark energy), and possibly understand the cause of the late-time cosmic acceleration. This mission is called *Euclid* from the name of the Greek mathematician who is regarded as the father of geometry.

The mission, with launch scheduled for 2020, will spend six years mapping the large-scale structure of the Universe for a region of 15000 deg^2 [10], equivalent to more than one-third of the sky (the star-dominated regions in the Milky Way must be excluded). This wide survey will be complemented by two 20 deg^2 deep surveys.

About two billion galaxies will be observed, up to redshift $z \sim 2$, so that the late-time cosmic acceleration period is completely covered. The number of observed galaxies per square arcminute is supposed to be $n_{g,arcmin} = 30$ ([11], p. 84).

The Euclid survey is based on essentially two probes:

1. weak gravitational lensing;
2. galaxy clustering,

Weak lensing is a technique which allows us to get information on dark energy and to map dark matter by

measuring the apparent distortion of galaxy images due to mass inhomogeneities along the line-of-sight. The galaxy clustering probe is based on accurate measurements of redshifts and distances of galaxies, in order to measure the baryon acoustic oscillations (BAO), a wiggle pattern in the clustering of galaxies which can be used as a standard ruler to measure the expansion of the Universe, and to obtain information on the statistical properties of the galaxy field, such as the galaxy correlation function and the galaxy power spectrum described in Chapter 3. Both of the probes will be described with more details in the next sections.

Weak lensing requires high-quality images to perform accurate measurements of the weak lensing galaxy shear, and photometry at visible and infrared wavelengths in order to measure the distances of each lensed galaxy out to redshift $z \geq 2$. The galaxy clustering probe requires accurate measurements of spectroscopic redshifts for galaxies out to $z \geq 0.7$. Therefore, the Euclid payload consists of a 1.2 m Korsch telescope, designed to provide a large field of view, with two main instruments: a visual imager (VIS) and a near-infrared spectrometer and interferometer (NISP). The VIS provides high-quality images for the weak lensing probe; the NISP is designed to measure both spectroscopic and photometric redshifts. The photometric redshift for each of the galaxies used for the weak lensing probe will reach a precision of $\sigma_z/(1+z) \lesssim 0.05$; the redshift accuracy for each galaxy in the galaxy clustering probe will be given by $\sigma_z/(1+z) \lesssim 0.001$ [10].

Euclid will use weak lensing and galaxy clustering to put constraints on the dark energy equation of state, but it will not only explore dark energy: in fact, it will test all sectors of the cosmological model. For example, it will map the dark matter distribution with a very high accuracy, and also deviations from Gaussianity of initial perturbations will be measured with great precision, allowing to test a number of inflation models.

5.2 Galaxy clustering

Galaxies are not randomly distributed in the Universe: by observing the large-scale structure we can see that some regions are more dense than others. From the large scale structure of the Universe we can obtain some information about dark energy. The key observable is the galaxy power spectrum; therefore we will employ the concepts exposed in Chapter 3.

5.2.1 Matter power spectrum

We know that galaxies have started to form from the perturbations of pressureless matter after the radiation-matter equality, when the gravitational attraction became stronger than the pressure repulsion. In order to quantify the matter distribution, we can measure the correlation function or the power spectrum of the galaxies. But in order to derive the power spectrum of matter perturbations today, we need to know the evolution of the gravitational potential $\Phi(k,t)$ from the early Universe (after inflation) to present time.

During inflation the quantum fluctuations of a scalar field with a potential generate nearly scale-invariant density perturbations (which means that $P_\Phi^{(i)} \propto k^0 = const$). That is, inflation sets up initial conditions for the

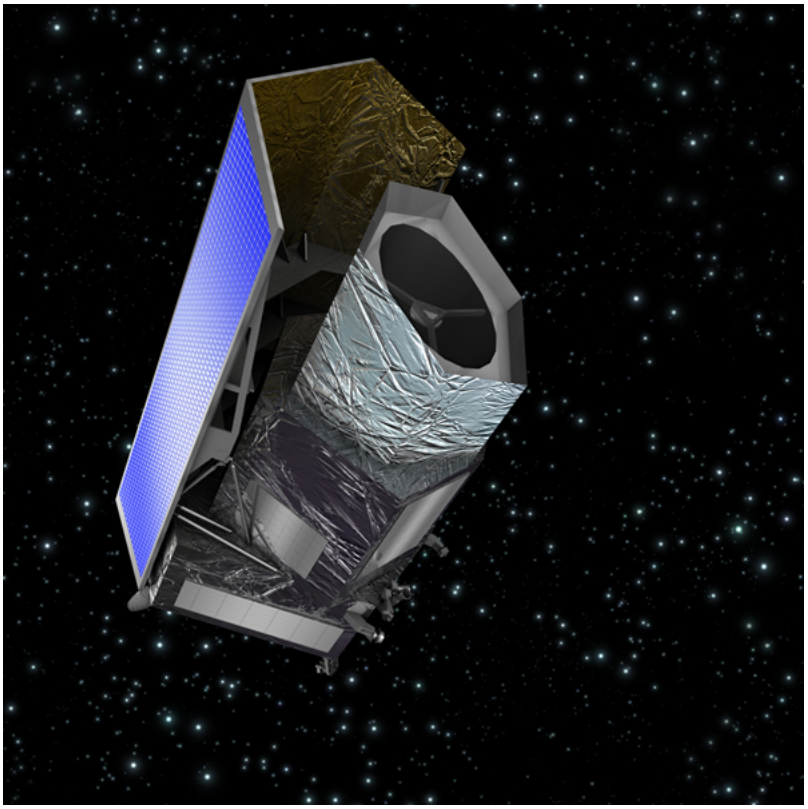

Figure 5.1: A reconstruction of how the Euclid satellite will appear in space after its launch.

gravitational potential; in particular, the initial power spectrum for Φ generated during inflation is

$$P_\Phi^{(i)} = \left\langle |\Phi(k,a_i)|^2 \right\rangle = \frac{50\pi^2}{9k^3} \left(\frac{k}{H_0}\right)^{n_s-1} \delta_H^2 \tag{5.1}$$

where n_s is the spectral index and δ_H^2 is the amplitude of the gravitational potential. The value $n_s = 1$ corresponds to the scale-invariant spectrum with $k^3 \left\langle |\Phi(k,a_i)|^2 \right\rangle = constant$.

In order to obtain the gravitational potential today, we have to solve the equation for $\Phi(k,t)$ from the radiation era to the present. The evolution of Φ depends on the scale k; we will analyse in the following what happens at small scales and large scales. The wavenumber k_{eq} that characterizes the border between small and large scales represents the scale that entered the Hubble radius at the radiation-matter equality: $k_{eq} = a_{eq}H(a_{eq})$.

From $H(a_{eq})/H_0 = \left(2\Omega_m^{(0)}/a_{eq}^3\right)^{1/2}$ we have:

$$k_{eq} = H_0\sqrt{\frac{2\Omega_m^{(0)}}{a_{eq}}} = 0.073\Omega_m^{(0)}h^2 Mpc^{-1}. \tag{5.2}$$

First, we will deal with large scales: $k \ll k_{eq}$. From equation (2.55), we had that in a single-fluid model Φ is constant; that is, in both the radiation and the matter era Φ remains nearly constant. We can verify this for the radiation era by solving equation (2.52) for $c_s^2 \simeq 1/3$, $\mathscr{H}' \simeq -\mathscr{H}^2$and $\mathscr{H} \simeq 1/\eta$:

$$\Phi'' + \frac{4}{\eta}\Phi' + \frac{k^2}{3}\Phi = 0. \tag{5.3}$$

The solution for initial conditions $\Phi = \Phi_I$ and $d\Phi/d\eta = 0$ at $\eta = 0$ is

$$\Phi(k,\eta) = 3\Phi_I \frac{\sin(k\eta/\sqrt{3}) - (k\eta/\sqrt{3})\cos(k\eta/\sqrt{3})}{(k\eta/\sqrt{3})^3} \tag{5.4}$$

and we have, for large scales ($k\eta \ll 1$), $\Phi(k,\eta) \simeq \Phi_I\left[1 - (k\eta)^2/10\right]$, that is,$\Phi$ is nearly constant. Notice that equation (5.4) is also valid for small scales, since it comes from (2.52).

We still have to find out how Φ evolves in the transition between the two eras.

In order to take into account the effects of the collisions between baryons and photons, one can treat them as imperfect fluids (see for details [5], section 4.9); the collisions are described by the Boltzmann equation:

$$\frac{df}{dt} = C[f] \tag{5.5}$$

where f is the distribution function and $C[f]$ describes a collision term.

By solving the Einstein equation for the (00) component (2.45) together with the perturbation equation (2.49) and the Boltzmann equation (5.5) in the super-horizon approximation $k \ll \mathscr{H}$, with the initial conditions $\Phi_i = \Phi(0)$ and $(d\Phi/dy)_i = 0$ we obtain

$$\Phi(y) = \Phi(0)\frac{9y^3 + 2y^2 - 8y - 16 + 16\sqrt{y+1}}{10y^3} \tag{5.6}$$

with $y = a/a_{eq}$. We notice that, for $y \to \infty$, the gravitational potential approaches $\Phi \to (9/10)\Phi(0)$: for super-horizon perturbations, the gravitational potential decreases by 10% during the radiation-matter transition.

Now let us discuss the behavior for small scales $k \gg k_{eq}$. These modes crossed inside the Hubble radius before the radiation-matter equality, and started to decay after the Hubble radius crossing. Since we are considering the radiation era, we can use equation (5.4) and we see that for $k\eta \gg 1$ the gravitational potential Φ decreases as $1/(k\eta)^2$ with oscillations. The larger the wavenumber k is, the earlier this decay started. So we can say that the amplitude of the gravitational potential is suppressed for perturbations on smaller scales. After the Universe enters the matter era, the amplitude of Φ approaches a constant value.

We have shown that the evolution of the gravitational potential depends on the scales of perturbations. In order to describe the evolution of Φ for each wavenumber k during the transition from the radiation era to the epoch at $a = a_T$, we introduce the *transfer function*:

$$T(k) = \frac{\Phi(k, a_T)}{\Phi_{LS}(k, a_T)}, \tag{5.7}$$

where $\Phi_{LS}(k, a_T)$ is the large-scale solution, decreased by an amount 9/10 compared to the primordial value $\Phi(k, a_i)$ generated from inflation:

$$\Phi_{LS}(k, a_T) = \frac{9}{10}\Phi(k, a_i). \tag{5.8}$$

The typical value for a_T is 0.03; for $a > a_T$ (during the matter era) the evolution becomes independent of k, as already said.

In general, the transfer function has to be derived numerically. Bardeen, Bond, Kaiser and Szalay (BBKS) provided a very popular fit of it [13]:

$$T(x) = \frac{\ln(1+0.171x)}{0.171x}\left[1 + 0.284x + (1.18x)^2 + (0.399x)^3 + (0.490x)^4\right]^{-1/4} \tag{5.9}$$

where $x = k/k_{eq}$.

The BBKS transfer function (5.9) reproduces the behavior for large and small scales that we have exposed before: for large scales ($x \ll 1$) we have $T(x) \simeq 1$, that is, $\Phi(k, a_T) = \frac{9}{10}\Phi(k, a_i)$ as expected. For small scales ($x \gg 1$) the transfer function behaves like $T(x) \propto (\ln k)/k^2$, and the gravitational potential $\Phi(k, a_T)$ is suppressed for increasing k.

During the matter-dominated era, $\Phi \simeq constant$. But when the late-time cosmic acceleration starts, the potential Φ is expected to vary again. We introduce the *growth function* $D(a)$ in order to quantify this variation:

$$\frac{\Phi(a)}{\Phi(a_T)} \equiv \frac{D(a)}{a} \tag{5.10}$$

where $a > a_T$.

Combining equations (5.7), (5.8) and (5.10) yields the following expression for the gravitational potential at present time (with $a_0 = 1$):

$$\Phi(k, a_0) = \frac{9}{10}\Phi(k, a_i)T(k)D(a_0). \tag{5.11}$$

Now we can proceed to calculate the matter power spectrum today. If we ignore the dark energy perturbations with respect to the matter perturbations, we have that the (00) component of Einstein equations (2.45) in the sub-horizon approximation $k \ll \mathscr{H}$ reduces to

$$k^2\Phi = 4\pi G a^2 \rho_m \delta_m \tag{5.12}$$

and using the relations $\rho_m = \rho_m^{(0)}/a^3$ and $\Omega_m^{(0)} = 8\pi G\rho_m^{(0)}/(3H_0^2)$, we get the following expression for the matter perturbation δ_m:

$$\delta_m(k, a) = \frac{2k^2 a}{3\Omega_m^{(0)} H_0^2}\Phi(k, a). \tag{5.13}$$

From equations (5.1), (5.11), (5.13) we finally have the expression for the matter power spectrum at present time:

$$P_{\delta_m} \equiv \left\langle |\delta_m(k, a_0)|^2 \right\rangle = \frac{2\pi^2 \delta_H^2}{\left(\Omega_m^{(0)}\right)^2}\left(\frac{k}{H_0}\right)^{n_s} T^2(k)D^2(a_0)H_0^{-3}. \tag{5.14}$$

On large scales, the matter power spectrum behaves as $P_{\delta_m} \propto k^{n_s}$, while on small scales $P_{\delta_m} \propto k^{n_s-4}(\ln k)^2$. This means the power spectrum has a peak for $k = k_{eq}$.

5.2.2 Relation between observed and theoretical power spectra

What we want to achieve is to extract information about the cosmology from the power spectrum. The first step to do is to estabilish which relation exists between the real data and the (theoretical) present matter power spectrum (5.14). Then we will see how to translate the information on P_{δ_m} into constraints for the cosmological parameters, by means of the Fisher matrix formalism.

Let us start with the first step. First of all, we have to remark that the cosmological model influences the spectrum in many ways: for example, it affects the wavenumbers k and the volume V in which the spectrum is calculated. What we actually observe is angles and redshifts concerning the various galaxies. In order to

obtain a power spectrum from real data, we need to assume a reference cosmology so that we can convert the angles and redshifts into distances or wave vectors.

It can be found that the wavenumber modulus k and the direction cosine $\mu = k \cdot \hat{r}/k$ in the reference and in a generic cosmology are related by [5]

$$k = Qk_r, \tag{5.15}$$

$$\mu = \frac{H\mu_r}{H_r Q}, \tag{5.16}$$

where the r at the pedex indicates the quantities for the reference cosmology, and

$$Q = \frac{\sqrt{H^2 d^2 \mu_r^2 - H_r^2 d_r^2 (\mu_r^2 - 1)}}{H_r d}. \tag{5.17}$$

d being the angular diameter distance (1.60).

Since the power spectrum $P(k) = V\delta_k^2$ depends on the volume V in which we measure the perturbations, we also have to calculate how the volume depends on the cosmology. The following relation is found to hold [5]:

$$V = V_r \frac{H_r d^2}{H d_r^2}. \tag{5.18}$$

The power spectrum for the true cosmology can be now converted into the power spectrum for the reference cosmology by multiplying by V_r/V and by converting k, μ into $k_{r,}\mu_r$. Hence

$$P_r(k_{r,}z) = \frac{H(z)d_r^2(z)}{H_r(z)d^2(z)} P(Rk_r, z). \tag{5.19}$$

At this point, we can find a relation between the observed galaxy power spectrum $P_{r,obs}(k_r, \mu_r; z)$ (calculated using the reference cosmology) and the theoretical matter power spectrum at present time $P(k, z = 0)$ (5.14) .We can write the spectrum at any z by multiplying the present spectrum by the growth factor squared: $P(k,z) = D^2(z)P(k,0)$, where

$$D(z) \equiv \frac{\delta_m(z)}{\delta_m(0)}. \tag{5.20}$$

Then, we can use the bias factor $b^2(z)$ from equation (3.42) to relate the galaxy power spectrum to the matter power spectrum, and finally we must introduce a factor $(1 + \beta\mu^2)^2$ in order to take into account the redshift distortion (see equation (3.50)). Collecting everything yields:

$$P_{r,obs}(k_r, \mu_r; z) = \frac{H(z)d_r^2(z)}{H_r(z)d^2(z)} D^2(z) b^2(z) \left[1 + \beta(z)\mu^2\right]^2 P(k, z = 0). \tag{5.21}$$

A note on the explicit form of the growth factor. The parameter β is defined by $\beta \equiv f/b$, and $f = \dot{\delta}_m/(H\delta_m)$ is the growth rate, which can be approximated by $f \simeq \Omega_m^\gamma(z)$, recalling equation (3.30). If we use this approximation, then the growth factor has the form

$$D(z) = \exp\left[\int_z^0 \Omega_m^\gamma(\tilde{z})\frac{d\tilde{z}}{1+\tilde{z}}\right]. \tag{5.22}$$

We can complete equation (5.21) by including the redshift error in the observed galaxy power spectrum. Since $dr = dz/H(z)$, where r is the comoving distance (1.48) with $c = a_0 = 1$, an error σ_z in redshift transforms into an error $\sigma_r = \sigma_z/H(z)$ in distance. If we suppose that the observed radial distances r are Gaussian distributed around the true distances r_0

$$f(r, r_0) = \frac{1}{\sqrt{2\pi}\sigma_r} e^{-(r-r_0)^2/(2\sigma_r^2)}, \tag{5.23}$$

then the observed correlation function is given by the convolution

$$\xi(\sigma, r_0) = \int_0^\infty \xi(\sigma, r) f(r, r_0) dr. \tag{5.24}$$

Performing a Fourier transformation, the convolution becomes a product:

$$P = P_{r,obs} e^{-k^2\mu^2\sigma_r^2} \tag{5.25}$$

so that the galaxy power spectrum with redshift correction becomes:

$$P_g(k, \mu; z) = \frac{H(z)d_r^2(z)}{H_r(z)d^2(z)} D^2(z) b^2(z) \left[1 + \beta(z)\mu^2\right]^2 P(k, z=0) e^{-k^2\mu^2\sigma_r^2}. \tag{5.26}$$

Notice that expression (5.26) relates the observed galaxy power spectrum to the cosmological parameters (i.e. $\Omega_m^{(0)}$, n_s, H_0, etc.), which are included in $P(k, z=0)$. We will see in section 5.4 how to use the galaxy power spectrum to constrain these parameters.

5.3 Weak lensing

5.3.1 Weak gravitational lensing from perturbed photon propagation

We now want to deal with the propagation of photons in a perturbed Universe. Light propagation in General Relativity is ruled by the following equations: the null condition

$$k^\mu k_\mu = 0 \tag{5.27}$$

and the geodesic equation

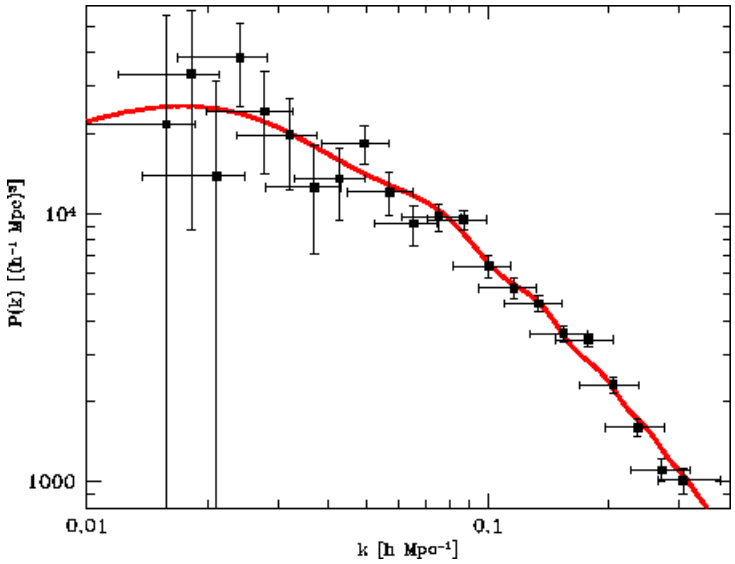

Figure 5.2: Measured power spectrum of $L*$ galaxies from SDSS data [12].

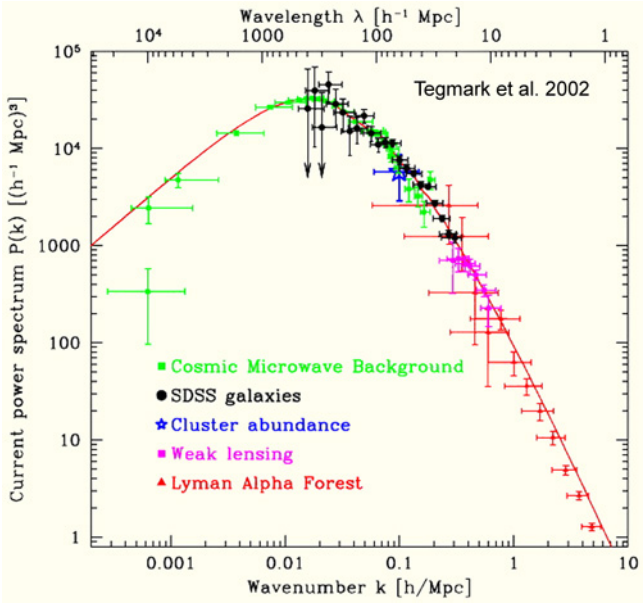

Figure 5.3: Power spectrum constraints from different surveys [12].

$$\frac{dk^\mu}{d\lambda_s} + \Gamma^\mu_{\alpha\beta} k^\alpha k^\beta = 0, \tag{5.28}$$

where λ_s is a parameter which can be always converted to the conformal time η using the $\mu = 0$ geodesic equation. Solving the two equations (5.27), (5.28) in the perturbed metric (2.12) gives the general equations of photon propagation; the solution will give the variation in the photon's frequency and path due to the inhomogeneities in the metric.

We can split the momentum vector $k^\mu = dx^\mu/d\lambda_s$ into a background and a perturbed value

$$k^\mu = \hat{k}^\mu + \delta k^\mu. \tag{5.29}$$

The geodesic equation for index $\mu = 0$ at background level gives simply

$$\frac{d\hat{k}_0}{d\lambda_s} = -2\mathscr{H}(\hat{k}_0)^2, \tag{5.30}$$

if we consider a photon propagating along direction r so that the perturbation equation in flat space is $d\eta = dr$ and use $\Gamma^0_{00} = \mathscr{H}$ for the FLRW metric with the conformal time η; this can be integrated to give

$$\hat{k}_0 = \frac{d\eta}{d\lambda_s} \propto a^{-2}. \tag{5.31}$$

This equation allows us to convert λ_s into η.

Then we can use equation (5.29) to derive the perturbed null condition and the geodesic equations at first order. It can be shown [5] that for the $\mu = 0$ geodesic equation, one has

$$\frac{d(\delta k^0/k^0)}{d\eta} = -\left(\frac{\partial\Phi}{\partial\eta} + \frac{\partial\Psi}{\partial\eta} + 2\Psi_{,r}\right), \tag{5.32}$$

while for the spatial equations for the directions $\mu = i = 1,2$ orthogonal to the propagation direction r:

$$\frac{d^2x^i}{d\lambda_s^2} + 2\mathscr{H}\frac{d\eta}{d\lambda_s}\frac{dx^i}{d\lambda_s} = \left(\frac{d\eta}{d\lambda_s}\right)^2 (\Phi_{,i} - \Psi_{,i}). \tag{5.33}$$

Equation (5.32) leads to the Sachs-Wolfe effect, that is, the change of a photon's redshift due to its passing through a gravitational potential; equation (5.33) leads to weak lensing, the deviation of a light ray passing through the same potential.

Let us discuss the second one. From equations (5.31) and (5.33), we can obtain the propagation equations for $i = 1,2$:

$$\frac{d^2x^i}{dr^2} = \psi_{,i} \tag{5.34}$$

where

$$\psi = \Phi - \Psi \tag{5.35}$$

is the *lensing potential*, which in standard General Relativity is equal to $\psi = 2\Phi = -2\Psi$. The displacement vector $x = (x_1, x_2)$ is small; then we can put $x^i = r\theta^i$, where r is the distance of the source, and write (5.34) as

$$\frac{d^2}{dr^2}(r\theta^i) = \psi_{,i}\,. \tag{5.36}$$

The light ray reaches the observer at $r = 0$ along the direction (θ_0^1, θ_0^2). Integrating the last equation yields therefore:

$$\theta^i = \theta_0^i + \frac{1}{r}\int_0^r dr'' \int_0^{r'} dr' \psi_{,i}\,(r'\theta_0^1, r'\theta_0^2, r') \tag{5.37}$$

where the integration constant has been chosen equal to θ_0^i so that the angle does not change for $\psi = 0$. The integral variables respect the following ordering: $r' < r'' < r$, $0 < r' < r$. Performing the integration in r'' yields

$$\theta^i = \theta_0^i + \int_0^r dr' \left(1 - \frac{r'}{r}\right) \psi_{,i}\,(r'\theta_0^1, r'\theta_0^2, r'). \tag{5.38}$$

Two light rays separated by a small interval Δx will then obey the equation

$$\Delta\theta^i = \Delta\theta_0^i + \Delta\theta_0^j \int_0^r dr' \left(1 - \frac{r'}{r}\right) r' \psi_{,ij}\,(r'\theta_0^1, r'\theta_0^2, r'), \tag{5.39}$$

where a term $r'\psi_{,ij}$ appears due to the variation of $\psi_{,i}$ with respect to θ_0^j $(j = 1, 2)$. If we consider a light source at $r = r_s$, we have an equation which connects the separation $\Delta\theta^i$ on the source plane (at a distance r) to the separation $\Delta\theta_0^i$ observed at $r = 0$.

We can describe this distortion effect using a symmetric matrix A_{ij}:

$$A_{ij} \equiv \frac{\partial\,\theta_s^i}{\partial\,\theta_0^j} = \delta_{ij} + D_{ij} \tag{5.40}$$

where D_{ij} is called *distortion tensor* and it is equal to

$$D_{ij} = \int_0^{r_s} dr' \left(1 - \frac{r'}{r_s}\right) r' \psi_{,ij} = \begin{pmatrix} -\kappa_{wl} - \gamma_1 & -\gamma_2 \\ -\gamma_2 & -\kappa_{wl} + \gamma_1 \end{pmatrix}. \tag{5.41}$$

The parameter

$$\kappa_{wl} \equiv -\frac{1}{2}\int_0^{r_s} dr' \left(1 - \frac{r'}{r_s}\right) r' \,(\psi_{,11} + \psi_{,22}\,) \tag{5.42}$$

is called *convergence* and describes the magnification of the source image, while the two parameters

$$\gamma_1 = -\frac{1}{2}\int_0^{r_s} dr' \left(1 - \frac{r'}{r_s}\right) r' \left(\psi_{,11} - \psi_{,22}\right) \tag{5.43}$$

$$\gamma_2 = -\int_0^{r_s} dr' \left(1 - \frac{r'}{r_s}\right) r' \psi_{,12} \tag{5.44}$$

are the two components of the *shear field* and describe the distortion of the source image.

5.3.2 Convergence power spectrum

Let us now see how to extract information on the cosmology from the weak lensing effect.

First of all, we observe that an intrinsically circular object is distorted from the weak lensing effect into an elliptical one. It can be shown [5] that the ellipticity of the object is related to the shear components γ_1, γ_2. It can be also shown that the measured ellipticity is the sum of two components: one of them is due to weak lensing, while the other one is a noise component. The power specrum of the noise component can be derived from equation (3.25) by substituting the weights w_i with the average intrinsic ellipticity γ_{int}^2; for N sources in a volume V the noise (intrinsic) power spectrum is given by

$$P_{int} = \gamma_{int}^2 \frac{V}{N} \tag{5.45}$$

with $\gamma_{int} \simeq 0.22$.

Up to now we have considered only the sources at a given comoving distance r, but we can add up all the transformation matrices for many sources at different distances. We consider a number $n(r)dr$ of sources in a shell dr with the normalization $\int_0^\infty n(r)dr = 1$. We can then write the full transformation matrix D_{ij} as

$$D_{ij} = \int_0^\infty n(r')dr' \int_0^{r'} dr \left(1 - \frac{r}{r'}\right) r\psi_{,ij} = \int_0^\infty dr w(r) \psi_{,ij} \tag{5.46}$$

with

$$w(r) \equiv \int_r^\infty dr' \left(1 - \frac{r}{r'}\right) r n(r). \tag{5.47}$$

By means of the relation $dr = dz/H(z)$ we can write equation (5.46) as a function of the redshift z:

$$D_{ij} = \int_0^\infty \frac{dz}{H(z)} w(z) \psi_{,ij} [\theta_x r(z), \theta_y r(z), r(z)] \tag{5.48}$$

where $\theta^i = (\theta_x, \theta_y)$ are the angles in the source plane.

Now let us consider the convergence κ_{wl}:

$$\kappa_{wl} = -\frac{1}{2}(D_{11}+D_{22}) = -\frac{1}{2}\int_0^\infty dr w(r)\psi_{,ii} \tag{5.49}$$

where the sum over i is implicit. We want to project the 3-dimensional power spectrum of this field into a 2-dimensional power spectrum, by applying Limber's theorem. This theorem states that if we have a field $f(x,y,r)$ projected along the r-direction with some weight $w(r)$ normalized to unity:

$$F(\theta_x,\theta_y) = \int_0^\infty dr w(r) f(\theta_x r, \theta_y r, r) \tag{5.50}$$

then the two-dimensional power spectrum of F is given by

$$P(q) = \int_0^\infty dr \frac{w(r)^2}{r^2} p\left(\frac{q}{r}\right) \tag{5.51}$$

if $p(k)$ is the 3-dimensional power spectrum of f and q is the modulus of $q = (q_1,q_2)$.

In the case of κ_{wl} the theorem leads to the following *convergence power spectrum*:

$$P_{\kappa_{wl}}(q) = \frac{1}{4}\int_0^\infty dr \frac{w^2(r)}{r^2} P_{\psi,ii}\left(\frac{q}{r}\right) = \frac{1}{4}\int_0^\infty dz \frac{W^2(z)}{H(z)} P_{\psi,ii}\left(\frac{q}{r}\right) \tag{5.52}$$

with

$$W(z) \equiv \frac{w[r(z)]}{r(z)}. \tag{5.53}$$

An expression for the spectrum of $\psi_{,ii}$ must be found. Further calculations show that, in the absence of anisotropic stress (when $\psi = \Phi - \Psi = 2\Phi$), we can express $P_{,ii}$ as a function of the matter power spectrum:

$$P_{\psi,ii} = 9H^4\Omega_m^2(1+z)^{-4} P_{\delta_m}. \tag{5.54}$$

Equation (5.52) becomes then

$$P_{\kappa_{wl}}(q) = \frac{9H_0^3}{4}\int_0^\infty dz \frac{W^2(z)E^3(z)\Omega_m^2(z)}{(1+z)^4} P_{\delta_m}\left(\frac{q}{r(z)}\right) \tag{5.55}$$

with $E(z) = H(z)/H_0$ and

$$W(z) = \int_z^\infty \frac{d\tilde{z}}{H(\tilde{z})}\left[1 - \frac{r(z)}{r(\tilde{z})}\right] n[r(\tilde{z})]. \tag{5.56}$$

For large q we can write

$$q = \frac{l}{\pi} \tag{5.57}$$

and estimate the power spectrum as a function of the approximate multipole l.

The function $n[r(z)]$ is often given as a direct function of redshift z; in this case, we have to take into account that $n(z)dz = n(r)dr$, and therefore

$$n[r(z)] = n(z)H(z). \tag{5.58}$$

A typical parameterization for $n(z)$ is given by

$$n(z; z_0, \alpha) = z^2 \exp\left[-(z/z_0)^\alpha\right] \tag{5.59}$$

where α is fixed by observations (usually of order unity).

We have considered the convergence κ_{wl}, we may wonder what happens to the power spectrum of the components $\psi_{,ij}$ for $i \neq j$. Actually, it happens that a transformation on the shear fields γ_1, γ_2 can be done in order to make the power spectrum for $i \neq j$ vanish [5]. The convergence power spectrum is therefore the only quantity we need to extract cosmological information from weak lensing.

We can generalize expression (5.55) to the case in which we correlate sources in two redshift bins around z_i and z_j respectively. In this case (using also (5.57)) we have:

$$P_{ij}(l) = \frac{9H_0^3}{4} \int_0^\infty dz \frac{W_i(z) W_j(z) E^3(z) \Omega_m^2(z)}{(1+z)^4} P_{\delta_m}\left(\frac{l}{\pi r(z)}\right) \tag{5.60}$$

with

$$W_i(z) = \int_z^\infty \frac{d\tilde{z}}{H(\tilde{z})} \left[1 - \frac{r(z)}{r(\tilde{z})}\right] n_i[r(\tilde{z})] \tag{5.61}$$

and $n_i[r(z)]$ is the galaxy density for the i-th bin, which is usually the convolution of $n(z)$ with a Gaussian centered in z_i (for more details and for an explicit calculation, see section 6.4).

We derived expression (5.60) in the absence of anisotropic stress; one can show that, in the general case with anisotropic stress, (5.60) becomes

$$P_{ij}(l) = \frac{9H_0^3}{4} \int_0^\infty dz \frac{W_i(z) W_j(z) E^3(z) \Omega_m^2(z)}{(1+z)^4} \Sigma^2(z,l) P_{\delta_m}\left(\frac{l}{\pi r(z)}\right) \tag{5.62}$$

where $\Sigma^2(z,l)$ is the *modified gravity function* (a definition of Σ is postponed to section 6.1).

5.4 Fisher matrix

As announced before, the statistical tool of Fisher matrix formalism based on Bayesian statistics will be described in this section, an extremely powerful tool to extract cosmological information from observed data. In particular, we will show how it can be applied to supernovae, galaxy clustering and weak lensing surveys.

5.4.1 Likelihood function

Let x be a random variable with a certain probability distribution function (PDF) $f(x;\theta)$ that depends on an unknown parameter θ. Just to make an useful example to our case, x could be the apparent magnitude m of a supernova and θ could be its absolute magnitude M or a cosmological parameter appearing in (1.63), e.g. $\Omega_m^{(0)}$. Then the $f(x;\theta)$ is called a conditional probability of having the data x given the theoretical parameter θ.

Back to our example, we can suppose that the apparent magnitude m has a Gaussian PDF centered at its theoretical value (from (1.63))

$$m_{th} = 5 + \log_{10} d_L(z;\Omega_m^{(0)},\Omega_\Lambda^{(0)}) + constant \tag{5.63}$$

but we do not know one of the parameters (e.g. $\Omega_m^{(0)}$). $f(\bar{m};\bar{\Omega}_m^{(0)})$ tells us the probability of having a value $m=\bar{m}$ for the apparent magnitude if we fix the matter density parameter to $\Omega_m^{(0)} = \bar{\Omega}_m^{(0)}$.

If we have more than one variable x_1, x_2, x_3, then the probability to obtain x_i in the interval dx_i around the value x_i (for every i and for independent measures) is

$$f(x_i;\theta)d^n x_i \equiv \prod_i f_i(x_i;\theta)dx_i. \tag{5.64}$$

The value of $f(x_i;\theta)$ is different for every value of θ; we define as the *best value* of θ the one which maximizes $f(x_i,\theta)$ (all of the x_i are meant in the argument). The best θ is thus the parameter which "fits better" with the data x_i.

We can also have more than one parameter; in this case we define the best θ_i as those values which maximize the joint PDF $f(x_1,...,x_m;\theta_1,...,\theta_n) \equiv f(x_i,\theta_j)$.

The *maximum likelihood method* of parameter estimation consists in finding the parameters that maximize the *likelihood function* $f(x_i;\theta_j)$, i.e. solving the system

$$\frac{\partial f(x_i;\theta_j)}{\partial \theta_j} = 0, \tag{5.65}$$

for $j = 1,...,n$.

We denote the solutions of these equations as $\hat{\theta}_j$. They are functions of the data x_i, and are therefore random variables as the x_i are. The classical frequentist approach would be to try to determine the distribution of the $\hat{\theta}_j$s knowing the distribution of the x_i; but using this approach is computationally very demanding and, above all, we cannot include in the calculations what we already know about the theoretical parameters, i. e. the results of previous experiments.

We have to use then the so-called *Bayesian approach*: instead of considering the probability $f(x_i;\theta_j)$ of having the data given the theoretical model, we estimate the probability $L(\theta_j;x_i)$ of having the model given the data. This approach is based on the Bayes' theorem, which can be stated in the following way:

$$P(T;D) = \frac{P(D;T)P(T)}{P(D)}, \tag{5.66}$$

where we have used D to denote the data x_i and T to denote the theory (the parameters θ_j). $P(T;D)$ is the conditional probability of having the theory given the data, $P(D;T)$ is the conditional probability of having the data given the theory, while $P(T)$ and $P(D)$ are the probabilities of having the theory and the data, respectively, independently from each other. It follows that, in our case:

$$L(\theta_j;x_i) = \frac{f(x_i;\theta_j)p(\theta_j)}{g(x_i)}, \tag{5.67}$$

where $p(\theta_j)$ is called the *prior probability* for the θ_j and $g(x_i)$ is the PDF of the data x_i. The $p(\theta_j)$ can account for the information we already have on the θ_js, for example, the results of previous experiments.

Notice that the likelihood must be normalized to one, since it is a PDF too:

$$\int L(\theta_j;x_i)d^n\theta_j = 1 = \frac{\int f(x_i;\theta_j)p(\theta_j)d^n\theta_j}{g(x_i)} \tag{5.68}$$

which means that $g(x_i)$ is constrained from the normalization condition to be:

$$g(x_i) = \int f(x_i;\theta_j)p(\theta_j)d^n\theta_j \tag{5.69}$$

and, since it does not depend on θ_j, it has no role in the estimation of the parameters.

From $f(x_i;\theta_j)$ and the priors $p(\theta_j)$ we can obtain $L(\theta_j;x_i)$ (which can be indicated with $L(\theta_j)$ for simplicity). Once we have $L(\theta_j)$, we have to search the *maximum likelihood estimators*, the values $\hat{\theta}_i$ that maximize it; that is we have to solve

$$\frac{\partial L(\theta_i)}{\partial(\theta_i)} = 0 \tag{5.70}$$

for $i = 1,...,n$.

If we discard $g(x_i)$ in equation (5.67), we have that the normalization has to be recalculated: we redefine $\frac{L(\theta_i)}{N} \equiv L(\theta_i)$, where N is the new normalization constant

$$N = \int L(\theta_i)d^n\theta_i \tag{5.71}$$

with the integral extending to the whole parameter space.

From the new normalized $L(\theta_i)$ we can derive the confidence regions for the parameter. For example, the confidence region $R(\alpha)$ for the confidence level α (with $0 < \alpha < 1$) is the domain in the parameter space delimited by constant $L(\theta_i)$ such that

$$\int_{R(\alpha)} L(\theta_i)d^n\theta_i = \alpha. \tag{5.72}$$

A problem with which we have often to deal is to consider only a subset of the parameters θ_i, because often we have little information on some of them, or simply because we are not interested in them.

Consider the simple case of the likelihood depending on three parameters $\theta_1, \theta_2, \theta_3$. Suppose that we are not interested in θ_3. In order to eliminate the dependence of the likelihood from θ_3, we integrate out it:

$$L(\theta_1, \theta_2) = \int L(\theta_1, \theta_2, \theta_3) d\theta_3 \tag{5.73}$$

This procedure is called *marginalization*.

Sometimes one prefers to fix a parameter, rather than marginalize over it. This is useful when one wants to see what happens for values of the parameter which are particularly interesting. Then the result will depend on the fixed value of that parameter. When the value is used for which the likelihood is maximum, the likelihood is said to be *maximized* with respect to that parameter.

5.4.2 Fisher matrix

The likelihood method is conceptually not complicated, and in principle it can be applied in a variety of cases, but it has one problem: it is extremely computationally demanding when there are more than a few parameters, because $L(\theta_i)$ must be evaluated for many θ_i. Therefore, we need to find a method which can be implemented more easily. This is the method known as *Fisher matrix method*.

The idea is to approximate the full likelihood with a multivariate Gaussian distribution:

$$L \approx N \exp\left[-\frac{1}{2}\left(\theta_i - \hat{\theta}_i\right) F_{ij} \left(\theta_j - \hat{\theta}_j\right)\right], \tag{5.74}$$

where $\hat{\theta}_i$s are the maximum likelihood estimators and F_{ij} is the *Fisher matrix* and is equal to the inverse of the correlation matrix. The Gaussian approximation could be in general not very accurate, but we can expect it to hold near the peak of the distribution, that is, for θ_i near to $\hat{\theta}_i$.

If we expand the exponent of a generic likelihood near the peak, we have

$$\ln L(\theta_i) \approx \ln L(\hat{\theta}_i) + \frac{1}{2} \left.\frac{\partial^2 \ln L(\theta_i)}{\partial \theta_i \partial \theta_j}\right|_{ML} \left(\theta_i - \hat{\theta}_i\right) \left(\theta_j - \hat{\theta}_j\right) \tag{5.75}$$

where *ML* indicates that the derivative is evaluated at the peak (for the maximun likelihood estimators). The first derivatives are of course equal to zero since we are near the peak. Comparing this expression with equation (5.74), we see that N depends only on the data, and the Fisher matrix is defined as

$$F_{ij} \equiv - \left.\frac{\partial^2 \ln L(\theta_i)}{\partial \theta_i \partial \theta_j}\right|_{ML} \tag{5.76}$$

or as the average of (5.76) over the data distribution (the two definitions are equivalent in the approximation (5.74)):

$$F_{ij} \equiv -\left\langle \frac{\partial^2 \ln L(\theta_i)}{\partial\theta_i \partial\theta_j} \right\rangle = -\int \frac{\partial^2 \ln L(\theta_i)}{\partial\theta_i \partial\theta_j} L(x;\theta) dx. \tag{5.77}$$

Now the search for the likelihood peak can be much faster. However, one of the most useful features of the Fisher matrix method in Cosmology is that it allows us to simulate an experiment: instead of searching for the maximum likelihood estimators, we may take for the estimators the values obtained by fixing the parameters of the cosmological model to some fiducial values (e. g. the values for ΛCDM model); then, by generating a simulated data set (with values x_i and errors σ_i based on the expected performance of the experiment), we can calculate the approximated likelihood (5.74) and find the confidence errors for the parameters θ_i. This last step can be achieved quite easily by means of the Fisher matrix (5.76). In fact, it can be shown that the diagonal of the inverse Fisher matrix contains the fully marginalized 1σ-errors of the corresponding parameters (that is, the errors on each parameter after marginalizing over all others), and this is the minimal error one can hope to achieve (according to Cramer-Rao theorem):

$$\sigma^2(\theta_i) = \left(F^{-1}\right)_{ii}. \tag{5.78}$$

The Fisher matrix has a number of properties which make calculations very simple: here we summarize the most important (without proof).

Change of parameters If we want to obtain the Fisher matrix for a new set of parameters y_i from the one calculated for a set x_i, we have just to multiply the Fisher matrix on the left and on the right by the Jacobian matrix of the transformation:

$$F^{(y)}_{lm} = J_{il} F^{(x)}_{ij} J_{jm} \tag{5.79}$$

where sum over indices is implicit and

$$J_{ji} = \left.\left(\frac{\partial x_j}{\partial y_i}\right)\right|_{ML} \tag{5.80}$$

is the Jacobian matrix evaluated on the maximum likelihood estimators.

Maximization If we want to maximize the likelihood with respect to some parameters, we simply remove the corresponding rows and columns from the Fisher matrix.

Marginalization If we want to marginalize over some parameters, we have to remove the corresponding rows and columns from the *inverse* of the Fisher matrix.

Combining results If we want to add priors to a Fisher matrix, or to combine different matrices from different experiments or forecasts, we have to add up all the Fisher matrices:

$$F_{ij}^{(tot)} = F_{ij}^{(1)} + F_{ij}^{(2)}. \tag{5.81}$$

Hereafter we propose some calculations in explicit cases which will be useful in the following.

5.4.3 Likelihood for supernovae

If we simulate an experiment with N supernovae at redshifts z_i with errors σ_i on redshifts and apparent magnitudes m_i, we can calculate the theoretical value $m_{th,i}$ from equation (1.63) by choosing a fiducial cosmological model and fixing the cosmological parameters that appear in d_L. We can write

$$m_{th,i} = \alpha + \mu_i \tag{5.82}$$

where

$$\mu_i = 5\log_{10}\hat{d}_L(z_i,\theta_j), \tag{5.83}$$

$$\alpha = M + 25 - 5\log_{10}H_0 \tag{5.84}$$

and $\hat{d}_L = d_L H_0$.

The likelihood can be supposed to be Gaussian. Since we know little about α, we can marginalize over it. We therefore integrate the likelihood in $d\alpha$:

$$L(\theta_j) = N\int d\alpha \exp\left[-\frac{1}{2}\sum_i \frac{(m_i-\mu_i-\alpha)^2}{\sigma_i^2}\right]. \tag{5.85}$$

Performing the integration and absorbing the integration constant in N yields

$$L(\theta_j) = N\exp\left[-\frac{1}{2}\left(S_2 - \frac{S_1^2}{S_0}\right)\right] \tag{5.86}$$

where

$$S_0 = \sum_i \frac{1}{\sigma_i^2}, \tag{5.87}$$

$$S_1 = \sum_i \frac{y_i}{\sigma_i^2}, \tag{5.88}$$

$$S_2 = \sum_i \frac{y_i^2}{\sigma_i^2} \tag{5.89}$$

and $y_i = m_i - \mu_i$.

5.4.4 Fisher matrix for power spectrum

Let us now derive the Fisher matrix for a power spectrum. We will start from the case of the galaxy power spectrum and then proceed with the convergence power spectrum for weak lensing.

We suppose that a future experiment will measure the Fourier coefficients δ_k of a galaxy distribution and their power spectrum calculated for m wavenumbers k_i in some redshift bin $[z, z+\Delta z]$. The total power spectrum (including the Poissonian noise) is given by Δ_k^2 defined in equation (3.23):

$$\Delta_k^2 = \langle \delta_k \delta_k^* \rangle = \langle \delta_k \delta_{-k} \rangle = P(k,z) + \frac{1}{n}. \tag{5.90}$$

If we assume the galaxy distribution to be well approximated by a Gaussian random field (i.e. the real and complex parts of the coefficients δ_{k_i}obey the Gaussian statistics), and that the measures at every k_i are statistically independent, we can write the likelihood:

$$L = \frac{1}{(2\pi)^{m/2} \prod_i \Delta_i} \exp\left[-\frac{1}{2} \sum_i^m \frac{\delta_i^2}{\Delta_i^2} \right] \tag{5.91}$$

where $\delta_i = Re\delta_{k_i}$ and $\Delta_i = \Delta_{k_i}$.

When we simulate a future experiment, $P(k,z)$ is taken to be the theoretical spectrum of our fiducial model described by the fiducial parameters $p_j^{(F)}$. Then:

$$\mathscr{L} = -\ln L = \frac{m}{2} \ln(2\pi) + \sum_i \ln \Delta_i + \sum_i \frac{\delta_i^2}{2\Delta_i^2}. \tag{5.92}$$

From the definition (5.77), the Fisher matrix for a single redshift bin is

$$F_{lm} = -\left\langle \frac{\partial^2 \mathscr{L}}{\partial p_l \partial p_m} \right\rangle = \sum \left[\frac{\Delta_{,lm}}{\Delta} - \frac{\Delta_{,l}\Delta_{,m}}{\Delta^2} - \langle \delta^2 \rangle \left(\frac{\Delta_{,lm}}{\Delta^3} - 3\frac{\Delta_{,l}\Delta_{,m}}{\Delta^4} \right) \right], \tag{5.93}$$

where we suppressed the index i for brevity and $\Delta_{,l}$ denotes differentiation with respect to the l-th parameter. This is equal to:

$$F_{lm} = \frac{1}{2} \sum_i \frac{\partial \ln P_i}{\partial p_l} \frac{\partial \ln P_i}{\partial p_m} \left(\frac{nP_i}{1+nP_i} \right)^2. \tag{5.94}$$

We can now obtain a more compact expression by approximating the sum over k_i with an integral over k; to do this, we have to count the number accessible modes. The Fourier volume in the interval $[k, k+dk]$ and in the cosine interval $d\mu$ is $2\pi k^2 dk d\mu$, but the effective number of modes is limited by the size of the survey volume and by the shot noise. Modes larger than the survey volume cannot be measured; too short modes are unreliable. To accont for these limitation we discretize the Fourier space by dividing the Fourier volume by

$$V_{cell} = \frac{(2\pi)^3}{V_{survey}} \tag{5.95}$$

so that the number of modes in the survey volume is

$$N_{modes} = \frac{2\pi k^2 dk d\mu}{V_{cell}} = \frac{V_{survey} k^2 dk d\mu}{(2\pi)^2}. \tag{5.96}$$

The integral form of the Fisher matrix is therefore given by

$$F_{lm} = \frac{1}{8\pi^2} \int_{-1}^{+1} d\mu \int_{k_{min}}^{k_{max}} k^2 dk \frac{\partial \ln P(k,\mu)}{\partial p_l} \frac{\partial \ln P(k,\mu)}{\partial p_m} \left[\frac{nP(k,\mu)}{nP(k,\mu)+1} \right]^2 V_{survey}. \tag{5.97}$$

The factor

$$V_{eff} = \left[\frac{nP(k,\mu)}{nP(k,\mu)+1} \right]^2 V_{survey} \tag{5.98}$$

can be seen as an effective volume.

Notice that the Fisher matrix (5.97) is relative to a single redshift bin; if we have more than one bin, we can build the total Fisher matrix by summing all the Fisher matrices for each bin.

In the case of weak lensing, we can similarly derive the Fisher matrix for the convergence power spectrum (5.62), since $P_{ij}(l)$ is a linear function of P_{δ_m}. However, instead of calculating P_{ij} at all l's, we can calculate it at some interval Δl and then interpolate, considering that there are $(2l+1)$ modes for each multipole l. The final result is:

$$F_{\alpha\beta} = f_{sky} \sum_l \frac{(2l+1)\Delta l}{2} \frac{\partial P_{ij}(l)}{\partial p_\alpha} C^{-1}_{jk} \frac{\partial P_{km}(l)}{\partial p_\beta} C^{-1}_{mi} \tag{5.99}$$

(sum over indices implicit), where the *covariance matrix* C is given by

$$C_{jk} = P_{jk} + \delta_{jk} \gamma^2_{int} n_j^{-1} \tag{5.100}$$

and n_j is the number of galaxies per steradians in the j-th bin.

Chapter 6

Fisher Matrix for the Anisotropic Stress η

6.1 Anisotropic stress η from model-independent observables

A couple of questions which is very interesting to answer are: which quantities can we observe without assuming a parameterization for dark energy? Can we use these quantities to constrain the models? These questions have been dealt with in the paper by Amendola et al., 2012 [4].

The authors start from the following quite general hypotheses:

a) the geometry of the Universe is well described by small perturbations living in a FLRW background metric (1.3);

b) the matter component is pressureless or evolves in a known way;

c) the relation between galaxy and matter distributions can be modeled by a bias factor: $\delta_{gal} = b(k,a)\delta_m$ (this is the assumption (3.40), here the possible scale and time dependence has been explicited);

d) the late-time Universe is described by the action (with $\kappa^2 = 1$) $S = \int d^4x\sqrt{-g}\left(\frac{1}{2}R + \mathscr{L}_x + \mathscr{L}_m\right)$, where $\mathscr{L}_x$ is the dark energy Lagrangian;

e) the dark energy is ruled by the most general Lagrangian which depends on a single scalar field governed by second-order equations of motion; that is, $\frac{1}{2}R + \mathscr{L}_x$ will form the Horndeski Lagrangian (4.19).

From the analysis of the background Universe, under the hypotheses (a)-(c), a Friedmann equation can be obtained in the form

$$H^2 - H_0^2 \Omega_k^{(0)} a^{-2} = \frac{1}{3}(\rho_x + \rho_m). \tag{6.1}$$

From assumption (b), ρ_m evolves as a^{-3}. From the observations, one can measure distances $D(z)$ or directly the Hubble parameter $H(z)$; by combining the two, the present curvature parameter $\Omega_k^{(0)}$ can be estimated, and therefore the combined matter and dark energy content $1-\Omega_k$ at all times, from equation (6.1). If the cosmic fluid has only the two mentioned components, one can conclude that Ω_x and Ω_m can be both reconstructed from background observables, up to only one free parameter, namely $\Omega_m^{(0)}$. In fact, the following relation holds:

$$\Omega_x = 1 - \Omega_k - \Omega_m = 1 - \frac{H_0^2}{H^2}\left(\Omega_k^{(0)} a^{-2} + \Omega_m^{(0)} a^{-3}\right). \tag{6.2}$$

From galaxy clustering and weak lensing, they conclude that the following quantities are measurable using the two key observables of the two probes (the galaxy power spectrum and the convergence power spectrum, respectively):

$$A(z,k) = G(z) b(z) \sigma_8 \delta_{t,0}(k), \tag{6.3}$$

$$R(z,k) = G(z) f(z) \sigma_8 \delta_{t,0}(k), \tag{6.4}$$

$$L(z,k) = \Omega_{m0} \Sigma(z,k) G(z) \sigma_8 \delta_{t,0}(k) \tag{6.5}$$

where $G(z) = \exp\left[-\int_0^z \frac{f(\tilde{z})}{(1+\tilde{z})} d\tilde{z}\right]$ is the matter growth function, $f(z) = G'/G$ is the growth rate (the $'$ denotes derivatives with respect to time), σ_8 is the power spectrum normalization, $\delta_{t,0}(k) = \Omega_m^{(0)} \delta_{m,0} + \Omega_x^{(0)} \delta_{x,0}$ is the total density perturbation at present time and $\Sigma(k,z)$ is the modified gravity function introduced in section. It is defined as

$$\Sigma(k,z) = Y(1+\eta) \tag{6.6}$$

where

$$Y(k,z) = -\frac{2k^2 \Psi}{3\Omega_m \delta_m}, \tag{6.7}$$

$$\eta(k,z) = -\frac{\Psi}{\Phi}; \tag{6.8}$$

here η represents the *gravitational slip* or *dark energy anisotropic stress*.

Since $\delta_{t,0}(k)$ is the square root of the present power spectrum, it depends on a transfer function, which cannot be assumed without assuming a model for dark energy. This means that actually the only model-independent directly measurable quantities are ratios of A, R, L and their derivatives:

$$P_1(z) \equiv RA^{-1} = f/b, \tag{6.9}$$

$$P_2(k,z) \equiv LR^{-1} = \Omega_{m0}\Sigma/f, \tag{6.10}$$

$$P_3(z) \equiv R'/R = f + f'/f. \tag{6.11}$$

(dependencies are omitted for brevity).

Now, it happens that the anisotropic stress η and the function Y can be written, using assumption (e), in terms of the Horndeski Lagrangian functions K, G_{3-5} appearing in (4.19). In fact:

$$\eta = h_2 \left(\frac{1+k^2 h_4}{1+k^2 h_5} \right), \tag{6.12}$$

$$Y = h_1 \left(\frac{1+k^2 h_5}{1+k^2 h_3} \right), \tag{6.13}$$

where the functions h_{1-5} are quite complicated combinations of the Horndeski Lagrangian functions (for the relation between the two sets see [4],[9]). For ΛCDM model one has $h_{1,2} = 1$, $h_{3,4,5} = 0$, so that $\eta = Y = 1$ in this case. These relations are obtained in the quasi-static limit, that is, for scales inside the cosmological horizon ($k \gg 1$) and inside the Jeans length ($c_s k \gg 1$, where c_s is the sound speed).

Using the matter conservation equation, the definitions (6.7), (6.8) and relations (6.12), (6.13) one has:

$$\delta_m'' + \left(2 + \frac{H'}{H} \right) \delta_m' = -k^2 \Psi = \frac{3}{2} \Omega_m \delta_m h_1 \left(\frac{1+k^2 h_5}{1+k^2 h_3} \right) \tag{6.14}$$

or

$$f' + f^2 + \left(2 + \frac{H'}{H} \right) f = \frac{3}{2} \Omega_m h_1 \left(\frac{1+k^2 h_5}{1+k^2 h_3} \right). \tag{6.15}$$

From (6.10), (6.11), one has further

$$f = \frac{\Omega_m^{(0)} \Sigma}{P_2}, \tag{6.16}$$

$$f' = \frac{P_3 \Omega_m^{(0)} \Sigma}{P_2} - \left(\frac{\Omega_m^{(0)} \Sigma}{P_2} \right)^2. \tag{6.17}$$

The quantity Σ can be written as a function of the Horndeski Lagrangian functions as

$$\Sigma = Y(1+\eta) = \frac{h_6(1+k^2h_7)}{(1+k^2h_3)}, \tag{6.18}$$

with $h_6 = h_1(1+h_2)$, $h_7 = (h_5+h_4h_2)/(1+h_2)$.

At the end, the following relation is found to hold between model-independent observables (6.9)-(6.11) and the HL functions $h_{2,}h_{4,}h_5$:

$$\frac{3P_2H_0^2(1+z)^3}{2H^2\left(P_3+2+\frac{H'}{H}\right)} - 1 = \eta = h_2\left(\frac{1+k^2h_4}{1+k^2h_5}\right). \tag{6.19}$$

The remaining part of this Thesis uses the first part of this relation to make some forecasts on the constraints on the anisotropic stress η for the ESA *Euclid* survey using the Fisher matrix formalism described in section 5.4. A forecast on the model-independent parameters A,R,L and on the Hubble parameter $E(z) = H(z)/H_0$ will be performed using the Euclid expected performance values; data from a supernova survey will be added too in order to improve the constraints on E. Then we will project the results onto P_1,P_2,P_3 and finally on η by means of the Fisher matrix formalism. We will consider two cases:

1. η depending on redshift z only;
2. η constant at all scales and redshifts (as for example in the ΛCDM case, where we have $\eta = 1$).

Notice that the second part of (6.19) can be used to make a forecast on the HL functions h_2,h_4,h_5. This part of the work will be performed in a paper in preparation by Amendola, Fogli, Guarnizo, Kunz, Vollmer.

6.2 Forecasts for the anisotropic stress η

Our objective is to forecast the error on the observable quantity η defined as (6.19)

$$\frac{3P_2H_0^2(1+z)^3}{2H^2\left(P_3+2+\frac{H'}{H}\right)} - 1 = h_2\left(\frac{1+k^2h_4}{1+k^2h_5}\right) = \eta \tag{6.20}$$

or

$$\frac{3P_2(1+z)^3}{2E^2\left(P_3+2+\frac{E'}{E}\right)} - 1 = h_2\left(\frac{1+k^2h_4}{1+k^2h_5}\right) = \eta \tag{6.21}$$

using $E(z) = H(z)/H_0$.

The functions $P_{1,}P_{2,}P_3$ defined by equations (6.9)-(6.11) can be defined by means of the power-spectrum-independent parameters:

$$\bar{A}(z) = G(z)b(z)\sigma_8, \tag{6.22}$$

$$\bar{R}(z) = G(z)f(z)\sigma_8, \tag{6.23}$$

$$\bar{L}(z,k) = \Omega_{m0}\Sigma(z,k)G(z)\sigma_8. \tag{6.24}$$

We consider three kind of observations for a future survey (i.e. the ESA Euclid survey): galaxy clustering, weak lensing and supernovae. We estimate the errors on parameters $\{\bar{A},\bar{R},\bar{L},E\}$ for different bins in redshift using the Fisher matrix formalism and then combine the results to obtain the errors on η in each bin. We will assume ΛCDM as a fiducial model and the Bardeen formula as model for the power spectrum for the linear regime. The fiducial parameters have been taken from the WMAP-9-year data [14] and are reported in Table 6.1. Calculations in the following sections have been performed using units Mpc/h for distances, with $c = 1$.

Parameter	*Value*
h	0.6955
$\Omega_m^{(0)}$	0.2835
$\Omega_\Lambda^{(0)}$	0.7165
w	-1
σ_8	0.818
n_s	0.9616
k_{eq}	0.01000/h (h/Mpc)

Table 6.1: Fiducial parameters for ΛCDM from WMAP-9-year data (wmap9+spt+act+snls3+bao+h0).

6.3 Galaxy clustering

The galaxy power spectrum can be written from equation (5.26) as

$$P(k) = (A + R\mu^2)^2 e^{-k^2\mu^2\sigma_r^2} = (\bar{A} + \bar{R}\mu^2)^2 \delta_{t,0}^2(k) e^{-k^2\mu^2\sigma_r^2}, \tag{6.25}$$

where the factor $Hd_r^2/H_r d^2$ can be absorbed in the normalization σ_8 and

$$\mu = \frac{\vec{k}\cdot\vec{l}}{kl}, \tag{6.26}$$

$$\sigma_r = \delta z/H(z), \tag{6.27}$$

in our case $\sigma_r = 0.001(1+z)$, from the Euclid specifications ([11], p.83).

The Fisher matrix for a given redshift bin (centered at $\hat{z}$) is given in general by equation (5.97), which can be written as

$$F_{ab} = \frac{1}{8\pi}\int_{-1}^{+1} d\mu \int_{k_{min}}^{k_{max}} k^2 dk V_{eff} D_a D_b, \tag{6.28}$$

where

$$D_a \equiv \frac{d\log P}{dp_a} \tag{6.29}$$

(the lower-case latin indexes are used here to avoid confusion with the greek ones, which will represent the different redshift bins in the following sections).

We want to calculate the Fisher matrix expliciting the Hubble parameter, therefore our parameters are $p_a = \{\bar{A}(\hat{z}), \bar{R}(\hat{z}), E(\hat{z})\}$, with $E = H(\hat{z})/H_0$. The derivatives D_a will be calculated at a fiducial model (i.e. ΛCDM). We assume that the present power spectrum in the real space is given by the approximation formula obtained by Bardeen et al., 1986 [13]:

$$\delta_{t,0}^2 \approxeq P_{Bardeen}(k) = c_{norm} T^2(k) k^{n_s}. \tag{6.30}$$

Notice that since we are considering the quasi-static limit, the dark energy clusters weakly and its contribution to the perturbation is negligible; therefore we can take $\delta_{t,0} \simeq \delta_{m,0}$ and apply the Bardeen formula, which is valid for the matter power spectrum.

The parameter c_{norm} can be obtained from equation (5.14), or can be equivalently fixed by the normalization condition

$$\sigma_8^2 = \frac{1}{2\pi^2}\int P_{Bardeen}(k) W_8^2(k) k^2 dk; \tag{6.31}$$

the index n_s is the spectral index (=0.9616 from the WMAP-9 -year data) and the transfer function is given by equation (5.9):

$$T(x) = \frac{\ln(1+0.171x)}{0.171x}\left[1+0.284x+(1.18x)^2+(0.399x)^3+(0.490x)^4\right]^{-1/4} \tag{6.32}$$

with $x = k/k_{eq}$.

The Bardeen power spectrum is then given by:

$$P_{Bardeen}(k) = c_{norm}\cdot\frac{\ln^2\left(1+0.171\frac{k}{k_{eq}}\right)}{0.171^2\left(\frac{k}{k_{eq}}\right)^2}\left[1+0.284\frac{k}{k_{eq}}+\left(1.18\frac{k}{k_{eq}}\right)^2+\left(0.399\frac{k}{k_{eq}}\right)^3+\left(0.490\frac{k}{k_{eq}}\right)^4\right]^{-1/2}\cdot k^{n_s} \tag{6.33}$$

(see Figure 6.1), and using equations (6.25), (6.33) we can write the power spectrum in redshift space as

$$P(k) = (\bar{A} + \bar{R}\mu^2)^2 \cdot P_{Bardeen}(k) e^{-k^2\mu^2\sigma_r^2}. \tag{6.34}$$

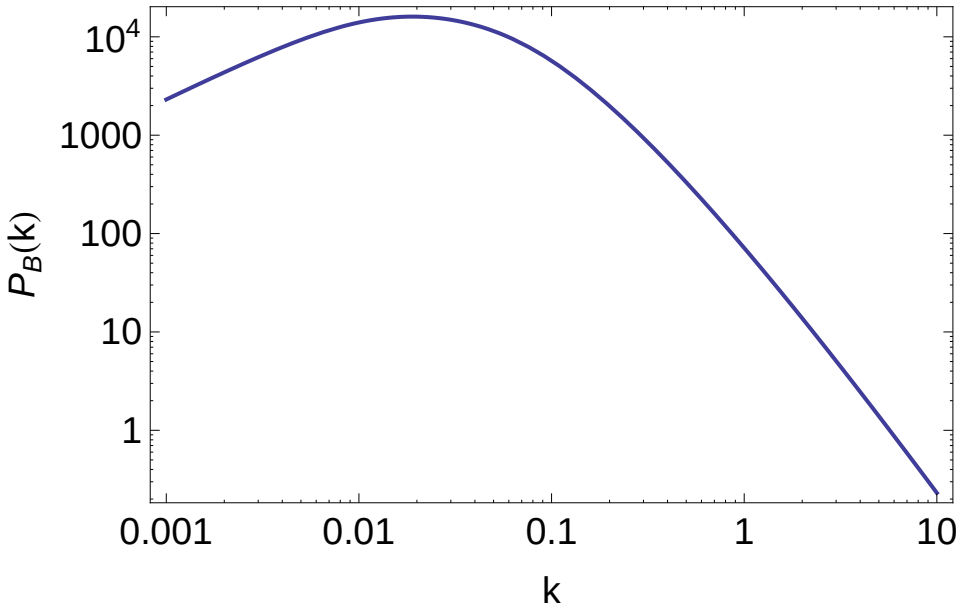

Figure 6.1: Bardeen power spectrum $P_B(k)$ as a function of k.

Calculation of the derivatives D_α

We need to express k, μ as functions of E, therefore we can use the coordinate exchange (5.15)-(5.16):

$$\begin{cases} k = & Qk_r \\ \mu = & \frac{H\mu_r}{H_r Q} = \frac{E\mu_r}{E_r Q} \end{cases}, \tag{6.35}$$

where k_r, μ_r are the wavevector and the direction cosine in a reference cosmology (i.e. ΛCDM) and Q is given by (5.17)

$$Q = \frac{\sqrt{H^2 d^2 \mu_r^2 - H_r^2 d_r^2 (\mu_r^2 - 1)}}{H_r d} = \frac{\sqrt{E^2 d^2 \mu_r^2 - E_r^2 d_r^2 (\mu_r^2 - 1)}}{E_r d}, \tag{6.36}$$

being d the angular diameter distance (1.60)

For the parameters $\bar{A}, \bar{R}$ we have:

$$\frac{\partial \log P}{\partial \bar{A}} = \frac{2}{(\bar{A}+\bar{R}\mu^2)}; \tag{6.37}$$

$$\frac{\partial \log P}{\partial \bar{R}} = \frac{2\mu^2}{(\bar{A}+\bar{R}\mu^2)}. \tag{6.38}$$

We now proceed calculating the derivative:

$$\frac{d \log P}{dE} = \frac{\partial \log P}{\partial k}\cdot\frac{\partial k}{\partial E} + \frac{\partial \log P}{\partial \mu}\cdot\frac{\partial \mu}{\partial E} + \frac{\partial \log P}{\partial d}\cdot\frac{\partial d}{\partial E}. \tag{6.39}$$

We have:

$$\frac{\partial \log P}{\partial k} = \frac{1}{P_B}\cdot\frac{dP_B}{dk} - 2k\mu^2\sigma_r^2, \tag{6.40}$$

$$\frac{\partial \log P}{\partial \mu} = \frac{4\bar{R}\mu}{(\bar{A}+\bar{R}\mu^2)} - 2k^2\mu\sigma_r^2, \tag{6.41}$$

with $P_B = P_{Bardeen}(k)$ for brevity.

In order to calculate $\frac{\partial \log P}{\partial d}$, we notice that the dependence of P on d is fully contained in the parameter Q. Therefore we can write:

$$\begin{aligned}\frac{\partial \log P}{\partial d} &= \frac{1}{P}\cdot\frac{\partial P}{\partial d} = \\ &= \frac{1}{P}\cdot\left[2(\bar{A}+\bar{R}\mu^2)\cdot 2\bar{R}\mu\frac{\partial \mu}{\partial d}P_B e^{-k^2\mu^2\sigma_r^2} + (\bar{A}+\bar{R}\mu^2)^2\frac{\partial P_B}{\partial k}\cdot\frac{\partial k}{\partial d}e^{-k^2\mu^2\sigma_r^2} + \right. \\ &\left. -(\bar{A}+\bar{R}\mu^2)^2 P_B e^{-k^2\mu^2\sigma_r^2}\left(2k\mu^2\sigma_r^2\cdot\frac{\partial k}{\partial d} + 2k^2\mu\sigma_r^2\cdot\frac{\partial \mu}{\partial d}\right)\right],\end{aligned}$$

where

$$\begin{aligned}\frac{\partial k}{\partial d} &= k_r\frac{\partial Q}{\partial d} \\ \frac{\partial \mu}{\partial d} &= -\frac{E\mu_r}{E_r Q^2}\frac{\partial Q}{\partial d}\end{aligned}$$

and

$$\frac{\partial Q}{\partial d} = \frac{2E^2d^2\mu_r^2E_r - 2E_r\left(E^2d^2\mu_r^2 - E_r^2d_r^2(\mu_r^2-1)\right)}{2E_r^2d^2\sqrt{E^2d^2\mu_r^2 - E_r^2d_r^2(\mu_r^2-1)}}. \tag{6.42}$$

Now we calculate:

$$\frac{\partial k}{\partial E} = \frac{\partial}{\partial E}(Qk_r) = \tag{6.43}$$

$$= k_r \cdot \frac{2Ed^2\mu_r^2}{2\sqrt{E^2d^2\mu_r^2 - E_r^2d_r^2(\mu_r^2-1)}} = \tag{6.44}$$

$$= k_r \frac{E}{E_r^2}\mu_r^2 \cdot \frac{1}{Q} = \tag{6.45}$$

$$= \frac{k_r\mu_r}{E_r}\mu. \tag{6.46}$$

Calculation of $\frac{\partial \mu}{\partial E}$ will give:

$$\frac{\partial \mu}{\partial E} = \frac{\mu_r}{E_r}\frac{\partial}{\partial E}\left(\frac{E}{Q}\right) = \tag{6.47}$$

$$= \frac{\mu_r}{E_r} \cdot E_r d \cdot \frac{\sqrt{E^2d^2\mu_r^2 - E_r^2d_r^2(\mu_r^2-1)} - E \cdot 2Ed^2\mu_r^2 \frac{1}{2\sqrt{E^2d^2\mu_r^2 - E_r^2d_r^2(\mu_r^2-1)}}}{E^2d^2\mu_r^2 - E_r^2d_r^2(\mu_r^2-1)} = \tag{6.48}$$

$$= \frac{\mu_r}{E_r} \cdot \frac{1}{E_r d} \cdot \frac{1}{Q^2}\left[\sqrt{E^2d^2\mu_r^2 - E_r^2d_r^2(\mu_r^2-1)} - \frac{E^2d^2\mu_r^2}{\sqrt{E^2d^2\mu_r^2 - E_r^2d_r^2(\mu_r^2-1)}}\right] = \tag{6.49}$$

$$= \frac{\mu_r}{E_r} \cdot \frac{1}{Q^2}\left[Q - \frac{E^2d^2\mu_r^2}{E_r^2d^2} \cdot \frac{1}{Q}\right] = \tag{6.50}$$

$$= \frac{\mu}{E}\left[1-\mu^2\right], \tag{6.51}$$

while for $\frac{\partial d}{\partial E}$, taking the functional derivative, we have:

$$\frac{\partial d}{\partial E} = -\frac{1}{(1+z)H_0}\int_0^z \frac{d\tilde{z}}{E^2(\tilde{z})}. \tag{6.52}$$

However, the derivatives must be evaluated for the fiducial model in order to calculate the Fisher matrix. We then finally get:

$$\left.\frac{\partial \log P}{\partial \bar{A}}\right|_r = \frac{2}{(\bar{A}+\bar{R}\mu^2)}; \tag{6.53}$$

$$\left.\frac{\partial \log P}{\partial \bar{R}}\right|_r = \frac{2\mu^2}{(\bar{A}+\bar{R}\mu^2)}; \tag{6.54}$$

$$\left.\frac{\partial \log P}{\partial E}\right|_r = k \cdot \frac{1}{P_B}\frac{dP_B}{dk}\left[\frac{\mu^2}{E_r} + (\mu^2-1)\frac{1}{d}\frac{\partial d}{\partial E}\right] + \frac{4\bar{R}\mu^2(1-\mu^2)}{(\bar{A}+\bar{R}\mu^2)} \cdot \left[\frac{1}{E_r} + \frac{1}{d}\frac{\partial d}{\partial E}\right] - \frac{2k^2\mu^2\sigma_r^2}{E_r}, \tag{6.55}$$

where we have set $\mu_r \equiv \mu$, $k_r \equiv k$, $E \equiv E_r$ since they coincide for the fiducial model. It has been verified that the last term can be neglected since its contribution is small.

Calculation of the effective volume

Now we have to calculate the effective volume

$$V_{eff}(k,\mu) = \left[\frac{nP(k,\mu)}{nP(k,\mu)+1}\right]^2 V_{survey}, \tag{6.56}$$

where $P(k,\mu)$ is the galaxy power spectrum (6.25) with the assumption (6.30).

The volume V_{survey} is the comoving volume of the redshift shell in which the survey is performed. The physical volume element of the redshift shell $[z, z+dz]$ per unit solid angle is given, setting $c = 1$, by [15]:

$$\frac{dV_{phys}}{d\Omega dz} = d^2(z) \cdot \frac{1}{H_0} \cdot \frac{1}{E(z)(1+z)}, \tag{6.57}$$

where $d(z)$ is the angular diameter distance (1.60) and $E(z) \equiv H(z)/H_0$ is given by

$$E(z) = \left[\Omega_r^{(0)}(1+z)^4 + \Omega_m^{(0)}(1+z)^3 + \Omega_{DE}^{(0)}(1+z)^{3(1+w)} + \Omega_K^{(0)}(1+z)^2\right]^{1/2}. \tag{6.58}$$

Notice that we are using H_0 expressed in units $c \cdot h/Mpc$: $H_{0(nat)} = H_{0(phys)}/c_{(phys)} = 100/c_{(phys)} \simeq 1/3000$, where $c_{(phys)}$ is the speed of light in km/s.

The comoving volume element is given by the physical one multiplied by a factor $(1+z)^3$. To obtain the survey volume of the shell $[z_{min}, z_{max}]$ we have to integrate over the redshift interval and over the solid angle Ω. The survey volume is then:

$$V_{survey} = \frac{\Omega \cdot d^2(z_{min})}{H_0} \int_{z_{min}}^{z_{max}} \frac{(1+z)^2}{E(z)} dz \tag{6.59}$$

Calculation of the Fisher matrix

We can now calculate the Fisher matrix

$$F_{ab} = \frac{1}{8\pi} \int_{-1}^{+1} d\mu \int_{k_{min}}^{k_{max}} k^2 dk V_{eff}(k,\mu) \left.\frac{d\log P}{dp_a}\right|_r \left.\frac{d\log P}{dp_b}\right|_r. \tag{6.60}$$

We can write it as:

$$F_{ab} = \frac{1}{8\pi} \int_{-1}^{+1} d\mu \int_{k_{min}}^{k_{max}} k^2 dk \frac{n^2P^2}{[nP+1]^2} V_{survey} M_{ab}(k,\mu), \tag{6.61}$$

where $M_{\alpha\beta}$ is the matrix obtained from the products of the derivatives:

$$M_{ab}(k,\mu) = \left.\frac{d\log P}{dp_a}\right|_r \left.\frac{d\log P}{dp_b}\right|_r. \tag{6.62}$$

Therefore, we can write the elements of the matrix $M_{ab}(k,\mu) = \begin{pmatrix} M_{\bar{A}\bar{A}} & M_{\bar{A}\bar{R}} & M_{\bar{A}E} \\ M_{\bar{R}\bar{A}} & M_{\bar{R}\bar{R}} & M_{\bar{R}E} \\ M_{E\bar{A}} & M_{E\bar{R}} & M_{EE} \end{pmatrix}$ as:

$$M_{\bar{A}\bar{A}} \equiv \left(\frac{d\log P}{d\bar{A}}\bigg|_r \right)^2 \tag{6.63}$$

et cetera.

Of course, $d_r = d_r(\hat{z})$ and $E_r = E_r(\hat{z})$ are calculated by putting the ΛCDM parameters and $z = \hat{z}$ in the formulas (1.60) and (6.58) respectively.

We have then calculated the Fisher matrix for each bin; if we want to take into account more than one redshift bin, we can calculate the Fisher matrix for each redshift bin and then build the total Fisher matrix block-wise. In our case we choose to consider bins of size $\Delta z = 0.1$ in the interval $0.65 < z < 2.05$; the values of n to be used in each bin are reported in [11], p.84 and in Table 6.2. We also consider bins of size $\Delta z = 0.2$; in this case the value of n for each bin is given by the average of the two corresponding values in the previous binning, given in Table .

An efficiency parameter ε_{eff} can be introduced in order to take into account the success rate of the survey in measuring redshifts. We then have $n = \varepsilon_{eff} \cdot n_{ref}$, being n_{ref} the reference value. We used $\varepsilon_{eff} = 1$ for the reference case, $\varepsilon_{eff} = 0.5$ for a pessimistic case and $\varepsilon_{eff} = 1.4$ for an optimistic case.

The integration limit k_{min} in the Fisher matrix can be taken to be equal to zero, because the integrand vanishes rapidly for small k; the small scale cut-off limit k_{max} is instead chosen to discard the nonlinear part of the spectrum. It is a good choice for k_{max} to impose $\sigma_R^2 = 0.25$ in equation (3.26), with $R = \pi/(2k_{max})$, where instead of $P(k)$ we consider the spectrum for the redshift z given by $P(k,z) = G^2(z)P_{Bardeen}(k)$, being $G(z)$ the growth function [16]. We will then have a different value of k_{max} for each redshift bin; the values of k_{max} use for each bin are also reported in Tables 6.2, 6.3, for the two cases $\Delta z = 0.1$ and $\Delta z = 0.2$, respectively.

z	$\hat{z}$	$n_{ref}(z) \times 10^{-3}$	k_{max}
0.65-0.75	0.7	1.25	0.162
0.75-0.85	0.8	1.92	0.172
0.85-0.95	0.9	1.83	0.183
0.95-1.05	1.0	1.68	0.194
1.05-1.15	1.1	1.51	0.206
1.15-1.25	1.2	1.35	0.218
1.25-1.35	1.3	1.20	0.232
1.35-1.45	1.4	1.00	0.245
1.45-1.55	1.5	0.80	0.260
1.55-1.65	1.6	0.58	0.274
1.65-1.75	1.7	0.38	0.290
1.75-1.85	1.8	0.35	0.306
1.85-1.95	1.9	0.21	0.323
1.95-2.05	2.0	0.11	0.341

Table 6.2: Values of the expected galaxy number densities n_{ref} for the *Euclid* survey in units of $(h/Mpc)^3$. Redshift interval: $0.65 < z < 2.05$, bin size $\Delta z = 0.1$.

z	$\hat{z}$	$n_{ref}(z) \times 10^{-3}$	k_{max}
0.65-0.85	0.75	1.59	0.167
0.85-1.05	0.95	1.76	0.188
1.05-1.25	1.15	1.43	0.212
1.25-1.45	1.35	1.10	0.238
1.45-1.65	1.55	0.69	0.267
1.65-1.85	1.75	0.37	0.298
1.85-2.05	1.95	0.16	0.332

Table 6.3: Values of the expected galaxy number densities n_{ref} for the *Euclid* survey in units of $(h/Mpc)^3$. Redshift interval: $0.65 < z < 2.05$, bin size $\Delta z = 0.2$.

In Figure 6.2 we show the structure of the Fisher matrix for galaxy clustering for $\Delta z = 0.1$ and $\Delta z = 0.2$; as an example, only the ones for $\varepsilon_{eff} = 1$ are shown.

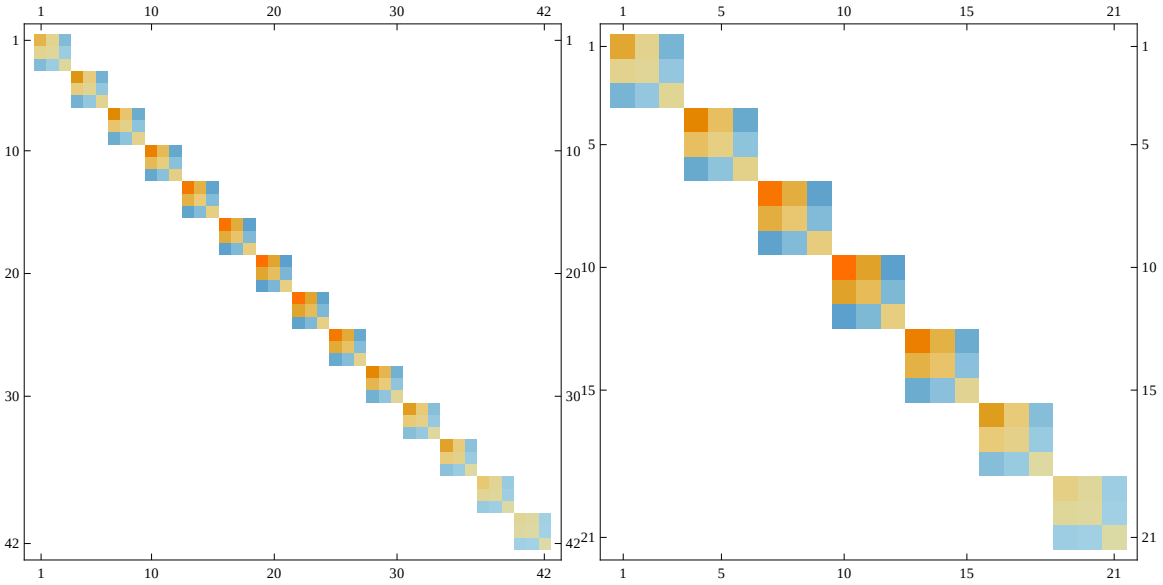

Figure 6.2: Structure of the Fisher matrix for galaxy clustering for bin size $\Delta z = 0.1$ (left) and $\Delta z = 0.2$ (right), with $\varepsilon_{eff} = 1$. Orange is for positive entries, blue for negative ones; color intensity represents the absolute value of the entry (the bigger the number, the darker the color).

Errors on P_1

It could be interesting to find the errors on P_1 given by the galaxy clustering only. If we want to find the error on the parameter $P_1 = \bar{R}/\bar{A}$, we have to transform the Fisher matrix for the parameters $\{\bar{A}, \bar{R}, E\}$ in the one for $\{\bar{A}, P_1, E\}$. The new Fisher matrix, according to equation (5.79), is given by:

$$F^{new} = J^T F J, \tag{6.64}$$

where J is the Jacobian of the transformation:

$$J = \begin{pmatrix} \frac{\partial \bar{A}}{\partial \bar{A}} & \frac{\partial \bar{A}}{\partial P_1} & \frac{\partial \bar{A}}{\partial E} \\ \frac{\partial \bar{R}}{\partial \bar{A}} & \frac{\partial \bar{R}}{\partial P_1} & \frac{\partial \bar{R}}{\partial E} \\ \frac{\partial E}{\partial \bar{A}} & \frac{\partial E}{\partial P_1} & \frac{\partial E}{\partial E} \end{pmatrix}. \tag{6.65}$$

Evaluating the single derivatives gives:

$$\frac{\partial \bar{A}}{\partial \bar{A}} = 1, \tag{6.66}$$

$$\frac{\partial \bar{A}}{\partial P_1} = -\frac{\bar{R}}{P_1^2} = -\frac{\bar{A}^2}{\bar{R}}, \tag{6.67}$$

$$\frac{\partial \bar{R}}{\partial P_1} = \bar{A}, \tag{6.68}$$

$$\frac{\partial E}{\partial E} = 1, \tag{6.69}$$

all other derivatives are equal to zero.

With J we can now evaluate the new Fisher matrix for each bin; the squared errors for the parameters $\{\bar{A}, P_2, E\}$ are on the diagonal of its inverse.

6.3.1 Errors from galaxy clustering only

Here we summarize the errors on the parameters obtained from the galaxy clustering only, with the two different choices for the bin size $\Delta z = 0.1$ and $\Delta z = 0.2$. For each choice of Δz, we did three different calculation using the three different values of the efficiency parameter ε_{eff} specified above.

6.3.1.1 Bin size $\Delta z = 0.1$

$\varepsilon_{eff} = 1$ **: reference case**

z_α	$\bar{A}(z_\alpha)$	$\Delta\bar{A}(z_\alpha)$	$\Delta\bar{A}(z_\alpha)(\%)$	$\bar{R}(z_\alpha)$	$\Delta\bar{R}(z_\alpha)$	$\Delta\bar{R}(z_\alpha)(\%)$	$E(z_\alpha)$	$\Delta E(z_\alpha)$	$\Delta E(z_\alpha)(\%)$
0.7	0.577	0.0038	0.67	0.460	0.0038	0.83	1.45	0.0101	0.74
0.8	0.551	0.0031	0.56	0.453	0.0029	0.65	1.54	0.0089	0.58
0.9	0.527	0.0027	0.52	0.444	0.0025	0.56	1.63	0.0081	0.50
1.0	0.504	0.0024	0.49	0.434	0.0022	0.51	1.73	0.0076	0.44
1.1	0.483	0.0023	0.47	0.424	0.0020	0.47	1.83	0.0073	0.40
1.2	0.464	0.0021	0.46	0.413	0.0018	0.44	1.93	0.0071	0.37
1.3	0.446	0.0020	0.45	0.402	0.0017	0.43	2.04	0.0071	0.35
1.4	0.429	0.0020	0.47	0.391	0.0017	0.43	2.15	0.0073	0.34
1.5	0.413	0.0021	0.51	0.381	0.0017	0.46	2.27	0.0079	0.35
1.6	0.398	0.0023	0.59	0.370	0.0020	0.53	2.39	0.0092	0.38
1.7	0.385	0.0029	0.75	0.360	0.0025	0.69	2.51	0.012	0.47
1.8	0.372	0.0030	0.81	0.350	0.0026	0.73	2.63	0.013	0.48
1.9	0.360	0.0043	1.2	0.341	0.0037	1.1	2.76	0.019	0.68
2.0	0.348	0.0072	2.1	0.332	0.0063	1.9	2.89	0.033	1.1

Table 6.4: Values, errors and percent errors on the parameters $\bar{A}, \bar{R}, E$ for every redshift bin from galaxy clustering only, $\Delta z = 0.1$, $\varepsilon_{eff} = 1$.

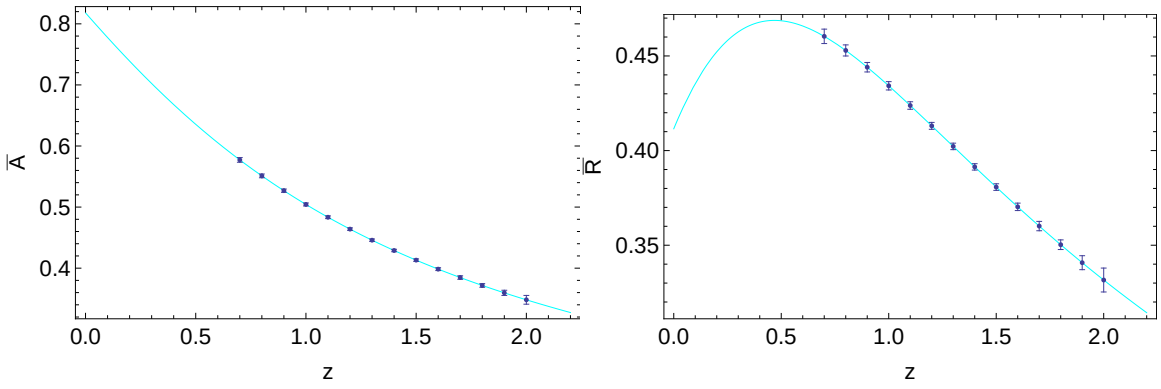

Figure 6.3: Errors on $\bar{A}$ (left) and $\bar{R}$ (right) from galaxy clustering, $\Delta z = 0.1$, $\varepsilon_{eff} = 1$.

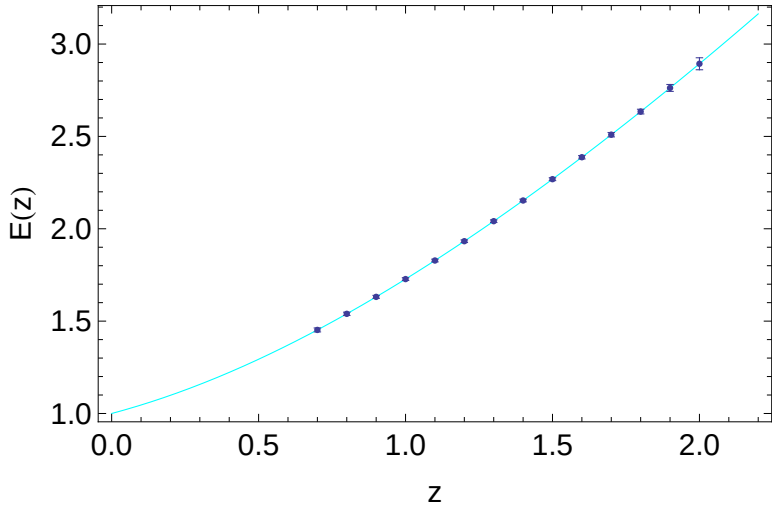

Figure 6.4: Errors on E from galaxy clustering, $\Delta z = 0.1$, $\varepsilon_{eff} = 1$.

z_α	$P_1(z_\alpha)$	$\Delta P_1(z_\alpha)$	$\Delta P_1(z_\alpha)(\%)$
0.7	0.798	0.0066	0.83
0.8	0.822	0.0053	0.65
0.9	0.843	0.0048	0.56
1.0	0.861	0.0044	0.51
1.1	0.877	0.0041	0.47
1.2	0.890	0.0039	0.44
1.3	0.902	0.0038	0.43
1.4	0.913	0.0039	0.43
1.5	0.922	0.0042	0.46
1.6	0.929	0.0049	0.53
1.7	0.936	0.0064	0.69
1.8	0.942	0.0069	0.73
1.9	0.948	0.010	1.1
2.0	0.952	0.018	1.9

Table 6.5: Values, errors and percent errors on the parameter P_1 for every redshift bin from galaxy clustering only, $\Delta z = 0.1$, $\varepsilon_{eff} = 1$.

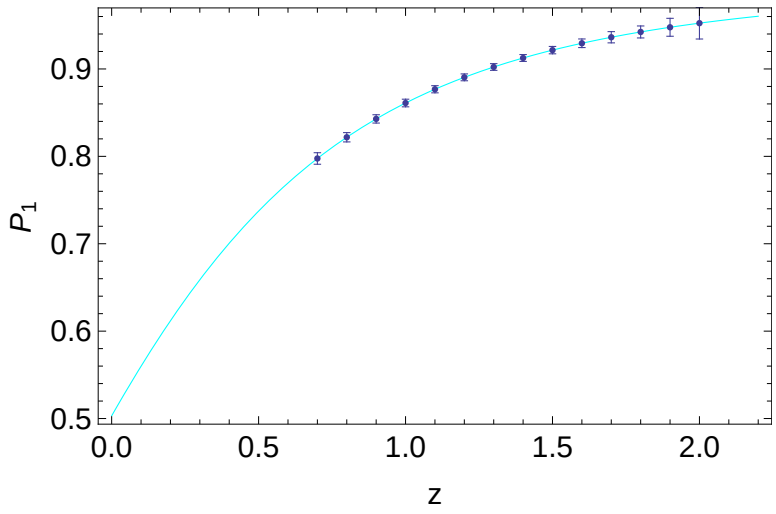

Figure 6.5: Errors on P_1 from galaxy clustering, $\Delta z = 0.1$, $\varepsilon_{eff} = 1$.

Taking into account, for example, Table 6.4 and Table 6.2, we can see that the errors' magnitude follows roughly the magnitude of n_{ref} in each bin; this is reasonable, since in the bins where we have a larger the number of galaxies we can get more statistical information and put better constraints on the parameters. In fact, the errors are smaller in the middle bins, where n_{ref} takes the higher values.

We can see, however, that the difference in percent errors for the same parameter in different bins is not larger than one order of magnitude.

A note on P_1: we can see that the percent error is the same as $\bar{R}$ in every bin; as we will see, this holds true independently of ε_{eff}. This happens because we replaced the set of parameters $\{\bar{A},\bar{R},E\}$ with the set $\{\bar{A},P_1,E\}$, where P_1 is just a combination of $\bar{R}$ and $\bar{A}$; therefore, the jacobian just rescales the absolute error, so that the percent error on P_1 is the same as on $\bar{R}$.

$\varepsilon_{eff} = 0.5$**: pessimistic case**

z_α	$\bar{A}(z_\alpha)$	$\Delta\bar{A}(z_\alpha)$	$\Delta\bar{A}(z_\alpha)(\%)$	$\bar{R}(z_\alpha)$	$\Delta\bar{R}(z_\alpha)$	$\Delta\bar{R}(z_\alpha)(\%)$	$E(z_\alpha)$	$\Delta E(z_\alpha)$	$\Delta E(z_\alpha)(\%)$
0.7	0.577	0.00445	0.77	0.460	0.0046	0.99	1.45	0.013	0.86
0.8	0.551	0.0035	0.63	0.453	0.0034	0.75	1.54	0.010	0.66
0.9	0.527	0.0031	0.59	0.444	0.0030	0.67	1.63	0.0094	0.58
1.0	0.504	0.0029	0.57	0.434	0.0027	0.62	1.73	0.0090	0.52
1.1	0.483	0.0027	0.56	0.424	0.0025	0.59	1.83	0.0089	0.49
1.2	0.464	0.0026	0.57	0.413	0.0024	0.58	1.93	0.0090	0.46
1.3	0.446	0.0026	0.58	0.402	0.0023	0.58	2.04	0.0092	0.45
1.4	0.429	0.0027	0.63	0.391	0.0024	0.61	2.15	0.0099	0.46
1.5	0.413	0.0029	0.71	0.381	0.0026	0.68	2.27	0.011	0.49
1.6	0.398	0.0035	0.87	0.370	0.0031	0.83	2.39	0.014	0.58
1.7	0.385	0.0046	1.2	0.360	0.0041	1.1	2.51	0.019	0.75
1.8	0.372	0.0049	1.3	0.350	0.0043	1.2	2.63	0.021	0.79
1.9	0.360	0.0074	2.1	0.341	0.0066	1.9	2.76	0.032	1.2
2.0	0.348	0.013	3.8	0.332	0.012	3.6	2.89	0.060	2.1

Table 6.6: Values, errors and percent errors on the parameters $\bar{A},\bar{R},E$ for every redshift bin from galaxy clustering only, $\Delta z = 0.1$, $\varepsilon_{eff} = 0.5$.

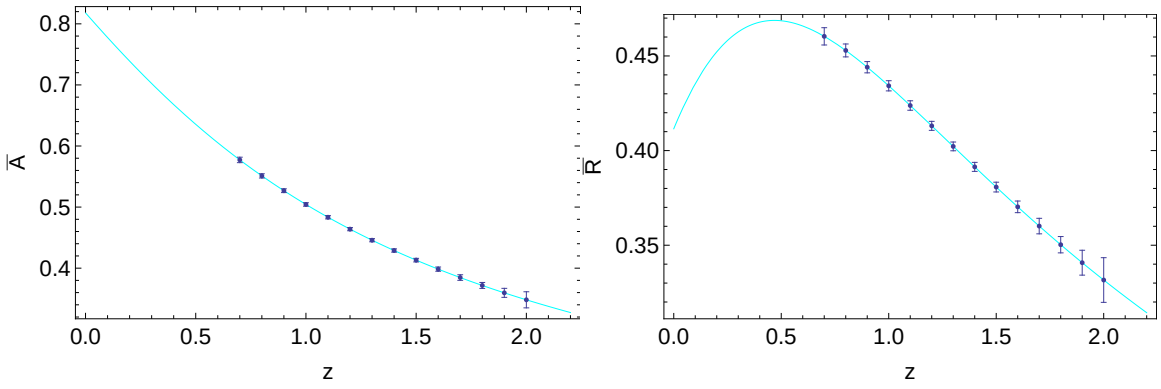

Figure 6.6: Errors on $\bar{A}$ (left) and $\bar{R}$ (right) from galaxy clustering, $\Delta z = 0.1$, $\varepsilon_{eff} = 0.5$.

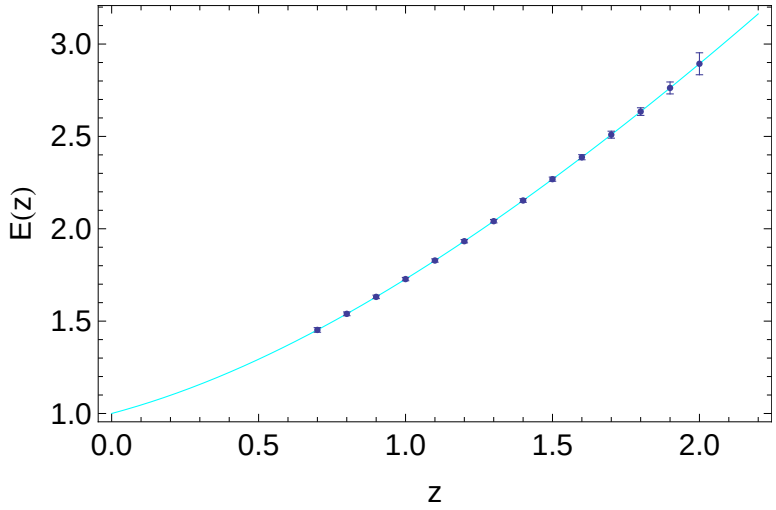

Figure 6.7: Errors on E from galaxy clustering, $\Delta z = 0.1$, $\varepsilon_{eff} = 0.5$.

z_α	$P_1(z_\alpha)$	$\Delta P_1(z_\alpha)$	$\Delta P_1(z_\alpha)(\%)$
0.7	0.798	0.0079	0.99
0.8	0.822	0.0062	0.75
0.9	0.843	0.0057	0.67
1.0	0.861	0.0053	0.62
1.1	0.877	0.0052	0.59
1.2	0.890	0.0051	0.58
1.3	0.902	0.0052	0.58
1.4	0.913	0.0056	0.61
1.5	0.922	0.0062	0.68
1.6	0.929	0.0077	0.83
1.7	0.936	0.011	1.1
1.8	0.942	0.012	1.2
1.9	0.948	0.018	1.9
2.0	0.952	0.034	3.6

Table 6.7: Values, errors and percent errors on the parameter P_1 for every redshift bin from galaxy clustering only, $\Delta z = 0.1$, $\varepsilon_{eff} = 0.5$.

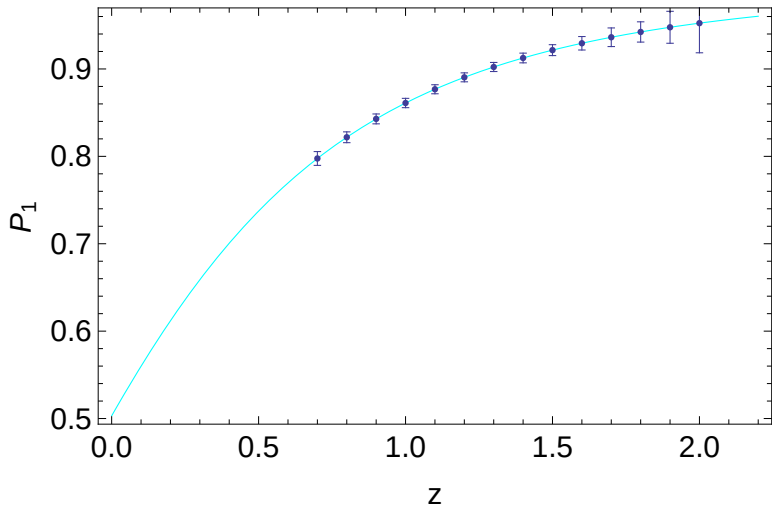

Figure 6.8: Errors on P_1 from galaxy clustering, $\Delta z = 0.1$, $\varepsilon_{eff} = 0.5$.

As we can see, the percent errors on the three parameters depend slightly on the value of ε_{eff} in the first bins, but ε_{eff} has stronger effects in the last bins, where the number of galaxy is smaller and therefore there is less statistics.

$\varepsilon_{eff} = 1.4$**: optimistic case**

z_α	$\bar{A}(z_\alpha)$	$\Delta\bar{A}(z_\alpha)$	$\Delta\bar{A}(z_\alpha)(\%)$	$\bar{R}(z_\alpha)$	$\Delta\bar{R}(z_\alpha)$	$\Delta\bar{R}(z_\alpha)(\%)$	$E(z_\alpha)$	$\Delta E(z_\alpha)$	$\Delta E(z_\alpha)(\%)$
0.7	0.577	0.0037	0.63	0.460	0.00358	0.78	1.45	0.010	0.70
0.8	0.551	0.0030	0.54	0.453	0.00279	0.62	1.54	0.0085	0.55
0.9	0.527	0.0026	0.49	0.444	0.00236	0.53	1.63	0.0077	0.47
1.0	0.504	0.0023	0.46	0.434	0.00205	0.47	1.73	0.0072	0.41
1.1	0.483	0.0021	0.44	0.424	0.00182	0.43	1.83	0.0068	0.37
1.2	0.464	0.0020	0.42	0.413	0.00165	0.40	1.93	0.0065	0.34
1.3	0.446	0.0018	0.41	0.402	0.00153	0.38	2.04	0.0064	0.31
1.4	0.429	0.0018	0.42	0.391	0.00147	0.38	2.15	0.0065	0.30
1.5	0.413	0.0018	0.44	0.381	0.00149	0.39	2.27	0.0069	0.30
1.6	0.398	0.0020	0.50	0.370	0.00163	0.44	2.39	0.0078	0.33
1.7	0.385	0.0024	0.62	0.360	0.00198	0.55	2.51	0.0097	0.39
1.8	0.372	0.0024	0.66	0.350	0.00202	0.58	2.63	0.010	0.39
1.9	0.360	0.0034	0.93	0.341	0.00284	0.83	2.76	0.015	0.53
2.0	0.348	0.0054	1.6	0.332	0.00473	1.4	2.89	0.025	0.85

Table 6.8: Values, errors and percent errors on the parameters $\bar{A}, \bar{R}, E$ for every redshift bin from galaxy clustering only, $\Delta z = 0.1$, $\varepsilon_{eff} = 1.4$.

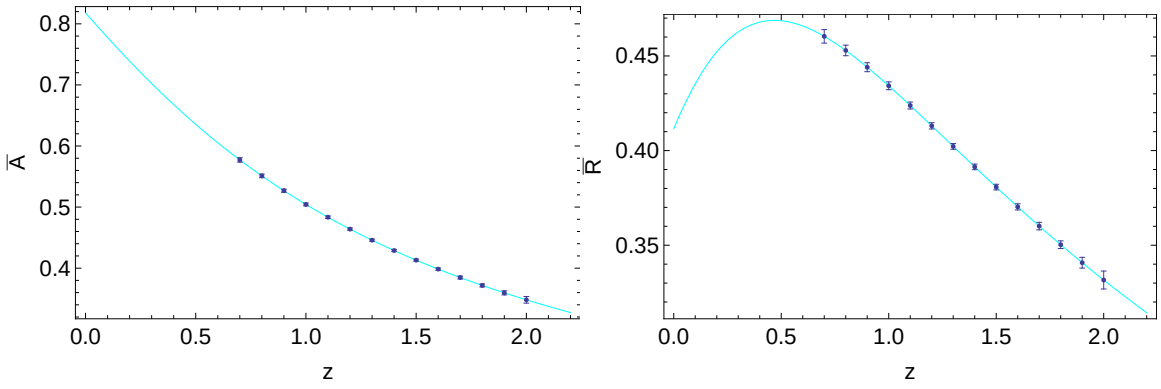

Figure 6.9: Errors on $\bar{A}$ (left) and $\bar{R}$ (right) from galaxy clustering, $\Delta z = 0.1$, $\varepsilon_{eff} = 1.4$.

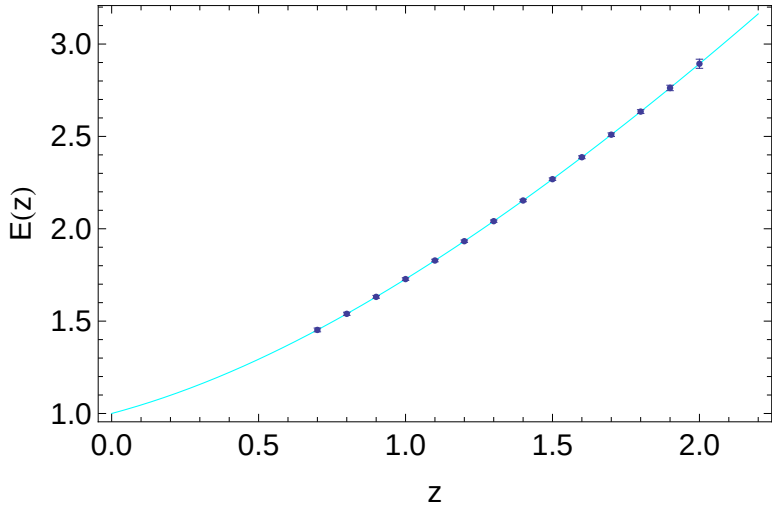

Figure 6.10: Errors on E from galaxy clustering, $\Delta z = 0.1$, $\varepsilon_{eff} = 1.4$.

z_α	$P_1(z_\alpha)$	$\Delta P_1(z_\alpha)$	$\Delta P_1(z_\alpha)(\%)$
0.7	0.798	0.0062	0.78
0.8	0.822	0.0051	0.62
0.9	0.843	0.0045	0.53
1.0	0.861	0.0041	0.47
1.1	0.877	0.0038	0.43
1.2	0.890	0.0036	0.40
1.3	0.902	0.0034	0.38
1.4	0.913	0.0034	0.38
1.5	0.922	0.0036	0.39
1.6	0.929	0.0041	0.44
1.7	0.936	0.0052	0.55
1.8	0.942	0.0054	0.58
1.9	0.948	0.0079	0.83
2.0	0.952	0.014	1.4

Table 6.9: Values, errors and percent errors on the parameter P_1 for every redshift bin from galaxy clustering only, $\Delta z = 0.1$, $\varepsilon_{eff} = 1.4$.

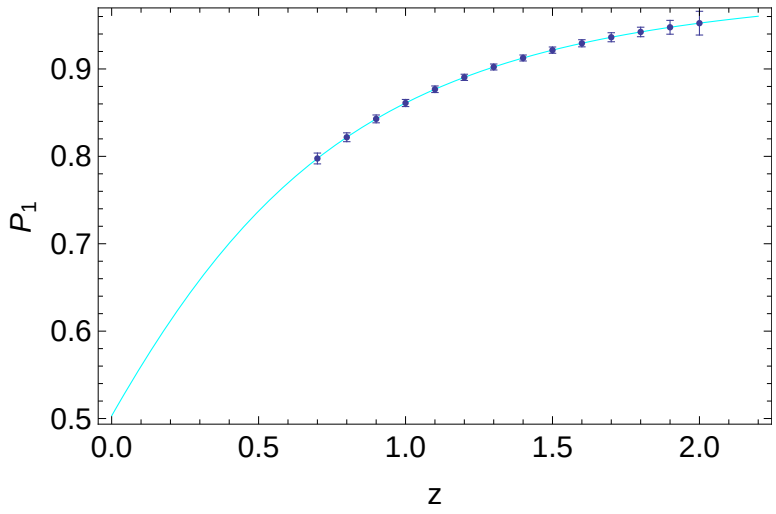

Figure 6.11: Errors on P_1 from galaxy clustering, $\Delta z = 0.1$, $\varepsilon_{eff} = 1.4$.

Again, the errors in the last bins are more influenced by the variation of ε_{eff}. In general, however, we can see from the comparison of Tables 6.6 and 6.8 that the difference in ε_{eff} can cause at most a difference of a factor of 2 to 2.5 in the percent error of the three parameters.

6.3.1.2 Bin size $\Delta z = 0.2$

$\varepsilon_{eff} = 1$ **: reference case**

z_α	$\bar{A}(z_\alpha)$	$\Delta\bar{A}(z_\alpha)$	$\Delta\bar{A}(z_\alpha)(\%)$	$\bar{R}(z_\alpha)$	$\Delta\bar{R}(z_\alpha)$	$\Delta\bar{R}(z_\alpha)(\%)$	$E(z_\alpha)$	$\Delta E(z_\alpha)$	$\Delta E(z_\alpha)(\%)$
0.75	0.564	0.0025	0.44	0.457	0.0024	0.53	1.50	0.0071	0.47
0.95	0.515	0.0019	0.36	0.439	0.0017	0.38	1.68	0.0056	0.34
1.15	0.473	0.0016	0.33	0.418	0.0014	0.32	1.88	0.0051	0.27
1.35	0.437	0.0014	0.33	0.397	0.0012	0.30	2.10	0.0051	0.24
1.55	0.406	0.0016	0.38	0.375	0.0013	0.34	2.33	0.0060	0.26
1.75	0.378	0.0021	0.55	0.355	0.0018	0.50	2.57	0.0087	0.34
1.95	0.354	0.0037	1.1	0.336	0.0032	0.96	2.83	0.017	0.59

Table 6.10: Values, errors and percent errors on the parameters $\bar{A}, \bar{R}, E$ for every redshift bin from galaxy clustering only, $\Delta z = 0.2$, $\varepsilon_{eff} = 1$.

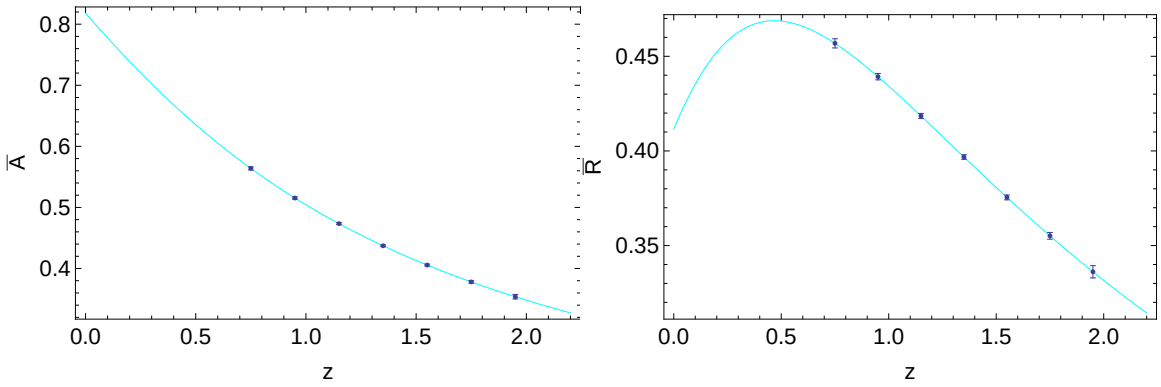

Figure 6.12: Errors on $\bar{A}$ (left) and $\bar{R}$ (right) from galaxy clustering, $\Delta z = 0.2$, $\varepsilon_{eff} = 1$.

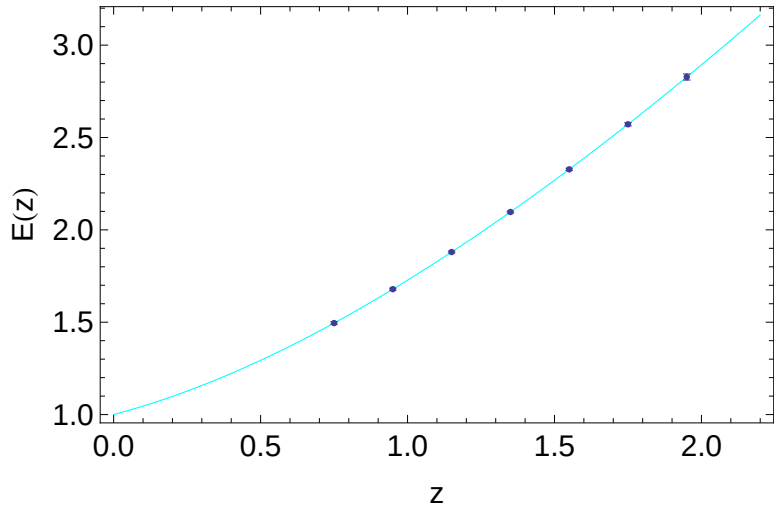

Figure 6.13: Errors on E from galaxy clustering, $\Delta z = 0.2$, $\varepsilon_{eff} = 1$.

z_α	$P_1(z_\alpha)$	$\Delta P_1(z_\alpha)$	$\Delta P_1(z_\alpha)(\%)$
0.75	0.810	0.0043	0.53
0.95	0.852	0.0033	0.38
1.15	0.884	0.0029	0.32
1.35	0.908	0.0028	0.30
1.55	0.926	0.0032	0.34
1.75	0.939	0.0047	0.50
1.95	0.950	0.0092	0.96

Table 6.11: Values, errors and percent errors on the parameter P_1 for every redshift bin from galaxy clustering only, $\Delta z = 0.2$, $\varepsilon_{eff} = 1$.

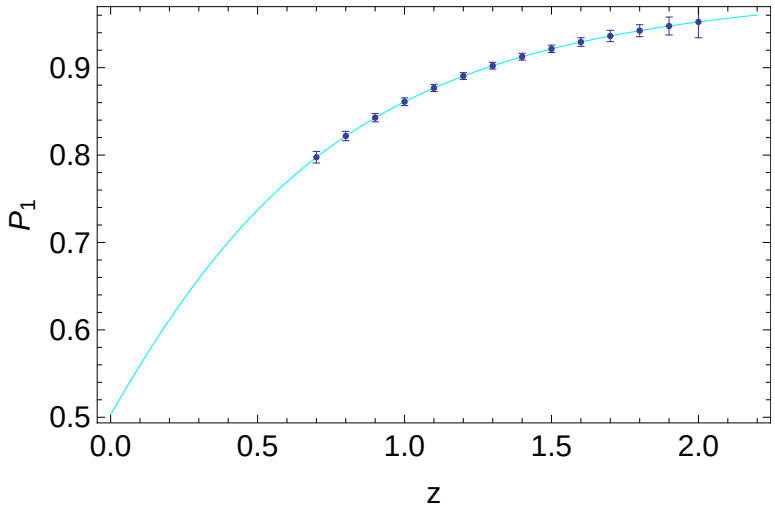

Figure 6.14: Errors on P_1 from galaxy clustering, $\Delta z = 0.2$, $\varepsilon_{eff} = 1$.

Comparing Tables 6.4 and 6.10, we can see that considering larger bins can reduce the uncertainties on the parameters (as expected, since the statistics is larger): we gain roughly a factor between 1.5 and 2 on the percent errors.

$\varepsilon_{eff} = 0.5$**: pessimistic case**

z_α	$\bar{A}(z_\alpha)$	$\Delta\bar{A}(z_\alpha)$	$\Delta\bar{A}(z_\alpha)(\%)$	$\bar{R}(z_\alpha)$	$\Delta\bar{R}(z_\alpha)$	$\Delta\bar{R}(z_\alpha)(\%)$	$E(z_\alpha)$	$\Delta E(z_\alpha)$	$\Delta E(z_\alpha)(\%)$
0.75	0.564	0.0029	0.51	0.457	0.0029	0.62	1.50	0.0081	0.55
0.95	0.515	0.0022	0.42	0.439	0.0020	0.46	1.68	0.0066	0.39
1.15	0.473	0.0019	0.40	0.418	0.0017	0.41	1.88	0.0064	0.34
1.35	0.437	0.0019	0.43	0.397	0.0017	0.42	2.10	0.0068	0.32
1.55	0.406	0.0022	0.55	0.375	0.0020	0.52	2.33	0.0087	0.37
1.75	0.378	0.0033	0.88	0.355	0.0030	0.84	2.57	0.014	0.54
1.95	0.354	0.0066	1.9	0.336	0.0059	1.8	2.83	0.029	1.0

Table 6.12: Values, errors and percent errors on the parameters $\bar{A}, \bar{R}, E$ for every redshift bin from galaxy clustering only, $\Delta z = 0.2$, $\varepsilon_{eff} = 0.5$.

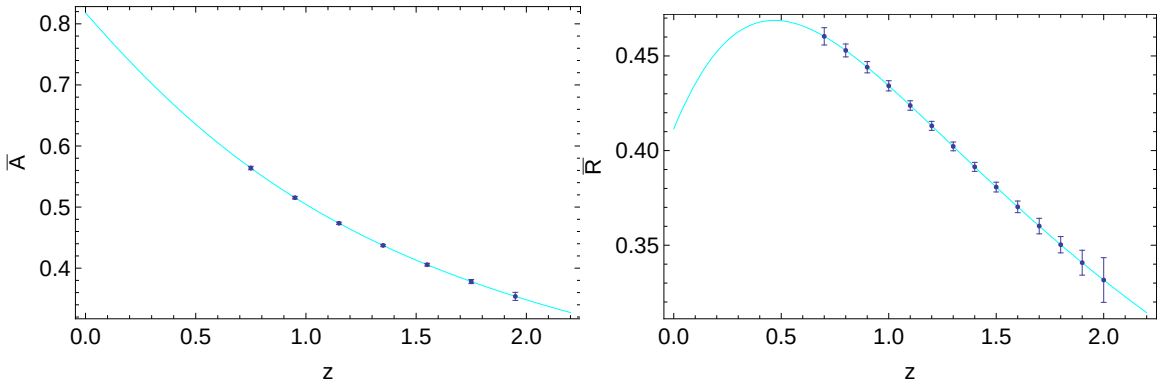

Figure 6.15: Errors on $\bar{A}$ (left) and $\bar{R}$ (right) from galaxy clustering, $\Delta z = 0.2$, $\varepsilon_{eff} = 0.5$.

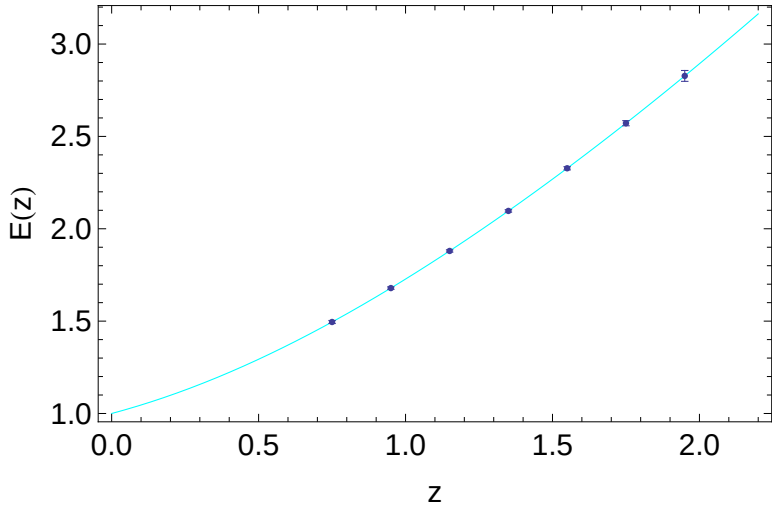

Figure 6.16: Errors on E from galaxy clustering, $\Delta z = 0.2$, $\varepsilon_{eff} = 0.5$.

z_α	$P_1(z_\alpha)$	$\Delta P_1(z_\alpha)$	$\Delta P_1(z_\alpha)(\%)$
0.75	0.810	0.0051	0.62
0.95	0.852	0.0039	0.46
1.15	0.884	0.0037	0.41
1.35	0.908	0.0038	0.42
1.55	0.926	0.0049	0.52
1.75	0.939	0.0078	0.84
1.95	0.950	0.017	1.8

Table 6.13: Values, errors and percent errors on the parameter P_1 for every redshift bin from galaxy clustering only, $\Delta z = 0.2$, $\varepsilon_{eff} = 0.5$.

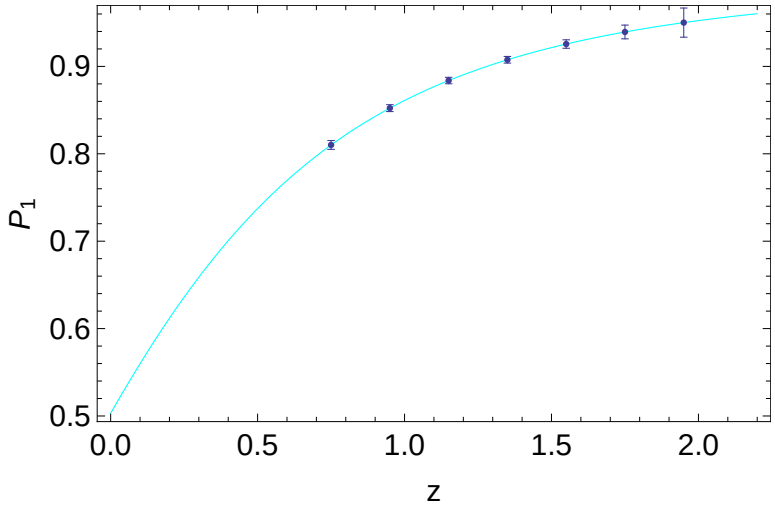

Figure 6.17: Errors on P_1 from galaxy clustering, $\Delta z = 0.2$, $\varepsilon_{eff} = 0.5$.

$\varepsilon_{eff} = 1.4$**: optimistic case**

z_α	$\bar{A}(z_\alpha)$	$\Delta\bar{A}(z_\alpha)$	$\Delta\bar{A}(z_\alpha)(\%)$	$\bar{R}(z_\alpha)$	$\Delta\bar{R}(z_\alpha)$	$\Delta\bar{R}(z_\alpha)(\%)$	$E(z_\alpha)$	$\Delta E(z_\alpha)$	$\Delta E(z_\alpha)(\%)$
0.75	0.564	0.0024	0.424	0.457	0.0023	0.50	1.50	0.0067	0.45
0.95	0.515	0.0018	0.341	0.439	0.0016	0.36	1.68	0.0053	0.32
1.15	0.473	0.0015	0.305	0.418	0.0012	0.30	1.88	0.0047	0.25
1.35	0.437	0.0013	0.295	0.397	0.0011	0.27	2.10	0.0046	0.22
1.55	0.406	0.0013	0.33	0.375	0.0011	0.29	2.33	0.0051	0.22
1.75	0.378	0.0017	0.45	0.355	0.0014	0.40	2.57	0.0071	0.27
1.95	0.354	0.0029	0.81	0.336	0.0025	0.73	2.83	0.013	0.45

Table 6.14: Values, errors and percent errors on the parameters $\bar{A}, \bar{R}, E$ for every redshift bin from galaxy clustering only, $\Delta z = 0.2$, $\varepsilon_{eff} = 1.4$.

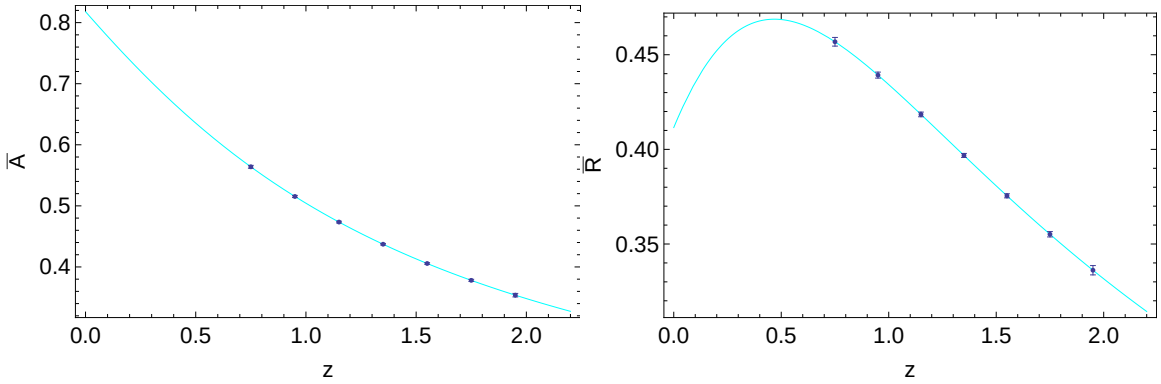

Figure 6.18: Errors on $\bar{A}$ (left) and $\bar{R}$ (right) from galaxy clustering, $\Delta z = 0.2$, $\varepsilon_{eff} = 1.4$.

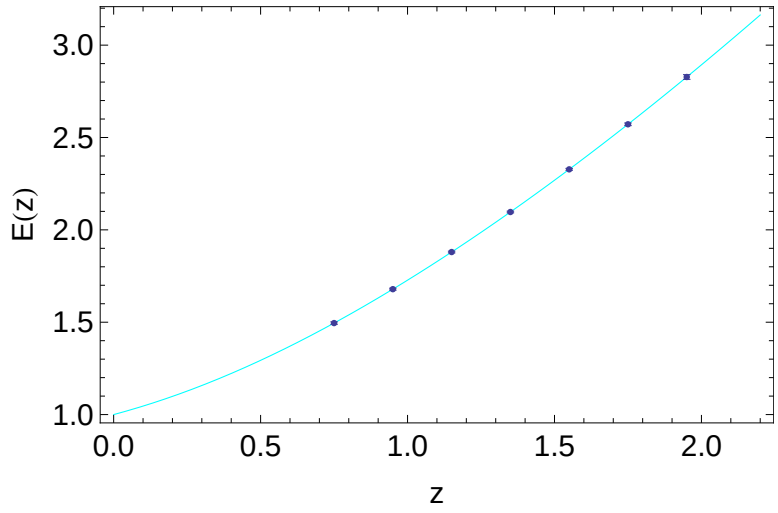

Figure 6.19: Errors on E from galaxy clustering, $\Delta z = 0.2$, $\varepsilon_{eff} = 1.4$.

z_α	$P_1(z_\alpha)$	$\Delta P_1(z_\alpha)$	$\Delta P_1(z_\alpha)(\%)$
0.75	0.810	0.0041	0.50
0.95	0.852	0.0031	0.36
1.15	0.884	0.0026	0.30
1.35	0.908	0.0024	0.27
1.55	0.926	0.0027	0.29
1.75	0.939	0.0037	0.40
1.95	0.950	0.0070	0.73

Figure 6.20: Values, errors and percent errors on the parameter P_1 for every redshift bin from galaxy clustering only, $\Delta z = 0.2$, $\varepsilon_{eff} = 1.4$.

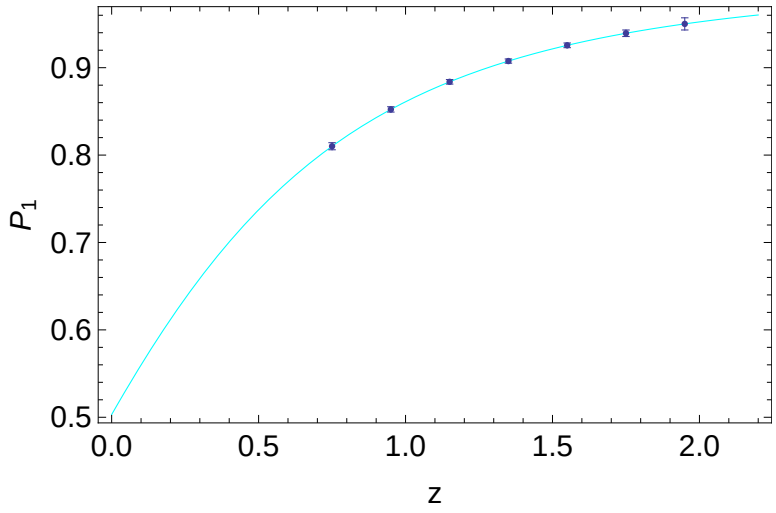

Figure 6.21: Errors on P_1 from galaxy clustering, $\Delta z = 0.2$, $\varepsilon_{eff} = 1.4$.

The effect of ε_{eff} is almost the same as in the case with smaller bins: there is about a factor-2.5-difference between the pessimistic and the optimistic case, and it is almost the same for all of the parameters.

6.4 Weak lensing

The lensing convergence power spectrum $P_{ij}(l)$ as a function of the multipole $l = k\pi$ for a survey divided into several redshift bins can be written as (5.62):

$$P_{ij}(l) = \frac{9H_0}{4}\int_0^\infty dz \frac{W_i(z)W_j(z)E^3(z)\Omega_m^2(z)}{(1+z)^4}\Sigma^2 P_{\delta_m}\left(\frac{l}{\pi r(z)}, z\right), \tag{6.70}$$

where H_0 is expressed in units $c \times h/Mpc$, the lensing window function is (5.61)

$$W_i(z) = \int_z^\infty \frac{d\tilde{z}}{E(\tilde{z})}\left[1 - \frac{r(z)}{r(\tilde{z})}\right] n_i(r(\tilde{z})), \tag{6.71}$$

$r(z)$ is the comoving distance (1.48), $E(z) = H(z)/H_0$, $\Omega_m(z) = \rho_{0m}(1+z)^3/\rho_{cr}(z)$ as usual and $n_i(r(z))$ is the bin galaxy density function (which will be better defined later).

It can be shown that the lensing convergence power spectrum can be written as

$$P_{ij}(l) = H_0 \int_0^\infty \frac{d\tilde{z}}{E(\tilde{z})} K_i(\tilde{z})K_j(\tilde{z})L(\tilde{z}, l)^2, \tag{6.72}$$

where

$$K_i(z) = \frac{3}{2}(1+z)W_i(z) \tag{6.73}$$

and

$$L(z,l) = \Omega_{0m}\Sigma G(z)\sigma_8\delta_{t,0}\left(k \to \frac{l}{\pi r(z)}\right), \tag{6.74}$$

being $\Omega_{0m} \equiv \Omega_m^{(0)}$, $\Sigma = 2$ for the fiducial model ΛCDM and $\delta_{t,0}^2(k) = P_{\delta_m}(k, z=0)$ the matter power spectrum at present time.

In fact, inserting the definitions (6.73) and (6.74) into equation (6.72), we get:

$$P_{ij}(k) = H_0 \int_0^{z_{max}} \frac{d\tilde{z}}{E(\tilde{z})}\frac{9}{4}(1+\tilde{z})^2 W_i(\tilde{z})W_j(\tilde{z})\Omega_{0m}^2\Sigma^2 G^2(z)\sigma_8^2\delta_{t,0}^2\left(\frac{k}{r(z)}\right). \tag{6.75}$$

where the scale k in $\delta_{t,0}^2$ is now divided by $r(z)$, according to the fact that $P_{\delta_m}(k,z) = G^2(z)\delta_{t,0}^2(k)$ and to Limber's theorem, which says that $P_{\delta_m}(k,z)$ must be evaluated for $k \to \frac{k}{r(z)}$.

In the condition of pressureless and uncoupled matter, the following identity holds:

$$\Omega_{0m}^2(1+z)^2 = \frac{E^4(z)\Omega_m^2(z)}{(1+z)^4}. \tag{6.76}$$

Therefore, we can write:

$$P_{ij}(l) = \frac{9H_0}{4}\int_0^\infty dz \frac{W_i(z)W_j(z)\Sigma^2 G^2(z)\sigma_8^2 E^3(z)\Omega_m^2(z)}{(1+z)^4} P_{\delta_m}\left(\frac{l}{\pi r(z)}, z=0\right) \tag{6.77}$$

which matches with equation (6.70) (the factor σ_8^2 accounts for the normalization of the power spectrum).

Assumption of Bardeen power spectrum

We assume again that the present matter power spectrum $\delta_{t,0}^2(k) = P_{\delta_m}(k, z=0)$ is given by the Bardeen approximation formula (6.30):

$$\delta_{t,0}^2(k) \approxeq P_{Bardeen}(k) = c_{norm}T^2(k)k^{n_s}, \tag{6.78}$$

where the normalization constant c_{norm} is fixed by the condition (6.31) and the transfer function is given by equation (5.9).

The power spectrum at any time will be given by $P_{\delta_m}(k,z) = G^2(z)P_{Bardeen}(k)$. Again, according to the Limber's theorem (5.51), to get an expression for $P_{ij}(l)$ we need to take into account $P_{\delta_m}\left(\frac{l}{\pi r(z)}, z\right)$, that is, we have to substitute $k \to \frac{l}{\pi r(z)}$ in the expression of the Bardeen spectrum (which contains the k-dependence of $P_{\delta_m}(k,z)$). That leads explicitly to

$$P_{\delta_m}\left(\frac{l}{\pi r(z)},z\right) = G^2(z)\cdot c_{norm}\frac{\ln^2(1+0.171\frac{l}{\pi r(z)k_{eq}})}{0.171^2\left(\frac{l}{\pi r(z)k_{eq}}\right)^2}\cdot$$
$$\cdot\left[1+0.284\frac{l}{\pi r(z)k_{eq}}+(1.18\frac{l}{\pi r(z)k_{eq}})^2+(0.399\frac{l}{\pi r(z)k_{eq}})^3+(0.490\frac{l}{\pi r(z)k_{eq}})^4\right]^{-1/2}\cdot\frac{l}{\pi r(z)}. \tag{6.79}$$

Total galaxy density function and galaxy density functions for each redshift bin

We are also assuming for the galaxy density $n(z)$ the common parameterization (see [17] and [18]):

$$n(z) = n_0 z^\alpha \exp\left[-(z/z_0)^\beta\right] \tag{6.80}$$

with $\alpha = 2$, $\beta = 3/2$ ([11], p.83), and the constant n_0 is fixed by the normalization condition

$$\int_0^\infty n(z)dz = n_{g,sterad}, \tag{6.81}$$

where $n_{g,sterad} = 3600\cdot\left(\frac{180}{\pi}\right)^2 n_{g,arcmin}$ is the total number of galaxies per steradian of the survey, and $n_{g,arcmin}$ is the same number per square arcminute (in the case of Euclid $n_{g,arcmin} = 30$, see [11], p. 84). In Figure 6.22 a plot of $n(z)$ as a function of z is given.

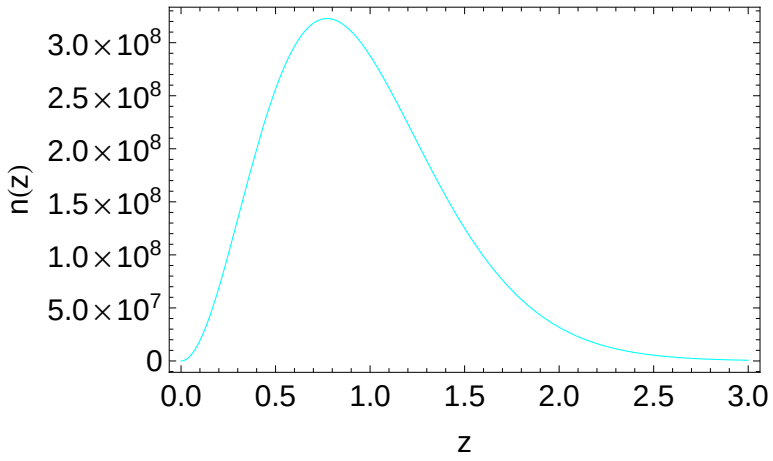

Figure 6.22: The galaxy density $n(z)$ for weak lensing.

To define the galaxy densities for each bin, we have to consider the fact that the observed (photometric) redshift of a galaxy is different from the true one, due to uncertainties (see [17]).

The (true) galaxy density $n_i(z)$ for the i-th (photometric) bin $z_{ph}^{(i)} < z_{ph} < z_{ph}^{(i+1)}$, is defined as the convolution of $n(z)$ with the probability distribution $p(z_{ph}|z)$ of the observed photometric redshifts z_{ph} given the true redshifts z:

$$n_i(z) = c_{n_i} \int_{z_{ph}^{(i)}}^{z_{ph}^{(i+1)}} dz_{ph} n(z) p(z_{ph}|z). \tag{6.82}$$

The probability distribution $p(z_{ph}|z)$ can be assumed to be a Gaussian centered at z_{ph} and with a RMS $\sigma_z = \Delta(1+z)$ at each redshift:

$$p(z_{ph}|z) = \frac{1}{\sqrt{2\pi}\sigma_z} \exp\left[-\frac{(z-z_{ph})^2}{2\sigma_z}\right] \tag{6.83}$$

($\Delta = 0.05$ in our case, from Euclid specifications [11], p.84). We can also take $\sigma = \Delta(1+z_i)$, z_i being the central redshift of the i-th bin (see [11], p. 93).

That is, $n_i(z)$ takes the form

$$n_i(z) = c_{n_i} \frac{1}{2} n(z) \left[erf(x_{i+1}) - erf(x_i)\right] \tag{6.84}$$

where $erf(x)$ is the error function and $x_i \equiv (z_{ph}^{(i)} - z)/(\sqrt{2}\sigma_z)$.

As a normalization constant c_{n_i} for the $n_i(z)$, we choose the inverse of the number of galaxies per steradian n_i belonging to the i-th bin:

$$n_i = \int_{z_{ph}^{(i)}}^{z_{ph}^{(i+1)}} n(z) dz \equiv \frac{1}{c_{n_i}}. \tag{6.85}$$

However, what appears in the definition (6.71) of $W_i(z)$ is $n_i(r(z))$. We have to remember that the densities are connected by $n(z)dz = n(r)dr$, and therefore $n(r(z)) = n(z)H(z)$. The definition (6.71) can be then rewritten as

$$W_i(z) = H_0 \int_z^\infty d\tilde{z} \left[1 - \frac{r(z)}{r(\tilde{z})}\right] n_i(\tilde{z}). \tag{6.86}$$

With these clarifications the lensing convergence power spectrum can be now calculated.

Figure 6.23 represents the $n_i(z)$ functions for the two choices of the bin size $\Delta z = 0.1$, $\Delta z = 0.2$. Figure 6.24 represents the window functions $K_i(z)$ in the same cases.

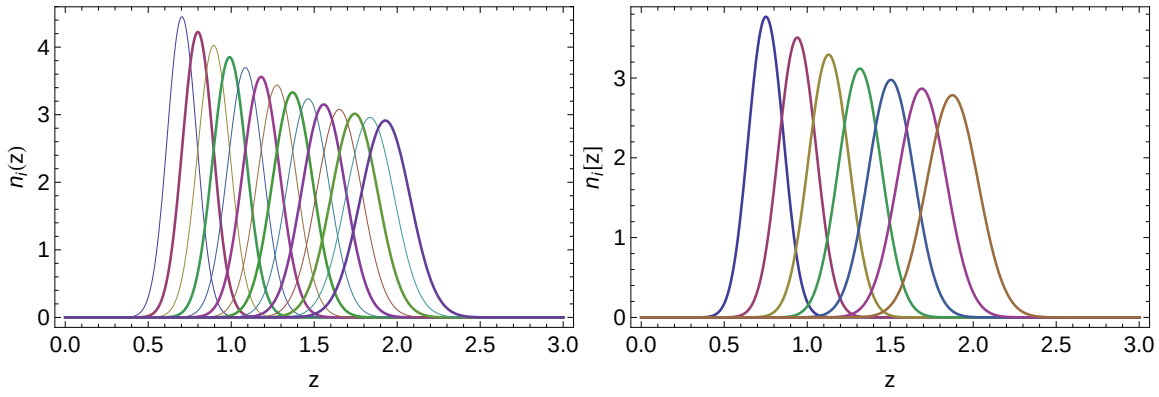

Figure 6.23: The galaxy densities $n_i(z)$ for a bin size $\Delta z = 0.1$ (left) and $\Delta z = 0.2$ (right).

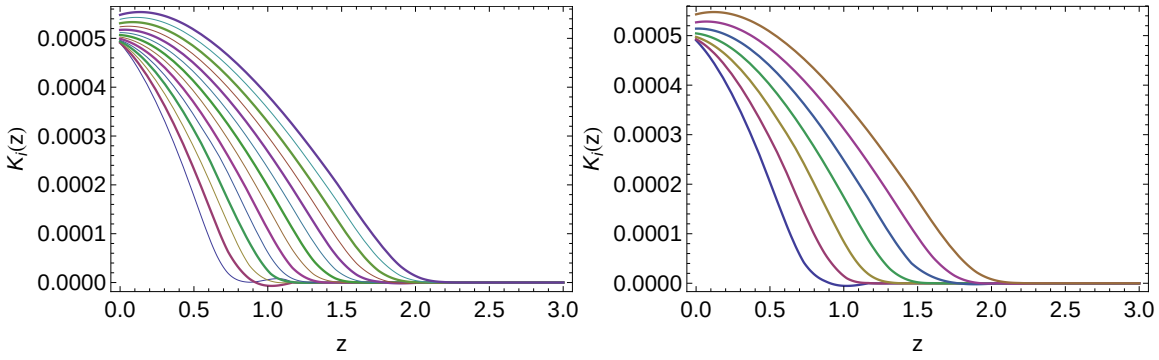

Figure 6.24: The window functions $K_i(z)$ for a bin size $\Delta z = 0.1$ (left) and $\Delta z = 0.2$ (right).

Fisher matrix calculation

We want to calculate the Fisher matrix, given by (5.99)

$$F_{\alpha\beta} = f_{sky} \sum_l \frac{(2l+1)\Delta l}{2} \frac{\partial P_{ij}(l)}{\partial p_\alpha} C^{-1}_{jk}(l) \frac{\partial P_{km}(l)}{\partial p_\beta} C^{-1}_{mi}(l), \tag{6.87}$$

summed over repeated indices, for the set of cosmological parameters $p_\alpha = \{\bar{L}(z_\alpha), E(z_\alpha)\}_{\alpha=1}^{n_{bins}}$, where

$$\bar{L}(z_\alpha) = \frac{L(z_\alpha, l)}{\delta_{t,0}\left(\frac{l}{\pi r(z)}\right)} = \Omega_{0m} \Sigma G(z_\alpha) \sigma_8, \tag{6.88}$$

with α running on the bins, and not over the parameters in each bin. It is also worth to stress that $\bar{L}(z_\alpha)$ do not depend on l because $\Sigma(k,z) = \Sigma$ has a fixed value for ΛCDM fiducial model.

The sum in l runs between $l_{min} = 100$ and l_{max} is calculated for each bin from the values of k_{max} in order to remain in the linear regime, for which the Bardeen approximation holds. To calculate $l_{max,i}$ for the i-th bin, we find the point $z_{med,i}(l)$ for which the integral defining P_{ij} for $i = j$ (6.72) can be splitted into two equal contributions $\int_0^{z_{med}}$ and $\int_{z_{med}}^{\infty}$, and then calculate $l_{max,i}$ as the solution of

$$\frac{l}{\pi r\left(z_{med,i}(l)\right)} = k_{max,i}. \tag{6.89}$$

The values for l_{max} for the two cases of $\Delta z = 0.1$ and $\Delta z = 0.2$ are reported in Tables 6.15 and 6.16, respectively.

$z\alpha$	k_{max}	l_{max}
0.7	0.162	430
0.8	0.172	520
0.9	0.183	600
1.0	0.194	700
1.1	0.206	800
1.2	0.218	910
1.3	0.232	1000
1.4	0.245	1100
1.5	0.260	1300
1.6	0.274	1400
1.7	0.290	1500
1.8	0.306	1700
1.9	0.323	1800
2.0	0.341	2000

Table 6.15: Values for l_{max} for each bin, $\Delta z = 0.1$.

z_α	k_{max}	l_{max}
0.75	0.167	480
0.95	0.188	650
1.15	0.212	850
1.35	0.238	1100
1.55	0.267	1300
1.75	0.298	1600
1.95	0.332	1900

Table 6.16: Values for l_{max} for each bin, $\Delta z = 0.2$.

The covariance matrix C_{ij} is given by (5.100)

$$C_{ij} = P_{ij} + \delta_{ij}\gamma_{int}^2 n_i^{-1} \tag{6.90}$$

with $\gamma_{int} = 0.22$ and n_i are the numbers of galaxies per steradian in each bin defined in equation (6.85).

We have to evaluate the derivatives $\frac{\partial P_{ij}(l)}{\partial p_\alpha}$ and the covariance matrix for a fiducial model, which we choose to be ΛCDM with the numerical values of the cosmological parameters taken from the WMAP-9-year data.

In order to calculate the derivative $\frac{\partial P_{ij}(l)}{\partial E(z_\alpha)}$, we have to take into account the fact that E appears also in the definition of the comoving distance. We then replace the regular definition of $E(z)$ with an interpolating function that goes smoothly through all points $(z_\alpha, E(z_\alpha))$ and $(0,1)$. Instead of depending on Ω_m, it now depends on all the parameters $E(z_\alpha)$, and so do all the quantities which depend on $E(z)$, like the comoving distance $r(z)$ and the window functions $K_i(z)$. For example, the convergence power spectrum is now dependent on the $E(z_\alpha)$values:

$$P_{ij} = P_{ij}(l, \{E(z_1), ..., E(z_{n_{bins}})\}). \tag{6.91}$$

The derivatives are then obtained by varying the fiducial values of $E(z_\alpha)$ by a small quantity ε (i.e. $\varepsilon \simeq 10^{-6}$):

$$\frac{\partial P_{ij}(l, \{E(z_1), ..., E(z_{n_{bins}})\})}{\partial E(z_\alpha)} =$$

$$= \frac{P_{ij}(l, \{E(z_1), ..., E(z_\alpha) + \varepsilon, ...E(z_{n_{bins}})\}) - P_{ij}(l, \{E(z_1), ..., E(z_\alpha) - \varepsilon, ...E(z_{n_{bins}})\})}{2\varepsilon} \tag{6.92}$$

$$\equiv J_{ij(2\alpha)}(l). \tag{6.93}$$

The derivative $\frac{\partial P_{ij}(l)}{\partial \bar{L}(z_\alpha)}$ can be instead calculated from

$$P_{ij}(l) = H_0 \int_0^\infty \frac{d\tilde{z}}{E(\tilde{z})} K_i(\tilde{z}) K_j(\tilde{z}) L(\tilde{z}, l)^2 = \sum_{\xi=0}^{\infty} \frac{\Delta z_\xi}{E(z_\xi)} K_i(z_\xi) K_j(z_\xi) L(z_\xi, l)^2. \tag{6.94}$$

for some bins indexed by ξ which coincide with the bins of the survey tomography in the survey range. We have

$$\frac{\partial P_{ij}(l)}{\partial \bar{L}(z_\alpha)} = 2H_0 \frac{\Delta z_\alpha}{E(z_\alpha)} K_i(z_\alpha) K_j(z_\alpha) \frac{L^2(z_\alpha, l)}{\bar{L}(z_\alpha)} \equiv J_{ij(2\alpha-1)}(l) \tag{6.95}$$

The matrix $J_{ij\alpha}$is then a $2n_{bins} \times 2n_{bins}$ matrix where the odd indexes are for the derivatives with respect to $\bar{L}(z_\alpha)$ for each bin and the even indexes are for the ones with respect to $E(z_\alpha)$.

The Fisher matrix can also be written as

$$F_{\alpha\beta} = f_{sky} \sum_l \frac{(2l+1)\Delta l}{2} Tr\left[J_\alpha(l) C^{-1}(l) J_\beta(l) C^{-1}(l)\right]. \tag{6.96}$$

On the diagonal of the inverse of F we will find the errors for $\bar{L}(z_1), E(z_1), \bar{L}(z_2), E(z_2), \ldots$ respectively. A plot of the structure for the weak lensing Fisher matrix in cases with $\Delta z = 0.1$ and $\Delta z = 0.2$ can be found in Figure 6.25.

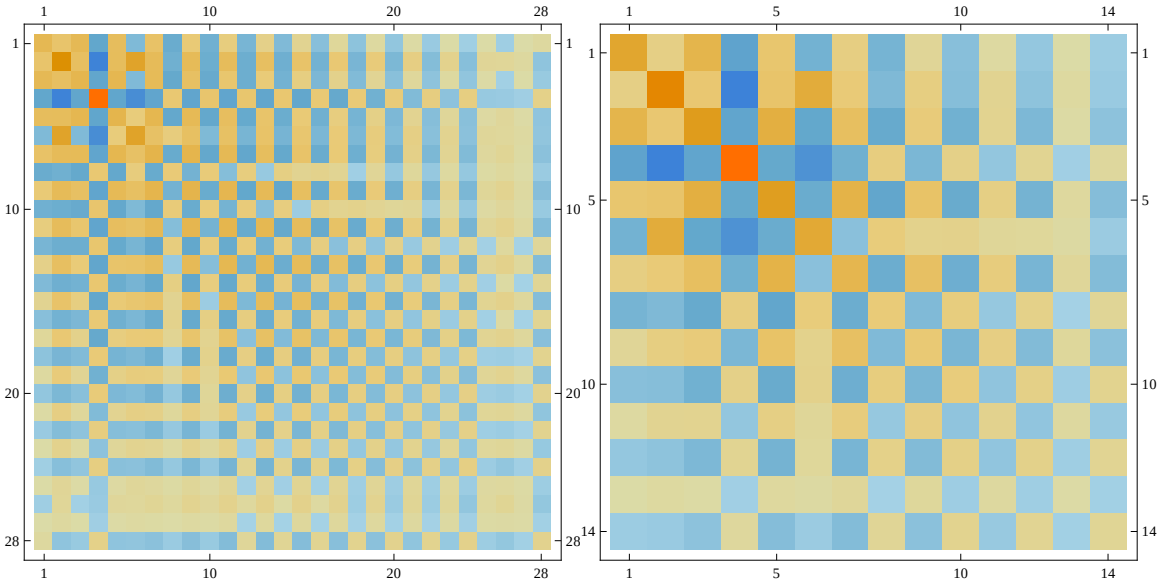

Figure 6.25: Structure of the weak lensing Fisher matrix in the cases $\Delta z = 0.1$ (left) and $\Delta z = 0.2$ (right). Orange is for positive entries, blue for negative ones; color intensity represents the absolute value of the entry (the bigger the number, the darker the color).

6.4.1 Errors from weak lensing only

Here we summarize the errors on the parameters obtained from the weak lensing only, with the two different choices for the bin size $\Delta z = 0.1$ and $\Delta z = 0.2$.

6.4.1.1 Bin size $\Delta z = 0.1$

z_α	$\bar{L}(z_\alpha)$	$\Delta\bar{L}(z_\alpha)$	$\Delta\bar{L}(z_\alpha)(\%)$	$E(z_\alpha)$	$\Delta E(z_\alpha)$	$\Delta E(z_\alpha)(\%)$
0.7	0.327	0.0079	2.4	1.45	0.0012	0.083
0.8	0.312	0.0096	3.1	1.54	0.0010	0.066
0.9	0.299	0.0094	3.2	1.63	0.0019	0.12
1.0	0.286	0.0098	3.4	1.73	0.038	2.2
1.1	0.274	0.012	4.3	1.83	0.058	3.2
1.2	0.263	0.016	6.2	1.93	0.074	3.8
1.3	0.253	0.023	9.3	2.04	0.089	4.4
1.4	0.243	0.036	15	2.15	0.11	5.1
1.5	0.234	0.067	29	2.27	0.14	6.3
1.6	0.226	0.14	60	2.39	0.19	8.1
1.7	0.218	0.31	140	2.51	0.26	10
1.8	0.211	0.98	460	2.63	0.21	8.1
1.9	0.204	3.7	1800	2.76	0.32	12
2.0	0.197	15	7700	2.89	0.30	10

Table 6.17: Values, errors and percent errors on the parameters $\bar{L}, E$ for every redshift bin from weak lensing only, $\Delta z = 0.1$.

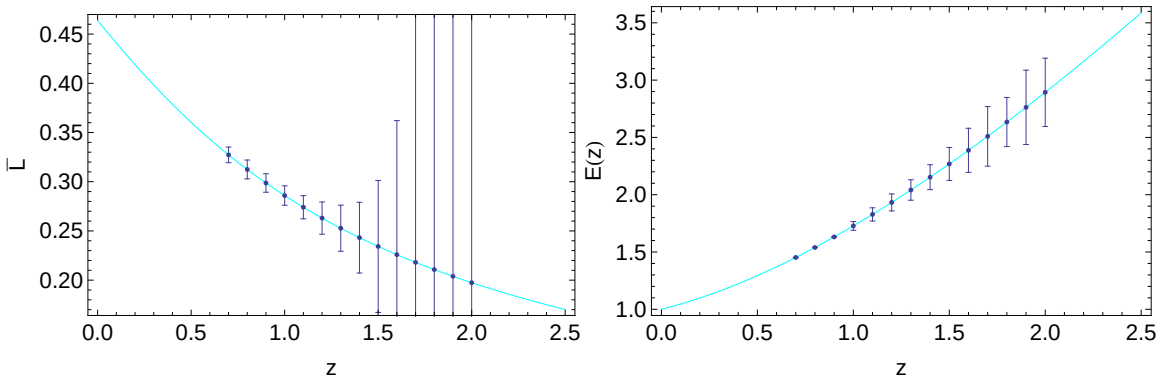

Figure 6.26: Errors on $\bar{L}, E$ from weak lensing, $\Delta z = 0.1$.

From Table 6.17, we can notice that there is a very strong difference in the errors for the same parameter depending on the bin: the percent errors in the first and in the last bin are about two orders of magnitude different in the case of E and more than three orders of magnitude in the case of L. We can conclude that the weak lensing method is very accurate for low redshift, but it does not put significant constraints on parameters at high redshift.

Comparing the errors on E from Tables 6.4 and 6.17, we can appreciate how weak lensing data can constrain the values on E about five-ten times better than galaxy clustering in the first three bins.

6.4.1.2 Bin size $\Delta z = 0.2$

z_α	$\bar{L}(z_\alpha)$	$\Delta\bar{L}(z_\alpha)$	$\Delta\bar{L}(z_\alpha)(\%)$	$E(z_\alpha)$	$\Delta E(z_\alpha)$	$\Delta E(z_\alpha)(\%)$
0.75	0.320	0.0026	0.82	1.50	0.0019	0.13
0.95	0.292	0.0029	0.99	1.68	0.0018	0.10
1.15	0.268	0.0038	1.4	1.88	0.0034	0.18
1.35	0.248	0.0077	3.1	2.10	0.024	1.2
1.55	0.230	0.028	12	2.33	0.047	2.0
1.75	0.214	0.18	85	2.57	0.089	3.5
1.95	0.201	2.0	1000	2.83	0.12	4.3

Table 6.18: Values, errors and percent errors on the parameters $\bar{L}, E$ for every redshift bin from weak lensing only, $\Delta z = 0.2$.

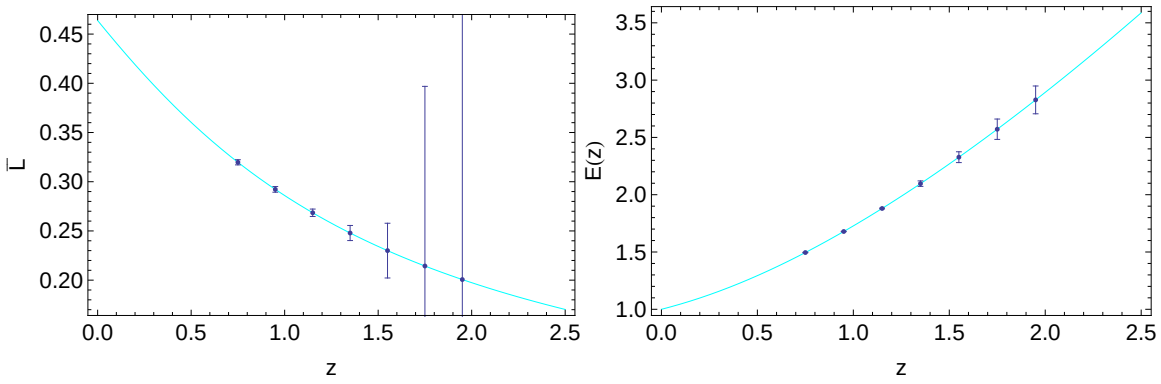

Figure 6.27: Errors on $\bar{L}$ (left) and E (right) from weak lensing, $\Delta z = 0.2$.

From Tables 6.17 and 6.18, we can see that considering larger bins significantly reduces the errors. On E we have a reduction in the errors of about two times (often significantly more), as we found in the galaxy clustering calculations. But the most significant improvement can be seen in the errors on L: here we gain about one order of magnitude with respect to the $\Delta z = 0.1$ case. We will see that this difference allows us to obtain much more tight constraints on the anisotropic stress η if we use larger bins.

6.5 Supernovae

Up to now, we have estimated the constraints we can get on the model-independent parameters $\bar{A}, \bar{R}, L$ and on Hubble dimensionless parameter E from the future *Euclid* probes. In order to put better constraints on E, we now want to add the information we can obtain from a supernova survey. We take into account a survey which will observe $\sim 10^3$ supernovae (say $n_{SN} = 2000$) of type Ia with redshift $z < 1.5$.

We now proceed with the calculation of the Fisher matrix for this experiment.

The likelihood function for the supernovae after marginalization of the offset is given by (5.86) (with $N = 1$):

$$\mathscr{L} = -\log L = \frac{1}{2}\left(S_2 - \frac{S_1^2}{S_0}\right), \tag{6.97}$$

where

$$S_n = \sum_i \frac{(m_i - \mu_i)^n}{\sigma_i^2} \tag{6.98}$$

and $\mu_i = 5\log \hat{d}_L(z_i)$. The dimensionless luminosity distance is

$$\hat{d}_L(z) = (1+z)\int_0^z \frac{d\tilde{z}}{E(\tilde{z})}. \tag{6.99}$$

This can be written as

$$\mathscr{L} = \frac{1}{2} X_i M_{ij} X_j, \tag{6.100}$$

where $X_i \equiv m_i - \mu_i$ and

$$M_{ij} = s_i s_j \delta_{ij} - \frac{s_i^2 s_j^2}{S_0} \tag{6.101}$$

(no sum) where $s_i = 1/\sigma_i$.The correlation matrix M^{-1} is independent of H. The Fisher matrix can be written as

$$F_{\alpha\beta} = \langle \frac{\partial \mathscr{L}}{\partial p_\alpha} \frac{\partial \mathscr{L}}{\partial p_\beta} \rangle, \tag{6.102}$$

where now the parameter is $p_\alpha = E$. So finally we have

$$F_{\alpha\alpha} = F_E = \langle (\frac{\partial \mu_i}{\partial p_\alpha} M_{ij} X_j)^2 \rangle = 25 Y_{i\alpha} M_{ij} Y_{m\alpha} M_{mk} \langle X_j X_k \rangle \tag{6.103}$$

$$= 25 Y_{i\alpha} M_{ij} Y_{m\alpha} M_{mk} M^{-1}_{jk} \tag{6.104}$$

$$= 25 Y_{i\alpha} M_{ij} Y_{j\alpha}, \tag{6.105}$$

where

$$Y_{i\alpha} \equiv \frac{\partial \log \hat{d}_i}{\partial p_\alpha} = \frac{1}{\hat{d}_i} \frac{\partial \hat{d}_i}{\partial E_\alpha} = -\frac{1}{\hat{d}_L(z_i)} \frac{\Delta z_\alpha}{E^2(z_\alpha)} (1+z_i) \Theta(z_i - z_\alpha). \tag{6.106}$$

We can in fact write

$$\hat{d}_i = (1+z_i) \sum_{j=0}^{i} \frac{\Delta z_j}{E_j} \tag{6.107}$$

so that

$$\frac{\partial \hat{d}_i}{\partial E_\alpha} = \frac{\Delta z_\alpha}{E_\alpha^2} (1+z_i) \Theta(z_i - z_\alpha). \tag{6.108}$$

The Fisher matrix for the parameter vector $p_\alpha = \{E(z_\alpha)\}$ with α running over the z-bins is

$$F_{\alpha\beta} = \langle (\frac{\partial \mu_i}{\partial p_\alpha} M_{ij} X_j)(\frac{\partial \mu_i}{\partial p_\beta} M_{ij} X_j) \rangle = 25 Y_{i\alpha} M_{ij} Y_{j\beta} \tag{6.109}$$

We have to make a choice to define the redshifts z_i and the uncertainties σ_i for the supernovae of the simulated experiment that appear in the Fisher matrix. We take as a reference the Union 2.1 catalogue [19] (580 SNIa in the range $0 < z \lesssim 1.5$, based on paper [20]). We assume that the survey will observe supernovae in the redshift range $0.65 < z < 1.45$, and divide that interval in bins of fixed size. The choices for the bin size are $\Delta z = 0.1$ and $\Delta z = 0.2$, in order to combine the SN Fisher matrix with the galaxy clustering and the weak lensing ones. We assume the total number of observed SN to be about $n_{SN} = 2000$ in that range. We further assume that the supernovae of the future survey will be distributed uniformly in each bin, respecting the proportions of the actual data (catalogue Union 2.1).

From the catalogue data, we count the number $n_{data,\alpha}$ of the supernovae in each bin; we also calculate the average error $\sigma_{data,\alpha}$ for each bin, which will be assumed to be the error for each of the supernovae of

the bin in our simulation: $\sigma_i = \sigma_{data,\alpha}$ (if the i-th SN is in the bin α). The number of observed SN in each bin in the simulation will be:

$$n_\alpha = n_{SN} \cdot \frac{n_{data,\alpha}}{\sum_\alpha n_{data,\alpha}}. \tag{6.110}$$

Since we assume the SN to be uniformly distributed in each bin, the redshift z_i for a SN in the bin α will be given by

$$z_i = z_{min,\alpha} + n_q \cdot \frac{\Delta z}{n_\alpha} \tag{6.111}$$

where $z_{min,\alpha}$ is the lower border of the bin and the index q, running from 1 to n_α, represents the position that the i-th supernova occupies in the bin.

Now that we have the z_is and the σ_is, the Fisher matrix can be calculated. A plot of the results can be seen in Figure 6.28, for the two cases of $\Delta z = 0.1$ and $\Delta z = 0.2$ respectively. In the Figure, rows and columns of zeros have been added for the bins which are not covered by the supernova survey.

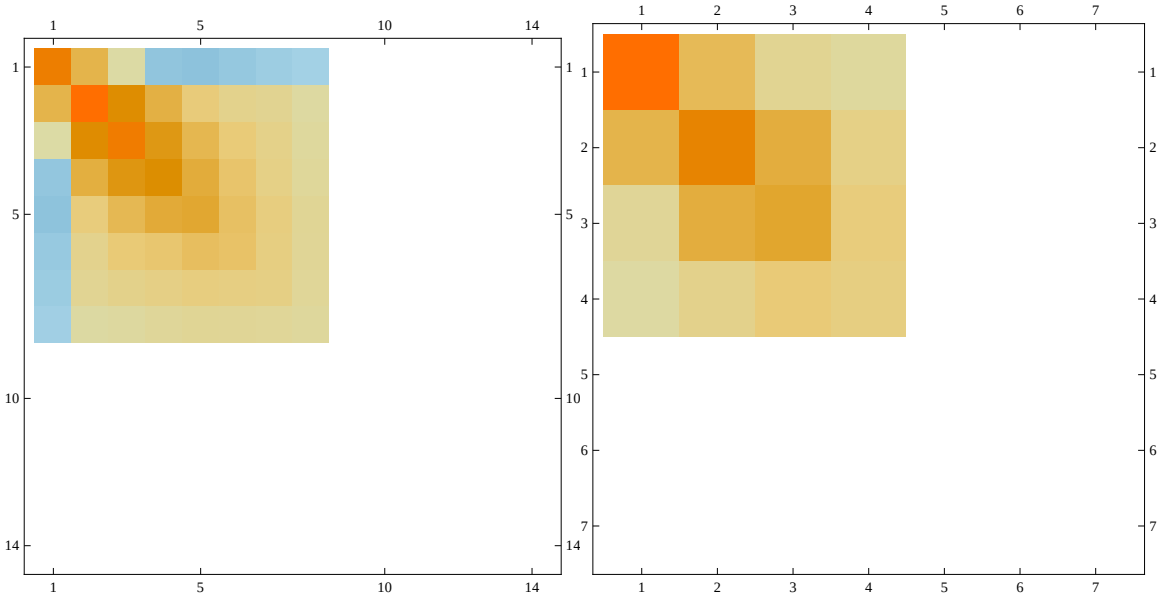

Figure 6.28: Structure of the supernovae Fisher matrix in the cases $\Delta z = 0.1$ (left) and $\Delta z = 0.2$ (right). Orange is for positive entries, blue for negative ones; color intensity represents the absolute value of the entry (the bigger the number, the darker the color).

6.5.1 Errors from the supernovae only

Here we summarize the errors on the parameters obtained from the supernovae only, with the two different choices for the bin size $\Delta z = 0.1$ and $\Delta z = 0.2$.

6.5.1.1 Bin size $\Delta z = 0.1$

z_α	$E(z_\alpha)$	$\Delta E(z_\alpha)$	$\Delta E(z_\alpha)(\%)$
0.7	1.45	0.064	4.4
0.8	1.54	0.065	4.2
0.9	1.63	0.091	5.6
1.0	1.73	0.13	7.3
1.1	1.83	0.19	11
1.2	1.93	0.26	13
1.3	2.04	0.29	14
1.4	2.15	0.45	21

Table 6.19: Values, errors and percent errors on the parameter E for every redshift bin from supernovae only, $\Delta z = 0.1$.

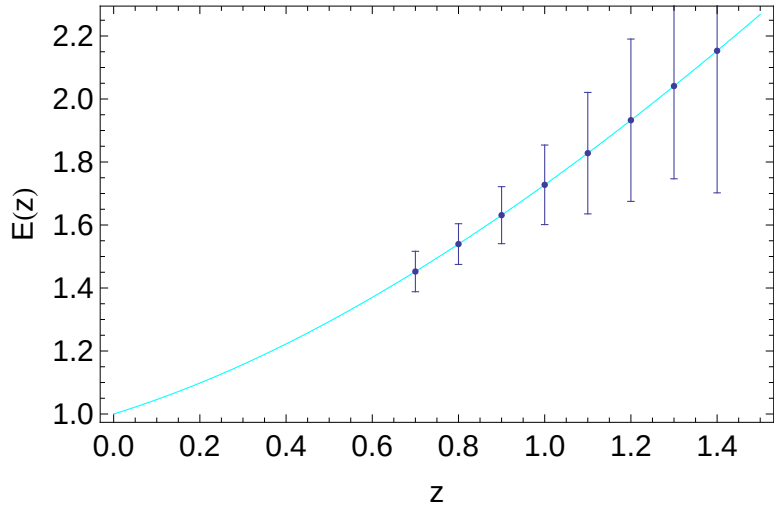

Figure 6.29: Errors on E from supernovae, $\Delta z = 0.1$.

6.5.1.2 Bin size $\Delta z = 0.2$

z_α	$E(z_\alpha)$	$\Delta E(z_\alpha)$	$\Delta E(z_\alpha)(\%)$
0.75	1.50	0.027	1.8
0.95	1.68	0.040	2.4
1.15	1.88	0.076	4.0
1.35	2.10	0.14	6.5

Table 6.20: Values, errors and percent errors on the parameter E for every redshift bin from supernovae only, $\Delta z = 0.2$.

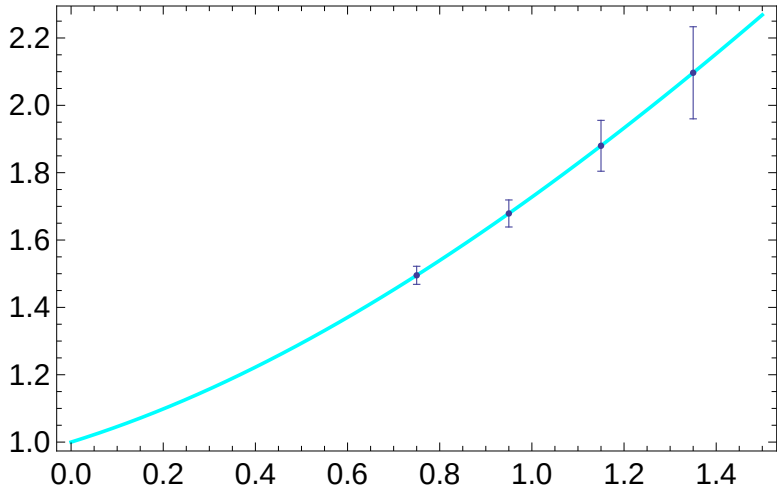

Figure 6.30: Errors on E from supernovae, $\Delta z = 0.2$.

In Tables 6.21, 6.22 we compare the errors obtained on the dimensionless Hubble parameter E from the galaxy clustering and weak lensing probes and from the supernova survey, in the cases $\Delta z = 0.1$ and $\Delta z = 0.2$ respectively. As we can see, the supernovae data do not give a significant contribution in constraining E. It must be said that the number $n_{SN} = 2000$ that we have chosen is quite conservative; but even considering a more optimistic survey with $n_{SN} = 10000$, the constraints coming from supernovae are quite weak. Errors for $n_{SN} = 10000$, $\Delta z = 0.2$ are reported in Table .

z_α	$E(z_\alpha)$	$\Delta E_{GC}(z_\alpha)(\%)$	$\Delta E_{WL}(z_\alpha)(\%)$	$\Delta E_{SN}(z_\alpha)(\%)$
0.7	1.45	0.74	0.083	4.4
0.8	1.54	0.58	0.066	4.2
0.9	1.63	0.50	0.12	5.6
1.0	1.73	0.44	2.2	7.3
1.1	1.83	0.40	3.2	11
1.2	1.93	0.37	3.8	13
1.3	2.04	0.35	4.4	14
1.4	2.15	0.34	5.1	21
1.5	2.27	0.35	6.3	-
1.6	2.39	0.38	8.1	-
1.7	2.51	0.47	10	-
1.8	2.63	0.48	8.1	-
1.9	2.76	0.68	12	-
2.0	2.89	1.1	10	-

Table 6.21: Percent errors on E from the three probes, $\Delta z = 0.1$ ($\varepsilon_{eff} = 1$ for galaxy clustering).

z_α	$E(z_\alpha)$	$\Delta E_{GC}(z_\alpha)(\%)$	$\Delta E_{WL}(z_\alpha)(\%)$	$\Delta E_{SN}(z_\alpha)(\%)$
0.75	1.50	0.47	0.13	1.8
0.95	1.68	0.34	0.10	2.4
1.15	1.88	0.27	0.18	4.0
1.35	2.10	0.24	1.2	6.5
1.55	2.33	0.26	2.0	-
1.75	2.57	0.34	3.5	-
1.95	2.83	0.59	4.3	-

Table 6.22: Percent errors on E from the three probes, $\Delta z = 0.2$ ($\varepsilon_{eff} = 1$ for galaxy clustering).

z_α	$E(z_\alpha)$	$\Delta E(z_\alpha)$	$\Delta E(z_\alpha)(\%)$
0.75	1.50	0.012	0.80
0.95	1.68	0.018	1.1
1.15	1.88	0.034	1.8
1.35	2.10	0.061	2.9

Table 6.23: Errors from supernovae for a survey with $n_{SN} = 10000$, $\Delta z = 0.2$.

6.6 Combining the matrices

All the matrices will be evaluated at the fiducial model, eg ΛCDM. Once we have the three Fisher matrices we insert them into a matrix for the full parameter vector

$$p_\alpha = \{\bar{A}, \bar{R}, \bar{L}, E\} \times n_z \tag{6.112}$$

Notice that we need also

$$\bar{R}' = -(1+z)\frac{[\bar{R}(z+\Delta z) - \bar{R}(z)]}{\Delta z} \tag{6.113}$$

and

$$E' = -(1+z)\frac{[E(z+\Delta z) - E(z)]}{\Delta z} \tag{6.114}$$

Since these are defined only in the first $n_{bins} - 1$ bins, we will have to cross out the rows and columns referring to the last bin to project onto η.

The structure for every bin will be:

$$\begin{pmatrix} \bar{A} & \bar{A}\bar{R} & 0 & \bar{A}E \\ \bar{A}\bar{R} & \bar{R} & 0 & \bar{R}E \\ 0 & 0 & \bar{L} & \bar{L}E \\ \bar{A}E & \bar{R}E & \bar{L}E & (E^{WL} + E^{SN} + E^{GC}) \end{pmatrix} \tag{6.115}$$

but the combined Fisher matrix will not be necessarily a block matrix, since the matrix for weak lensing is not. A plot of its structure for the two different choices of the bin size $\Delta z = 0.1$ and $\Delta z = 0.2$ is shown in Figure 6.31; the plots refer to the case in which $\varepsilon_{eff} = 1$ has been used for galaxy clustering.

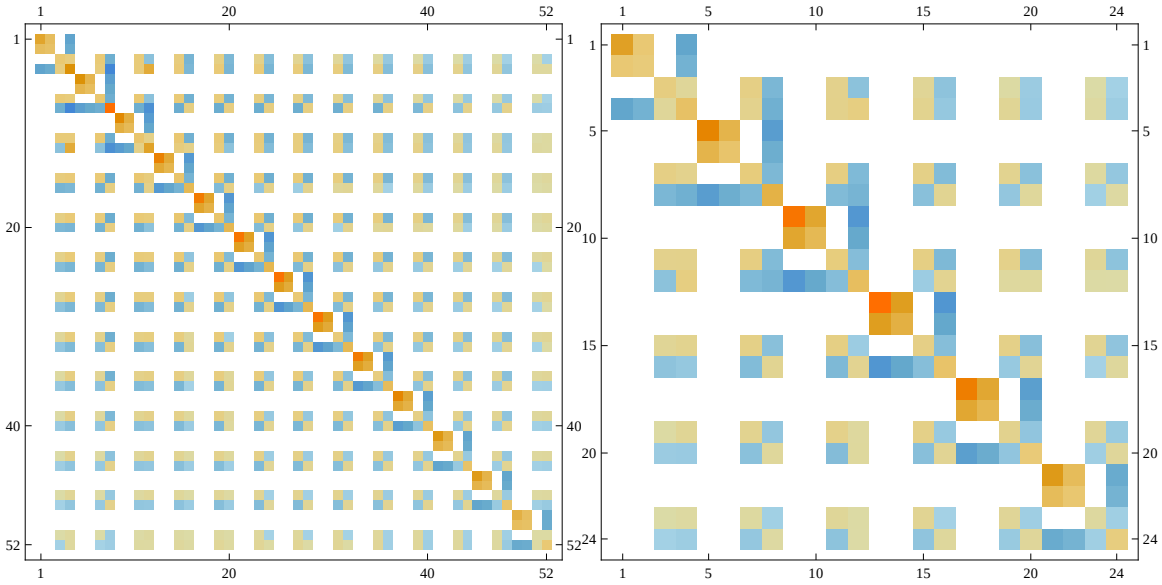

Figure 6.31: Structure of the combined Fisher matrix in the cases $\Delta z = 0.1$ (left) and $\Delta z = 0.2$ (right), with $\varepsilon_{eff} = 1$. Orange is for positive entries, blue for negative ones; color intensity represents the absolute value of the entry (the bigger the number, the darker the color).

This matrix must then be projected onto η. Is however interesting to produce an intermediate step, namely the matrix for $q_\alpha \equiv P_1, P_2, P_3, E$. According to equation (5.79), this is

$$F^{(q)}_{\alpha\beta} = F^{(p)}_{\gamma\delta} \frac{\partial p_\gamma}{\partial q_\alpha} \frac{\partial p_\delta}{\partial q_\beta} \tag{6.116}$$

or, in terms of matrices,

$$F^{(q)} = J_1^T F^{(p)} J_1, \tag{6.117}$$

where $F^{(p)}$ is the combined Fisher matrix without the columns referring to the last bin and $J_1$is the jacobian matrix of the transformation:

$$J_1 = \frac{\partial(p_1, ...)}{\partial(q_1, ...)}. \tag{6.118}$$

Since we have the new parameters as functions of the old ones, what we actually calculate is the inverse jacobian:

$$J_1^{-1} = \frac{\partial(q_1,...)}{\partial(p_1,...)} = \begin{pmatrix} \frac{\partial P_1(z_1)}{\partial \bar{A}(z_1)} & \frac{\partial P_1(z_1)}{\partial \bar{R}(z_1)} & \frac{\partial P_1(z_1)}{\partial \bar{L}(z_1)} & \frac{\partial P_1(z_1)}{\partial E(z_1)} & \frac{\partial P_1(z_1)}{\partial \bar{A}(z_2)} & \cdots \\ \frac{\partial P_2(z_1)}{\partial \bar{A}(z_1)} & \frac{\partial P_2(z_1)}{\partial \bar{R}(z_1)} & \frac{\partial P_2(z_1)}{\partial \bar{L}(z_1)} & \frac{\partial P_2(z_1)}{\partial E(z_1)} & & \\ \frac{\partial P_3(z_1)}{\partial \bar{A}(z_1)} & \frac{\partial P_{3\alpha}}{\partial \bar{R}(z_1)} & \frac{\partial P_3(z_1)}{\partial \bar{L}(z_1)} & \frac{\partial P_3(z_1)}{\partial E(z_1)} & & \\ \frac{\partial E(z_1)}{\partial \bar{A}(z_1)} & \frac{\partial E(z_1)}{\partial \bar{R}(z_1)} & \frac{\partial E(z_1)}{\partial \bar{L}(z_1)} & \frac{\partial E(z_1)}{\partial E(z_1)} & & \\ \frac{\partial P_1(z_2)}{\partial \bar{A}(z_1)} & & & & \ddots & \\ \vdots & & & & & \ddots \end{pmatrix} \tag{6.119}$$

so that

$$F^{(q)} = \left(\left(J_1^{-1} \right)^{-1} \right)^T F^{(p)} \left(J_1^{-1} \right)^{-1} \tag{6.120}$$

The non-zero terms in the jacobian J_1 are:

$$\frac{\partial P_1(z_\alpha)}{\partial \bar{A}(z_\alpha)} = -\frac{\bar{R}(z_\alpha)}{\bar{A}^2(z_\alpha)}; \tag{6.121}$$

$$\frac{\partial P_1(z_\alpha)}{\partial \bar{R}(z_\alpha)} = \frac{1}{\bar{A}(z_\alpha)}; \tag{6.122}$$

$$\frac{\partial P_2(z_\alpha)}{\partial \bar{R}(z_\alpha)} = -\frac{\bar{L}(z_\alpha)}{\bar{R}^2(z_\alpha)}; \tag{6.123}$$

$$\frac{\partial P_2(z_\alpha)}{\partial \bar{L}(z_\alpha)} = \frac{1}{\bar{R}(z_\alpha)}; \tag{6.124}$$

$$\frac{\partial P_3(z_\alpha)}{\partial \bar{R}(z_\alpha)} = \frac{(1+z_\alpha)\bar{R}(z_{\alpha+1})}{\Delta z \cdot \bar{R}^2(z_\alpha)}; \tag{6.125}$$

$$\frac{\partial P_3(z_\alpha)}{\partial \bar{R}(z_{\alpha+1})} = -\frac{(1+z_\alpha)}{\Delta z \cdot \bar{R}(z_\alpha)}; \tag{6.126}$$

$$\frac{\partial E(z_\alpha)}{\partial E(z_\alpha)} = 1. \tag{6.127}$$

In order to project on η, we can marginalize $F^{(q)}$ over $P_1$by eliminating the corresponding rows and columns from the inverse Fisher matrix (as stated in subsection 5.4.2), since η does not depend on it. A plot of the structure of this intermediate Fisher matrix for the two choices of the bin size can be found in Figure 6.32; the plots refer to the assumption $\varepsilon_{eff} = 1$ in the galaxy clustering calculations.

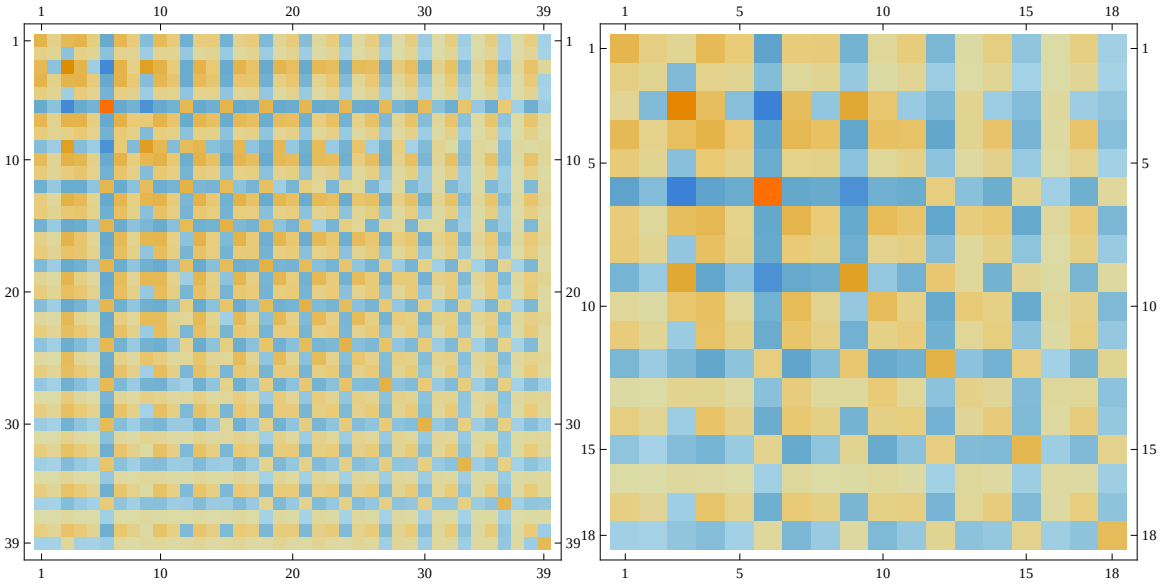

Figure 6.32: Structure of the intermediate Fisher matrix relative to the parameters $q_\alpha = \{P_2, P_3, E\}$ in the cases $\Delta z = 0.1$ (left) and $\Delta z = 0.2$ (right), with $\varepsilon_{eff} = 1$. Orange is for positive entries, blue for negative ones; color intensity represents the absolute value of the entry (the bigger the number, the darker the color).

It is then convenient to project the Fisher matrix for the set $q_\alpha = \{P_2, P_3, E\}$, that now we have, onto the one for the set $m_\alpha = \{P_2, P_3, \eta\}$, so that we have a square (and invertible) inverse jacobian.

$$F^{(m)}_{\lambda\nu} = F^{(q)}_{\alpha\beta} \frac{\partial q_\alpha}{\partial m_\lambda} \frac{\partial q_\beta}{\partial \eta_\nu} \tag{6.128}$$

that is

$$F^{(m)} = J_2^T F^{(q)} J_2 \tag{6.129}$$

with

$$J_2 = \frac{\partial(q_1, \ldots)}{\partial(m_1, \ldots)}. \tag{6.130}$$

In this case we compute directly the jacobian

$$J_2 = \frac{\partial(q_1,...)}{\partial(m_1,...)} = \begin{pmatrix} \frac{\partial P_2(z_1)}{\partial P_2(z_1)} & \frac{\partial P_2(z_1)}{\partial P_3(z_1)} & \frac{\partial P_2(z_1)}{\partial \eta(z_1)} & \frac{\partial P_2(z_1)}{\partial P_2(z_2)} & \cdots \\ \frac{\partial P_3(z_1)}{\partial P_2(z_1)} & \frac{\partial P_3(z_1)}{\partial P_3(z_1)} & \frac{\partial P_3(z_1)}{\partial \eta(z_1)} & & \\ \frac{\partial E(z_1)}{\partial P_2(z_1)} & \frac{\partial E(z_1)}{\partial P_3(z_1)} & \frac{\partial E(z_1)}{\partial \eta(z_1)} & & \\ \frac{\partial P_2(z_2)}{\partial P_2(z_1)} & & & \ddots & \\ \vdots & & & & \ddots \end{pmatrix} \tag{6.131}$$

and the non-zero terms are

$$\frac{\partial P_2(z_\alpha)}{\partial P_2(z_\alpha)} = 1 \tag{6.132}$$

$$\frac{\partial P_3(z_\alpha)}{\partial P_3(z_\alpha)} = 1 \tag{6.133}$$

$$\frac{\partial E(z_\alpha)}{\partial P_2(z_\alpha)} = \frac{3\left(1+z_\alpha\right)^3}{\left(\eta(z_\alpha)+1\right)\sqrt{\frac{4(1+z_\alpha)^2}{\Delta z^2}E^2\left(z_{\alpha+1}\right)+4\left(2P_3(z_\alpha)+4+2\frac{(1+z_\alpha)}{\Delta z}\right)\frac{3P_2(z_\alpha)(1+z_\alpha)^3}{\eta(z_\alpha)+1}}} \tag{6.134}$$

$$\begin{aligned}\frac{\partial E(z_\alpha)}{\partial P_3(z_\alpha)} = {} & \frac{6P_2(z_\alpha)(1+z_\alpha)^3}{\left(\eta(z_\alpha)+1\right)\left(2P_3(z_\alpha)+4+2\frac{(1+z_\alpha)}{\Delta z}\right)\sqrt{\frac{4(1+z_\alpha)^2}{\Delta z^2}E^2(z_{\alpha+1})+4\left(2P_3(z_\alpha)+4+2\frac{(1+z_\alpha)}{\Delta z}\right)\frac{3P_2(z_\alpha)(1+z_\alpha)^3}{\eta(z_\alpha)+1}}} + \\ & - \frac{2\left(1+z_\alpha\right)E(z_{\alpha+1})}{\Delta z\left(2P_3(z_\alpha)+4+2\frac{(1+z_\alpha)}{\Delta z}\right)^2} - \frac{\sqrt{\frac{4(1+z_\alpha)^2}{\Delta z^2}E^2(z_{\alpha+1})+4\left(2P_3(z_\alpha)+4+2\frac{(1+z_\alpha)}{\Delta z}\right)\frac{3P_2(z_\alpha)(1+z_\alpha)^3}{\eta(z_\alpha)+1}}}{\left(2P_3(z_\alpha)+4+2\frac{(1+z_\alpha)}{\Delta z}\right)^2}\end{aligned} \tag{6.135}$$

$$\frac{\partial E(z_\alpha)}{\partial \eta(z_\alpha)} = \frac{1}{2\sqrt{\frac{4(1+z_\alpha)^2}{\Delta z^2}E^2(z_{\alpha+1})+4\left(2P_3(z_\alpha)+4+2\frac{1+z_\alpha}{\Delta z}\right)\cdot\frac{3P_2(z_\alpha)(1+z_\alpha)^3}{\eta(z_\alpha)+1}}}\cdot\left(-\frac{6P_2(z_\alpha)\left(1+z_\alpha\right)^3}{\left(\eta(z_\alpha)+1\right)^2}\right) \tag{6.136}$$

$$\frac{\partial E(z_{\alpha+1})}{\partial \eta(z_\alpha)} = \frac{3P_2(z_\alpha)\Delta z\left(1+z_\alpha\right)^2}{2E(z_\alpha)\left(\eta(z_\alpha)+1\right)^2} \tag{6.137}$$

The last four equations are obtained by using the fact that

$$E'(z_\alpha) = -\left(1+z_\alpha\right)\frac{E(z_{\alpha+1})-E(z_\alpha)}{\Delta z}, \tag{6.138}$$

inverting the definition of η (6.21) with respect to $E(z_\alpha)$ and $E(z_{\alpha+1})$

$$E(z_\alpha) = \frac{\frac{2(1+z_\alpha)}{\Delta z}E(z_{\alpha+1}) + \sqrt{\frac{4(1+z_\alpha)^2}{\Delta z^2}E^2(z_{\alpha+1}) + 4\left(2P_3(z_\alpha)+4+2\frac{(1+z_\alpha)}{\Delta z}\right)\frac{3P_2(z_\alpha)(1+z_\alpha)^3}{\eta(z_\alpha)+1}}}{2\left(2P_3(z_\alpha)+4+2\frac{1+z_\alpha}{\Delta z}\right)} \tag{6.139}$$

$$E(z_{\alpha+1}) = -\frac{E(z_\alpha)\Delta z}{1+z_\alpha}\left[\frac{3P_2(z_\alpha)(1+z_\alpha)^3}{2E^2(z_\alpha)(\eta(z_\alpha)+1)} - P_3(z_\alpha) - 2 - \frac{1+z_\alpha}{\Delta z}\right] \tag{6.140}$$

and then deriving with respect to $P_2(z_\alpha), P_3(z_\alpha), \eta(z_\alpha)$.

We can then marginalize on P_2, P_3 to obtain the Fisher matrix for the $\eta(z_\alpha)$. Plots are shown in Figure 6.33.

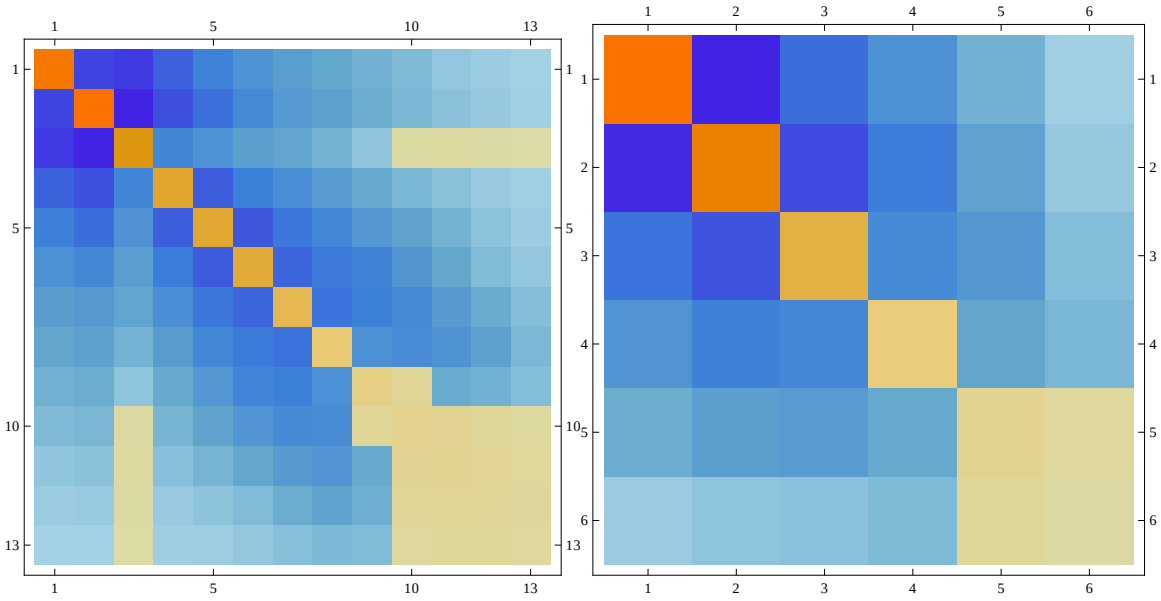

Figure 6.33: Structure of the intermediate Fisher matrix relative to the parameters $\eta(z_\alpha)$ in the cases $\Delta z = 0.1$ (left) and $\Delta z = 0.2$ (right), with $\varepsilon_{eff} = 1$. Orange is for positive entries, blue for negative ones; color intensity represents the absolute value of the entry (the bigger the number, the darker the color).

As a last step, we can assume that η is constant and $\eta = 1$ at every redshift (case 2 from section 6.1). This means that $\eta(z_\alpha) = \eta = 1$ for every α, so that

$$\frac{\partial \eta_\alpha}{\partial \eta} = 1 \tag{6.141}$$

and we can project the Fisher matrix for η_α on η.

6.6.1 Results

Here we summarize the final results, with the two different choices for the bin size $\Delta z = 0.1$ and $\Delta z = 0.2$.

6.6.1.1 Bin size $\Delta z = 0.1$

$\varepsilon_{eff} = 1$: **reference case**

z_α	$P_1(z_\alpha)$	$\Delta P_1(z_\alpha)$	$\Delta P_1(z_\alpha)(\%)$	$P_2(z_\alpha)$	$\Delta P_2(z_\alpha)$	$\Delta P_2(z_\alpha)(\%)$	$P_3(z_\alpha)$	$\Delta P_3(z_\alpha)$	$\Delta P_3(z_\alpha)(\%)$
0.7	0.798	0.0068	0.85	0.711	0.018	2.5	0.275	0.15	53
0.8	0.822	0.0054	0.66	0.690	0.021	3.1	0.352	0.13	36
0.9	0.843	0.0049	0.59	0.673	0.021	3.2	0.420	0.13	30
1.0	0.861	0.0048	0.56	0.659	0.022	3.3	0.480	0.13	28
1.1	0.877	0.0047	0.53	0.647	0.025	3.8	0.532	0.13	25
1.2	0.890	0.0047	0.52	0.637	0.032	5.0	0.578	0.13	22
1.3	0.902	0.0047	0.52	0.628	0.045	7.2	0.619	0.14	22
1.4	0.913	0.0051	0.55	0.621	0.072	12	0.654	0.15	22
1.5	0.922	0.0057	0.62	0.615	0.13	21	0.686	0.17	25
1.6	0.929	0.0069	0.75	0.610	0.28	45	0.713	0.22	31
1.7	0.936	0.0094	1.0	0.606	0.70	120	0.738	0.26	36
1.8	0.942	0.010	1.1	0.602	2.3	380	0.760	0.36	47
1.9	0.948	0.016	1.7	0.598	5.9	980	0.779	0.31	39

Table 6.24: Fiducial values, errors and percent errors for the parameters P_1, P_2, P_3 for every bin, $\Delta z = 0.1$, $\varepsilon_{eff} = 1$.

Looking at Table 6.24, we have that errors on P_1 are almost the same as the ones from galaxy clustering (Table 6.5); this is expected, since all of the information we have on $P_1 = \bar{R}/\bar{A}$ comes from galaxy clustering.

z_α	$\eta(z_\alpha)$	$\Delta\eta(z_\alpha)$	$\Delta\eta(z_\alpha)(\%)$
0.7	1.00	0.25	25
0.8	1.00	0.28	28
0.9	1.00	0.33	33
1.0	1.00	0.40	40
1.1	1.00	0.47	47
1.2	1.00	0.55	55
1.3	1.00	0.64	64
1.4	1.00	0.75	75
1.5	1.00	0.91	91
1.6	1.00	1.2	120
1.7	1.00	2.2	220
1.8	1.00	6.4	640
1.9	1.00	14	1400

Table 6.25: Fiducial values, errors and percent errors for the parameter η for every bin, $\Delta z = 0.1$, $\varepsilon_{eff} = 1$.

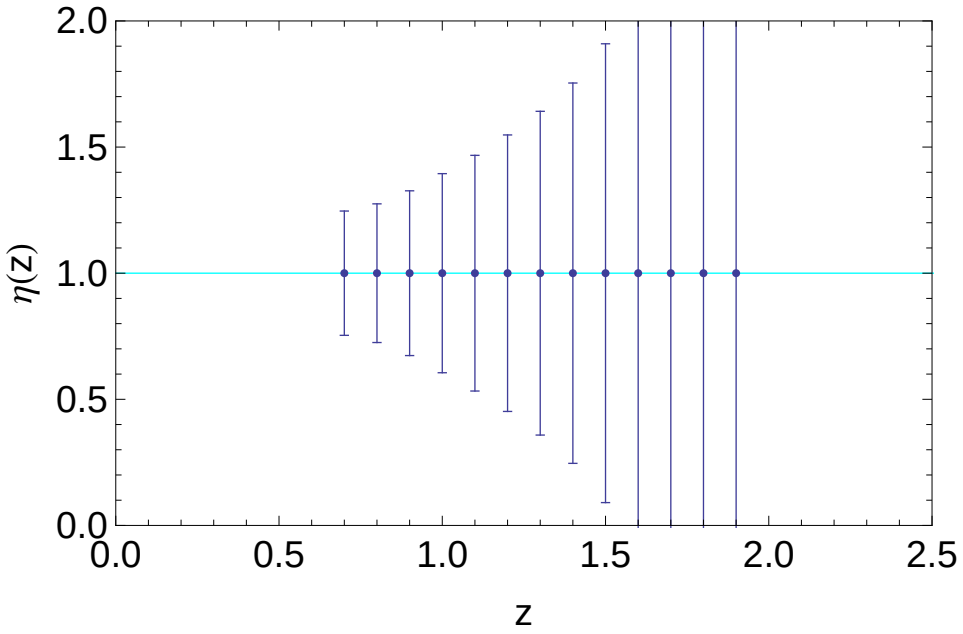

Figure 6.34: Errors on η, $\Delta z = 0.1$, $\varepsilon_{eff} = 1$.

In the last projection, where we assume $\eta = 1$, we get an uncertainty equal to

$$\Delta\eta = 0.19. \tag{6.142}$$

Notice that even if we consider η as dependent on z, the values with respect to which the error is calculated are the values obtained by using the fiducial parameters, so we should have $\eta = 1$ everywhere. However, the fiducial values for η we obtain from the calculations are not exactly equal to 1 (as ΛCDM would require) because we are using equations (6.19) for η with the approximate derivatives R' and E' defined in equations (6.113), (6.114) and also because we are using the interpolated version of E described in section 6.4 in order to make E dependent from the z_α; the values of η in Table 6.25, in Figure 6.34 and in all the next Tables and Figures concerning η have been therefore put equal to unity "by hand".

From Table 6.25, we see that with the choice $\Delta z = 0.1$ we can put acceptable constraints on η in the first bins, but in the last ones the errors are too large.

$\varepsilon_{eff} = 0.5$**: pessimistic case**

z_α	$P_1(z_\alpha)$	$\Delta P_1(z_\alpha)$	$\Delta P_1(z_\alpha)(\%)$	$P_2(z_\alpha)$	$\Delta P_2(z_\alpha)$	$\Delta P_2(z_\alpha)(\%)$	$P_3(z_\alpha)$	$\Delta P_3(z_\alpha)$	$\Delta P_3(z_\alpha)(\%)$
0.7	0.798	0.0084	1.05	0.711	0.018	2.5	0.275	0.17	63
0.8	0.822	0.0065	0.79	0.690	0.021	3.1	0.352	0.15	42
0.9	0.843	0.0060	0.72	0.673	0.021	3.2	0.420	0.15	37
1.0	0.861	0.0060	0.70	0.659	0.022	3.3	0.480	0.17	35
1.1	0.877	0.0061	0.69	0.647	0.025	3.8	0.532	0.17	32
1.2	0.890	0.0063	0.70	0.637	0.032	5.0	0.578	0.17	30
1.3	0.902	0.0066	0.73	0.628	0.045	7.2	0.619	0.19	30
1.4	0.913	0.0074	0.81	0.621	0.072	12	0.654	0.21	32
1.5	0.922	0.0086	0.94	0.615	0.13	21	0.686	0.26	38
1.6	0.929	0.011	1.2	0.610	0.28	46	0.713	0.36	50
1.7	0.936	0.016	1.7	0.606	0.70	120	0.738	0.44	60
1.8	0.942	0.018	1.9	0.602	2.3	380	0.760	0.62	82
1.9	0.948	0.029	3.1	0.598	5.9	980	0.779	0.54	70

Table 6.26: Fiducial values, errors and percent errors for the parameters P_1, P_2, P_3 for every bin, $\Delta z = 0.1$, $\varepsilon_{eff} = 0.5$.

As we can see, the error on $P_2 = \bar{L}/\bar{R}$ is almost independent of ε_{eff}: this can be explained by the fact that the percent errors on $\bar{R}$ (e.g. Table 6.4) are quite smaller than those on $\bar{L}$ from Table 6.17, which do not

depend on ε_{eff}, so that the contribution to the errors on P_2 given by the errors on $\bar{R}$ is negligible.

z_α	$\eta(z_\alpha)$	$\Delta\eta(z_\alpha)$	$\Delta\eta(z_\alpha)(\%)$
0.7	1.00	0.29	29
0.8	1.00	0.33	33
0.9	1.00	0.39	39
1.0	1.00	0.47	47
1.1	1.00	0.56	56
1.2	1.00	0.66	66
1.3	1.00	0.77	77
1.4	1.00	0.90	90
1.5	1.00	1.1	110
1.6	1.00	1.4	140
1.7	1.00	2.3	230
1.8	1.00	6.5	650
1.9	1.00	14	1400

Table 6.27: Fiducial values, errors and percent errors for the parameter η for every bin, $\Delta z = 0.1$, $\varepsilon_{eff} = 0.5$.

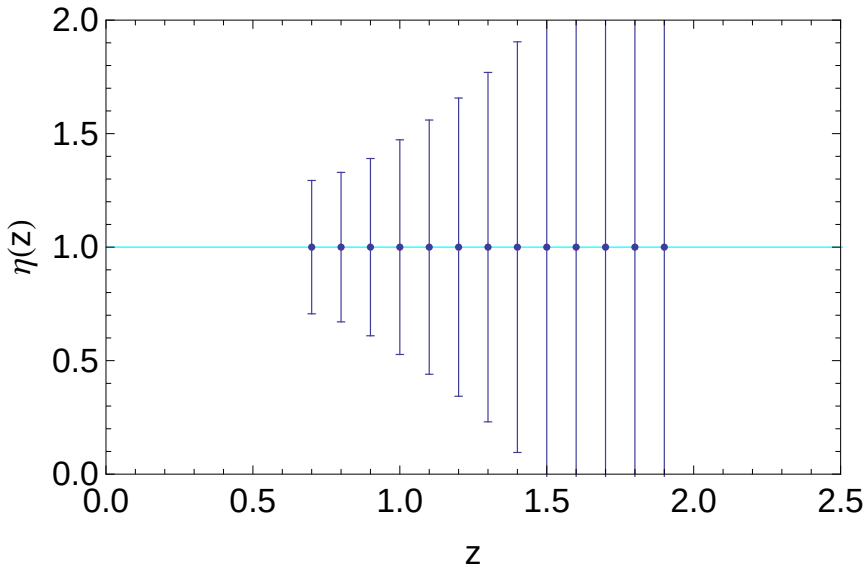

Figure 6.35: Errors on η, $\Delta z = 0.1$, $\varepsilon_{eff} = 0.5$.

In the last projection, where we assume $\eta = 1$, we get an uncertainty equal to

$$\Delta\eta = 0.23. \tag{6.143}$$

$\varepsilon_{eff} = 1.4$**: optimistic case**

z_α	$P_1(z_\alpha)$	$\Delta P_1(z_\alpha)$	$\Delta P_1(z_\alpha)(\%)$	$P_2(z_\alpha)$	$\Delta P_2(z_\alpha)$	$\Delta P_2(z_\alpha)(\%)$	$P_3(z_\alpha)$	$\Delta P_3(z_\alpha)$	$\Delta P_3(z_\alpha)(\%)$
0.7	0.798	0.0063	0.79	0.711	0.017	2.4	0.275	0.14	50
0.8	0.822	0.0051	0.62	0.690	0.021	3.1	0.352	0.12	34
0.9	0.843	0.0046	0.55	0.673	0.021	3.1	0.420	0.12	29
1.0	0.861	0.0044	0.52	0.659	0.022	3.3	0.480	0.12	26
1.1	0.877	0.0043	0.49	0.647	0.025	3.8	0.532	0.12	23
1.2	0.890	0.0042	0.47	0.637	0.032	5.0	0.578	0.12	20
1.3	0.902	0.0042	0.46	0.628	0.045	7.2	0.619	0.12	19
1.4	0.913	0.0044	0.48	0.621	0.072	12	0.654	0.13	19
1.5	0.922	0.0048	0.52	0.615	0.13	21	0.686	0.14	21
1.6	0.929	0.0057	0.61	0.610	0.28	45	0.713	0.18	25
1.7	0.936	0.0075	0.80	0.606	0.70	115	0.738	0.21	28
1.8	0.942	0.0081	0.86	0.602	2.3	380	0.760	0.28	36
1.9	0.948	0.012	1.3	0.598	5.9	980	0.779	0.24	30

Table 6.28: Fiducial values, errors and percent errors for the parameters P_1, P_2, P_3 for every bin, $\Delta z = 0.1$, $\varepsilon_{eff} = 1.4$.

z_α	$\eta(z_\alpha)$	$\Delta\eta(z_\alpha)$	$\Delta\eta(z_\alpha)(\%)$
0.7	1.00	0.23	23
0.8	1.00	0.26	26
0.9	1.00	0.31	31
1.0	1.00	0.37	37
1.1	1.00	0.44	44
1.2	1.00	0.52	52
1.3	1.00	0.60	60
1.4	1.00	0.71	71
1.5	1.00	0.86	86
1.6	1.00	1.2	120
1.7	1.00	2.1	210
1.8	1.00	6.4	640
1.9	1.00	14	1400

Table 6.29: Fiducial values, errors and percent errors for the parameter η for every bin, $\Delta z = 0.1$, $\varepsilon_{eff} = 1.4$.

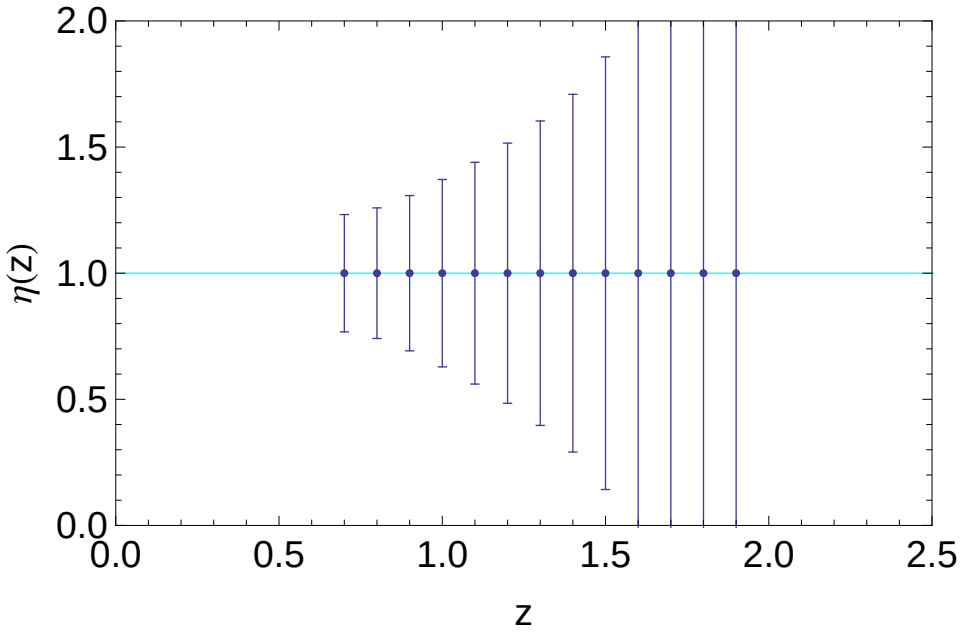

Figure 6.36: Errors on η, $\Delta z = 0.1$, $\varepsilon_{eff} = 1.4$.

In the last projection, where we assume $\eta = 1$, we get an uncertainty equal to

$$\Delta\eta = 0.18. \tag{6.144}$$

We can appreciate that the final errors on η do not depend strongly on ε_{eff}, and the conclusions for $\varepsilon_{eff} = 1$ are still valid for the pessimistic and optimistic case: we can have good constraints on η only in the first bins.

6.6.1.2 Bin size $\Delta z = 0.2$

$\underline{\varepsilon_{eff} = 1 : \textbf{reference case}}$

z_α	$P_1(z_\alpha)$	$\Delta P_1(z_\alpha)$	$\Delta P_1(z_\alpha)(\%)$	$P_2(z_\alpha)$	$\Delta P_2(z_\alpha)$	$\Delta P_2(z_\alpha)(\%)$	$P_3(z_\alpha)$	$\Delta P_3(z_\alpha)$	$\Delta P_3(z_\alpha)(\%)$
0.75	0.81	0.0044	0.54	0.700	0.0065	0.92	0.337	0.046	14
0.95	0.85	0.0034	0.40	0.665	0.0067	1.0	0.461	0.040	8.6
1.15	0.88	0.0032	0.36	0.642	0.0086	1.3	0.557	0.043	7.6
1.35	0.91	0.0035	0.38	0.625	0.018	2.9	0.631	0.051	8.1
1.55	0.93	0.0044	0.47	0.613	0.057	9.3	0.690	0.073	11
1.75	0.94	0.0070	0.74	0.604	0.22	37	0.736	0.065	8.8

Table 6.30: Fiducial values, errors and percent errors for the parameters P_1, P_2, P_3 for every bin, $\Delta z = 0.2$, $\varepsilon_{eff} = 1$.

z_α	$\eta(z_\alpha)$	$\Delta\eta(z_\alpha)$	$\Delta\eta(z_\alpha)(\%)$
0.75	1.00	0.086	8.6
0.95	1.00	0.12	12
1.15	1.00	0.16	16
1.35	1.00	0.22	22
1.55	1.00	0.32	32
1.75	1.00	0.70	70

Table 6.31: Fiducial values, errors and percent errors for the parameter η for every bin, $\Delta z = 0.2$, $\varepsilon_{eff} = 1$.

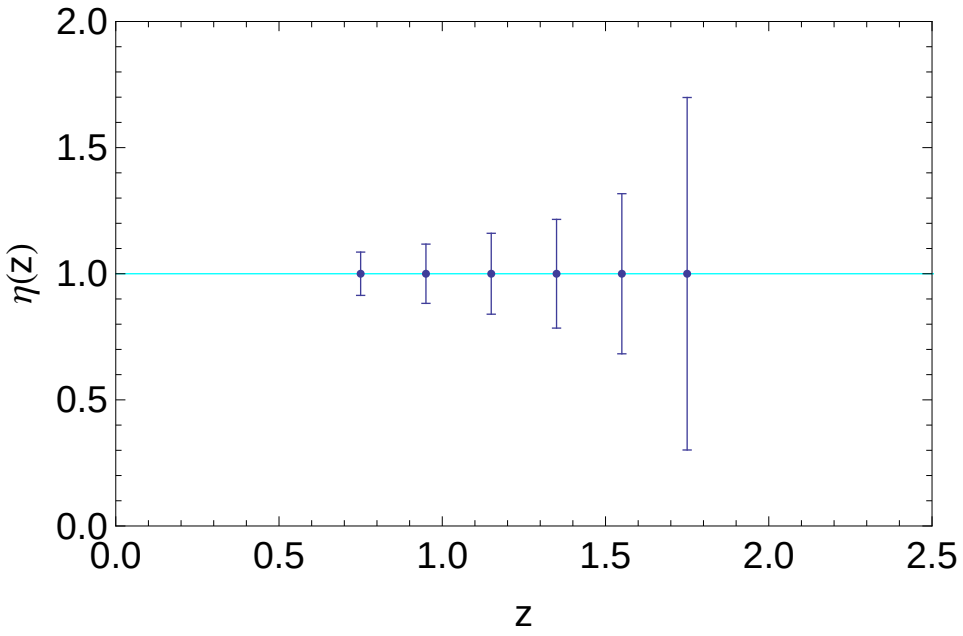

Figure 6.37: Errors on η, $\Delta z = 0.2$, $\varepsilon_{eff} = 1$.

In the last projection, where we assume $\eta = 1$, we get an uncertainty equal to

$$\Delta\eta = 0.070. \tag{6.145}$$

We can appreciate from the comparison of Tables 6.24 and 6.30 how considering larger bins has significantly reduced the errors on P_2 and P_3 by one-two orders of magnitude, and therefore also the constraints on η have improved very much, with the percent error not going beyond 70% (about 30% excluding the last bin).

Further, we gain roughly a factor 2.5 in the last projection, when we consider $\eta = 1$.

$\varepsilon_{eff} = 0.5$**: pessimistic case**

z_α	$P_1(z_\alpha)$	$\Delta P_1(z_\alpha)$	$\Delta P_1(z_\alpha)(\%)$	$P_2(z_\alpha)$	$\Delta P_2(z_\alpha)$	$\Delta P_2(z_\alpha)(\%)$	$P_3(z_\alpha)$	$\Delta P_3(z_\alpha)$	$\Delta P_3(z_\alpha)(\%)$
0.75	0.810	0.0053	0.66	0.700	0.0068	0.96	0.337	0.055	16
0.95	0.852	0.0043	0.50	0.665	0.0068	1.0	0.461	0.050	11
1.15	0.884	0.0042	0.48	0.642	0.0087	1.4	0.557	0.057	10
1.35	0.908	0.0049	0.54	0.625	0.018	2.9	0.631	0.074	12
1.55	0.926	0.0068	0.74	0.613	0.057	9.3	0.690	0.12	17
1.75	0.939	0.012	1.3	0.604	0.22	37	0.736	0.11	15

Table 6.32: Fiducial values, errors and percent errors for the parameters P_1, P_2, P_3 for every bin, $\Delta z = 0.2$, $\varepsilon_{eff} = 0.5$.

z_α	$\eta(z_\alpha)$	$\Delta\eta(z_\alpha)$	$\Delta\eta(z_\alpha)(\%)$
0.75	1.00	0.10	10
0.95	1.00	0.14	14
1.15	1.00	0.19	19
1.35	1.00	0.25	25
1.55	1.00	0.37	37
1.75	1.00	0.73	73

Table 6.33: Fiducial values, errors and percent errors for the parameter η for every bin, $\Delta z = 0.2$, $\varepsilon_{eff} = 0.5$.

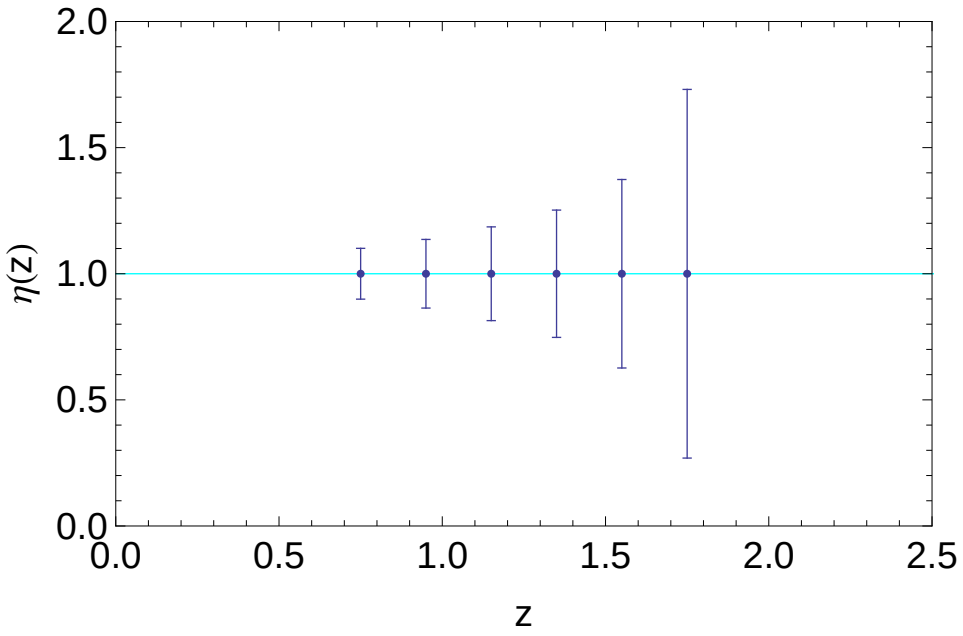

Figure 6.38: Errors on η, $\Delta z = 0.2$, $\varepsilon_{eff} = 0.5$.

In the last projection, where we assume $\eta = 1$, we get an uncertainty equal to

$$\Delta\eta = 0.083. \tag{6.146}$$

$\varepsilon_{eff} = 1.4$**: optimistic case**

z_α	$P_1(z_\alpha)$	$\Delta P_1(z_\alpha)$	$\Delta P_1(z_\alpha)(\%)$	$P_2(z_\alpha)$	$\Delta P_2(z_\alpha)$	$\Delta P_2(z_\alpha)(\%)$	$P_3(z_\alpha)$	$\Delta P_3(z_\alpha)$	$\Delta P_3(z_\alpha)(\%)$
0.75	0.810	0.0041	0.51	0.700	0.0064	0.91	0.337	0.043	13
0.95	0.852	0.0032	0.37	0.665	0.0066	0.99	0.461	0.037	7.9
1.15	0.884	0.0029	0.32	0.642	0.0085	1.3	0.557	0.038	6.9
1.35	0.908	0.0030	0.33	0.625	0.018	2.9	0.631	0.044	6.9
1.55	0.926	0.0036	0.39	0.613	0.057	9.2	0.690	0.059	8.6
1.75	0.939	0.0055	0.59	0.604	0.22	37	0.736	0.052	7.0

Table 6.34: Fiducial values, errors and percent errors for the parameters P_1, P_2, P_3 for every bin, $\Delta z = 0.2$, $\varepsilon_{eff} = 1.4$.

z_α	$\eta(z_\alpha)$	$\Delta\eta(z_\alpha)$	$\Delta\eta(z_\alpha)(\%)$
0.75	1.00	0.082	8.2
0.95	1.00	0.11	11
1.15	1.00	0.15	15
1.35	1.00	0.21	21
1.55	1.00	0.30	30
1.75	1.00	0.69	69

Table 6.35: Fiducial values, errors and percent errors for the parameter η for every bin, $\Delta z = 0.2$, $\varepsilon_{eff} = 1.4$.

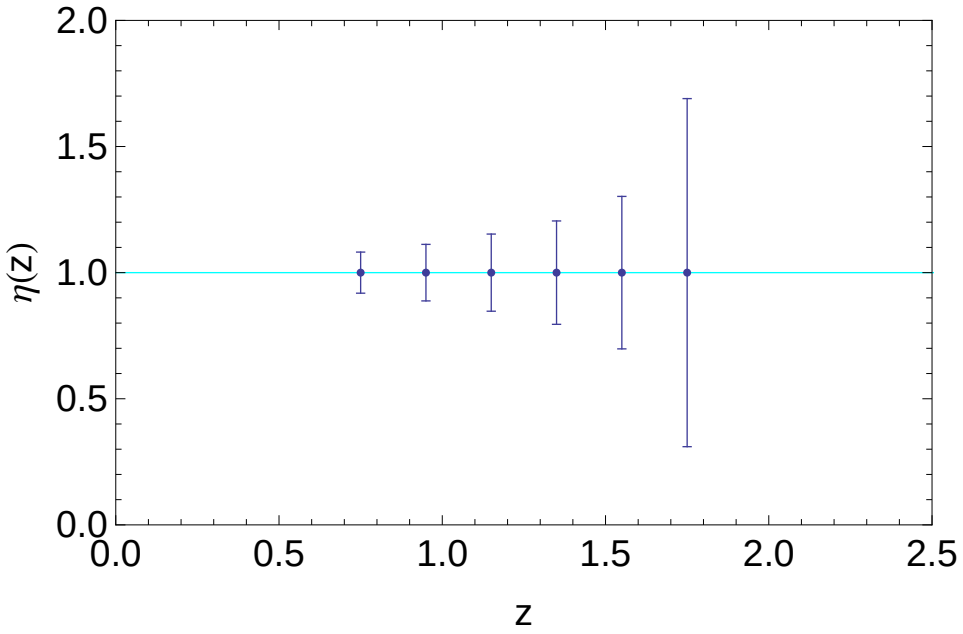

Figure 6.39: Errors on η, $\Delta z = 0.2$, $\varepsilon_{eff} = 1.4$.

In the last projection, where we assume $\eta = 1$, we get an uncertainty equal to

$$\Delta\eta = 0.066. \tag{6.147}$$

Also when we choose larger bins, then, we can conclude that the dependence on ε_{eff} is not very strong, since the final errors in Tables 6.33 and 6.35, that is, in the pessimistic and optimistic case, do not differ in a significant way.

Conclusions

In this Thesis we exposed the evidences for the accelerated expansion of the Universe, and explained why the cosmological constant Λ cannot be held as the definitive explanation for the late-time cosmic acceleration. We presented the main alternative dark energy models and talked about the importance of constraining them by means of accurate observations. In this framework, we introduced the European Space Agency *Euclid* mission and described its two main probes: galaxy clustering and weak lensing.

We then performed forecasts for the constraints on the dark energy anisotropic stress η by means of the Fisher matrix formalism, expressing η as a function of the model-independent parameters A, R, L defined in [4] and of the Hubble dimensionless parameter E. We used the specifications from the ESA *Euclid* survey [10, 11] for galaxy clustering and weak lensing surveys, to which we added information from a supernova survey in order to improve constraints on the Hubble dimensionless parameter E. We employed as fiducial parameters the ones for ΛCDM from WMAP-9-year data [14]. We considered the two cases in which (a) η depends on redshift only and (b) η is constant and equal to unity.

We computed the forecasts for surveys in the redshift interval $0.65 < z < 2.05$ and divided the interval in bins, using different values for the redshift size, $\Delta z = 0.1$ and $\Delta z = 0.2$.

We further considered three different values for the parameter ε_{eff}, which measures the efficiency of the galaxy clustering survey in measuring redshifts of the galaxies. The values of ε_{eff} that have been used are $\varepsilon_{eff} = 1$, $\varepsilon_{eff} = 0.5$ and $\varepsilon_{eff} = 1.4$, in order to take into account a reference, a pessimistic and an optimistic case, respectively.

The final results obtained for the constraints on η allow us to conclude as follows.

1. We can put much better constraints on η by choosing larger bins: the constraints using $\Delta z = 0.1$ are very weak for high redshifts, as often we get an uncertainty which is higher than 100%, while for $\Delta z = 0.2$ we manage to obtain errors below 40% in most bins (excluding the last); when we consider η as constant, we gain roughly a factor 2.5 in the accuracy.

2. The dependence of the final errors on the efficiency parameter ε_{eff} is not strong; the difference in the errors on η is of the order of few percentage points between the pessimistic and the optimistic case.

3. Adding data from supernovae does not bring us a great advantage, since the errors on E from galaxy clustering and weak lensing are significanlty lower than the constraints we can obtain from a supernova survey, if we consider a survey with $n_{SN} = 2000$ supernovae; further, we find that to have good constraints form supernovae we have surely to take into account a survey measuring more than $n_{SN} = 10000$ supernovae. In putting constraints on the Hubble dimensionless parameter E, we have that weak lensing is a very accurate method at low redshifts (below $z \simeq 1$), while the constraints from galaxy clustering are stronger at high redshifts.

Therefore, the present study shows how *Euclid* data will be able to put significant constraints on the dark energy anisotropic stress η, consistently with the great expectations on the *Euclid* mission.

It is also possible to project the constraints on η onto the Horndeski Lagrangian functions, therefore constraining the dark energy models belonging to the class of scalar-tensor theories. This part of the work will be performed in a paper in preparation by Amendola, Fogli, Guarnizo, Kunz and Vollmer.

Bibliography

[1] A. G. Riess et al., *Observational evidence from supernovae for an accelerating universe and a cosmological constant*, Astron. J. **116**, 1009 (1998).

[2] S. Perlmutter et al., Measurements of Ω and Λ from 42 high-redshift supernovae, Astrophs. J. **517**, 565 (1999).

[3] G. W. Horndeski, *Second-order scalar-tensor field equations in a four-dimensional space*, Int. J. Theor.Phys. 10, 363-384 (1974).

[4] L. Amendola, M. Kunz, M. Motta, I. D. Saltas, I. Sawicki, *Observables and unobservables in dark energy cosmology*, arXiv:1210.0439 (2012).

[5] L. Amendola and S.Tsujikawa, *Dark Energy: Theory and Observations*, Cambridge University Press (2010).

[6] W. Hillebrandt and J. C. Niemeyer, *Type IA Supernova Explosion Models*, Annual Review of Astronomy and Astrophysics 38 (1): 191–230; arXiv:astro-ph/0006305 (2000).

[7] A. Einstein, *Kosmologische Betrachtungen zur allgemeinen Relativitätstheorie* (Cosmological Considerations in the General Theory of Relativity), Koniglich Preußische Akademie der Wissenschaften, Sitzungsberichte (Berlin): 142–152 (1917).

[8] J. B. Kaler, *Stars*, Scientific American Library (1992).

[9] A. De Felice, T. Kobayashi, S. Tsujikawa, *Effective gravitational couplings for cosmological perturbations in the most general scalar-tensor theories*, arXiv:1108.4242 (2011)

[10] R.Laureijs et al., *Euclid Definition Study report*, arXiv:1110.3193 (2011).

[11] L. Amendola et al., *Cosmology and fundamental physics with the Euclid satellite,* arXiv:1206.1225v1 (2012).

[12] M. Tegmark et al., *The three-dimensional power spectrum of galaxies from the Sloan Digital Sky Survey,* Astrophys. J. 606:702-740 (2004).

[13] J. M. Bardeen, J. R. Bond, N. Kaiser and A. S. Szalay, *The statistics of peaks of Gaussian random fields*, Astrophys. J., 304:15 (1986).

[14] WMAP 9-year-data, Cosmological Parameters, http://lambda.gsfc.nasa.gov/product/map/current/params/all_parameters.pdf (2013).

[15] P. Peebles, *Physical Cosmology*, Princeton University Press (1994).

[16] H.-J. Seo and D. J. Eisenstein, *Probing Dark Energy with Baryonic Acoustic Oscillations from Future Large Galaxy Redshift Surveys,* Astrophys. J. 598:720-740 (2003).

[17] Z. Ma, W. Hu, D. Huterer, *Effects of photometric redshift uncertainties on weak lensing tomography*, Astrophys. J. 636:21-29 (2005).

[18] Y.-C. Cai and G. Bernstein, *Combining weak-lensing tomography and spectroscopic redshift surveys*, Mon. Not. R. Astron. Soc. **422**, 1045-1056 (2012)

[19] Union 2.1 Compilation, Magnitude vs. Redshift Table, http://supernova.lbl.gov/Union/figures/SCPUnion2.1_mu_vs_z.txt

[20] N. Suzuki et al., *The Hubble Space Telescope Cluster Supernova Survey: V. Improving the Dark Energy Constraints Above z>1 and Building an Early-Type-Hosted Supernova Sample*, arXiv:1105.3470v1 (2011).

Acknowledgements

I would like to thank professors Lauro Moscardini and Luca Amendola for the great opportunity they have given to me of developing this Thesis at the Institut für theoretische Physik (ITP), Heidelberg, Germany; an experience which has been very helpful to me, not only in scientific terms, and that I will always carry in my heart. I would also like to thank all the members of Professor Amendola's group and all the people who have made my stay in Heidelberg so pleasant and adventurous.

* * *

Se la vita è un libro, come spesso si dice, un altro capitolo è stato scritto (non solo metaforicamente). Questa tesi non è solo una selva di formule e grafici dall'arcano significato, ma rappresenta per me la fine di un lungo percorso. E alla fine di questo libro cartaceo, prima di voltare l'ultima pagina e metterlo a prendere polvere sullo scaffale più alto della libreria, vorrei ringraziare tutti quelli che che hanno camminato con me, sperando che questo momento mellifluo non provochi crisi di diabete agli interessati.

Grazie innanzitutto ai miei genitori, che mi hanno supportato (e soprattutto sopportato) per più di 24 anni, e grazie a tutti i parenti che mi hanno sempre sostenuto, in particolare alla zia Giancarla: ogni parola in più non vi renderebbe giustizia, quindi mi fermo qui.

Grazie alla prof.ssa Paola Giacconi, per l'entusiasmo con cui ha comunicato a noi "sbarbi" studenti di liceo la sua passione per la Fisica.

Grazie a don Sebastiano, che sicuramente apprezzerà la melensaggine di queste pagine, per le sue "Parole di Luce" e per avermi stangato quando ne avevo bisogno.

Grazie a Fabriz, Stiv, Lauretta, per i momenti di altissimo spessore cultural-filosofico-teologico, e soprattutto per quelli di altissima ignoranza.

Grazie a Ema, Rudi, Sandro, Rispo per le serate passate a cercare di conquistare il mondo (davanti a un risiko) e a immaginare di cambiarlo (davanti a una birra).

Grazie ad Alice, Elena, Molly, Eli, Miriam, Tony, Kallo, Giulia, Sciuri, Laura, Serena, Marika, Sofy e tutti gli amici della parrocchia di San Donnino (anche a quelli che si staranno lamentando perché non li ho citati), perché mi hanno aiutato a crescere insieme a loro.

Grazie alle suore e agli ospiti della Casa della Carità di San Giovanni in Persiceto, per avermi tenuto ancorato alla bellezza della concretezza e della realtà.

Grazie a Carlotta, Niccolò e Dome per le scorribande in giro per la città e per l'Europa; grazie a Eugenia, Sara, Chiara, Elia per le serate di vita mondana; grazie a Elena, perché mi ricorda che anche se siamo in giro per il mondo, ogni tanto è bello ritrovarsi nella propria città con la gente di sempre.

Grazie a tutti gli amici che ho incontrato e conosciuto nei corridoi, nelle aule, nella biblioteca del Dipartimento di Fisica, che hanno trascorso con me anche solo il tempo di un pranzo o di un caffè; grazie soprattutto e a quelli che mi hanno insegnato che si può parlare anche con chi non la pensa come te.

Grazie a chi c'è stato, a chi c'è e a chi ci sarà.

E a tutti, visto che non ve lo dico mai: vi voglio bene.